Radiative Processes

All e.m. radiation arises from transition between levels with difference in electric or magnetic moment

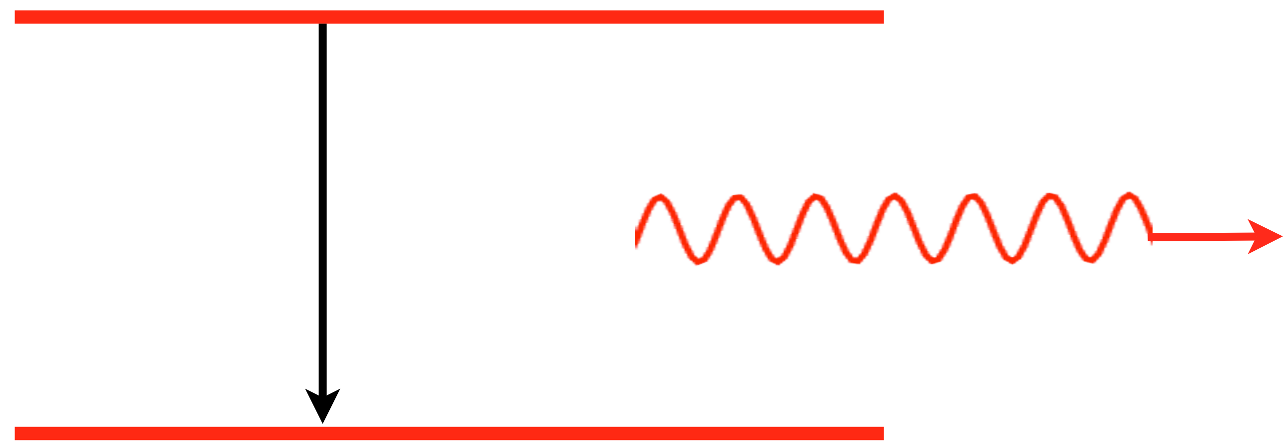

$$\nu = \frac{\Delta E}{h}$$

- Levels could be discrete or in continuum
- Between each pair of levels emisson and absorption
- Transitions dipole / higher multipole

$$\textit{Transition probability} \;\propto\; |\langle\, f \,|\, \exp(i\vec{k}.\vec{r})\; \vec{l}.\Sigma\vec{\nabla} \,|\, i \,\rangle|^2$$

[dipole approximation $\exp(i\vec{k}.\vec{r}) \;=\; 1$]

$$g_2 B_{21} = g_1 B_{12} \quad ; \quad A_{21} = 2h\nu^3 B_{21}/c^2$$

Continuum Radiation

$$P = \frac{2}{3c^3}(\ddot{d})^2 = \frac{2e^2}{3c^3}a^2$$

Classically any accelerated charge would radiate

Different physical situations involve different mechanisms of acceleration
- Radiation mechanism classified according to source of acceleration
- Radiation reaction slows the charge

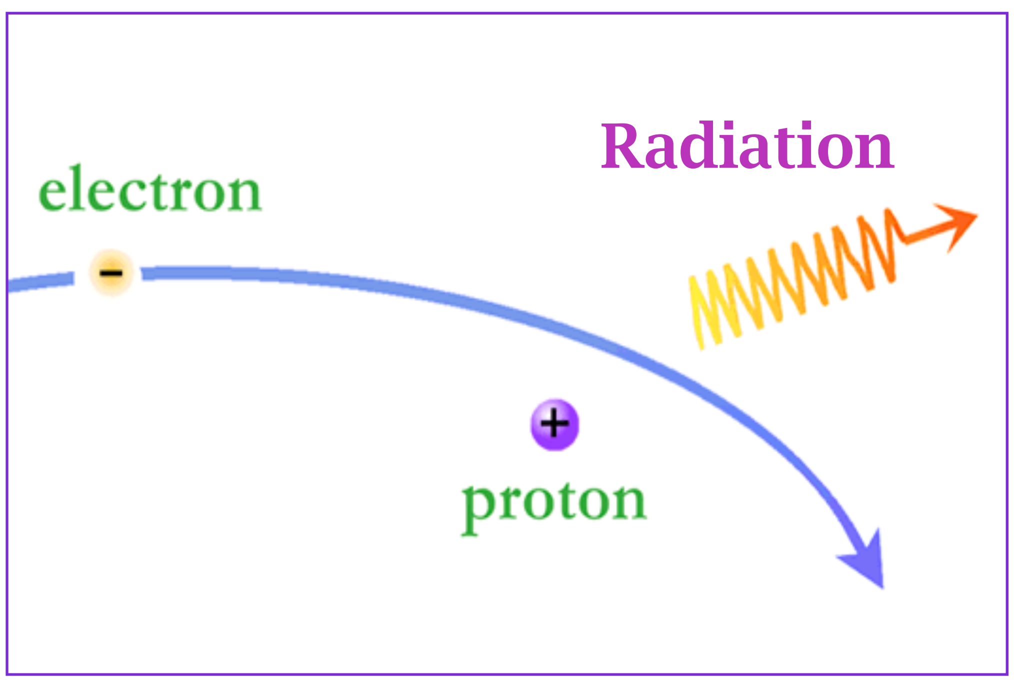

Bremsstrahlung

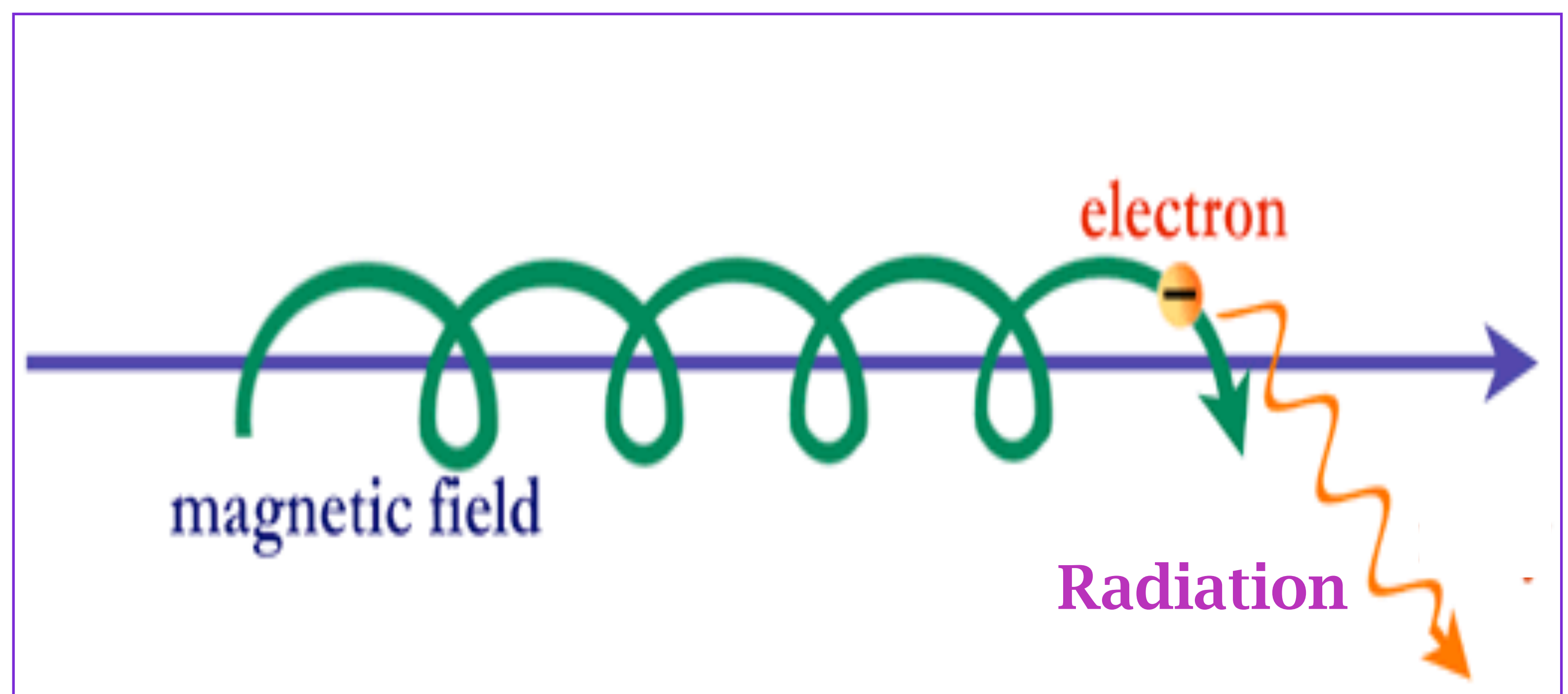

Synchrotron Radiation

Scattering processes

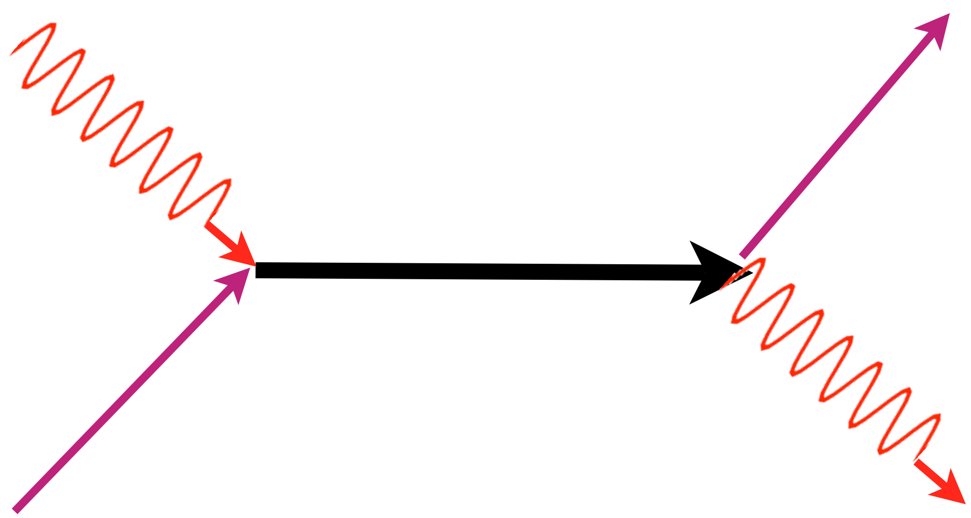

Non-resonant / resonant

Inverse Compton Scattering

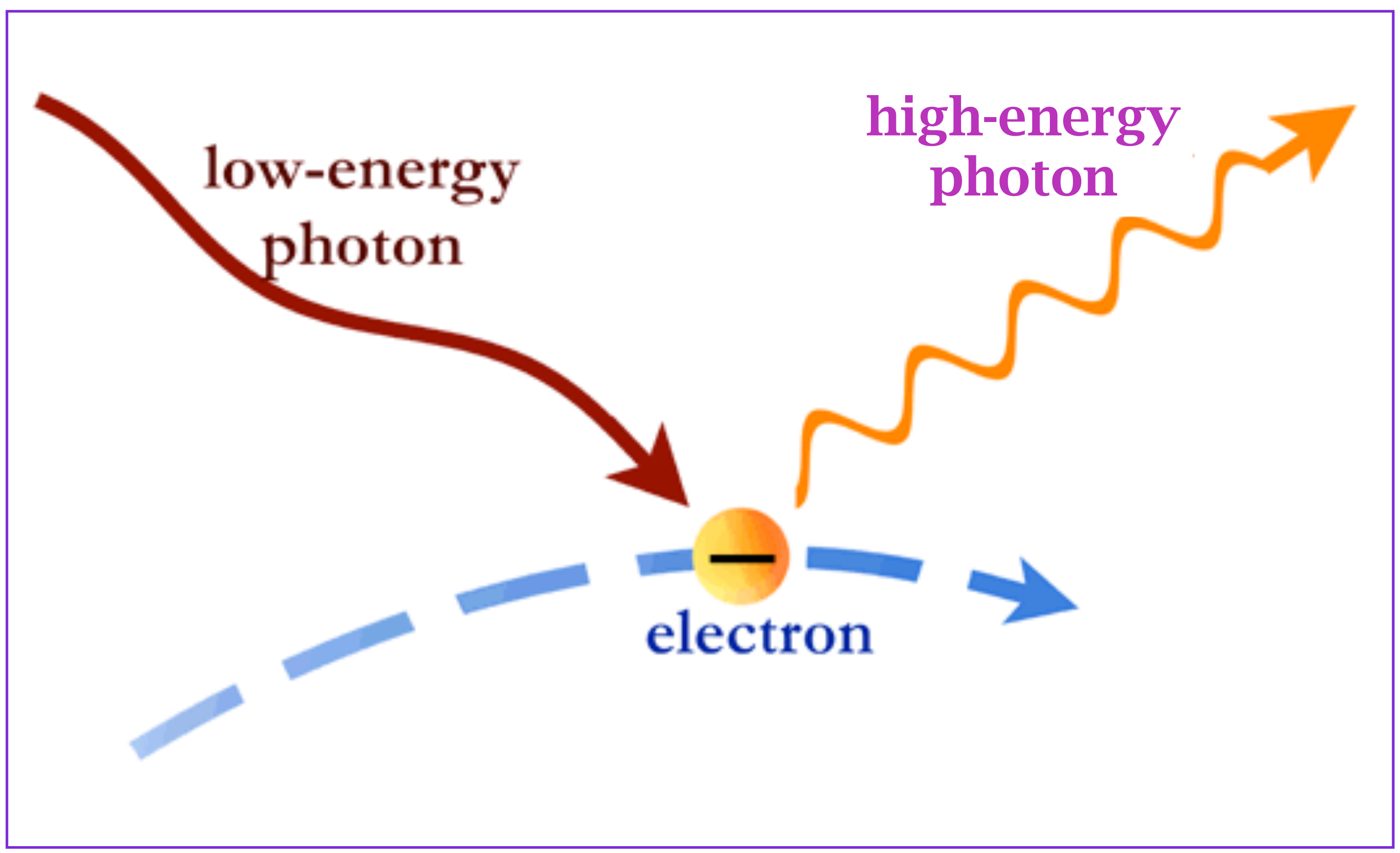

Related processes: Compton Scattering
Thomson Scattering

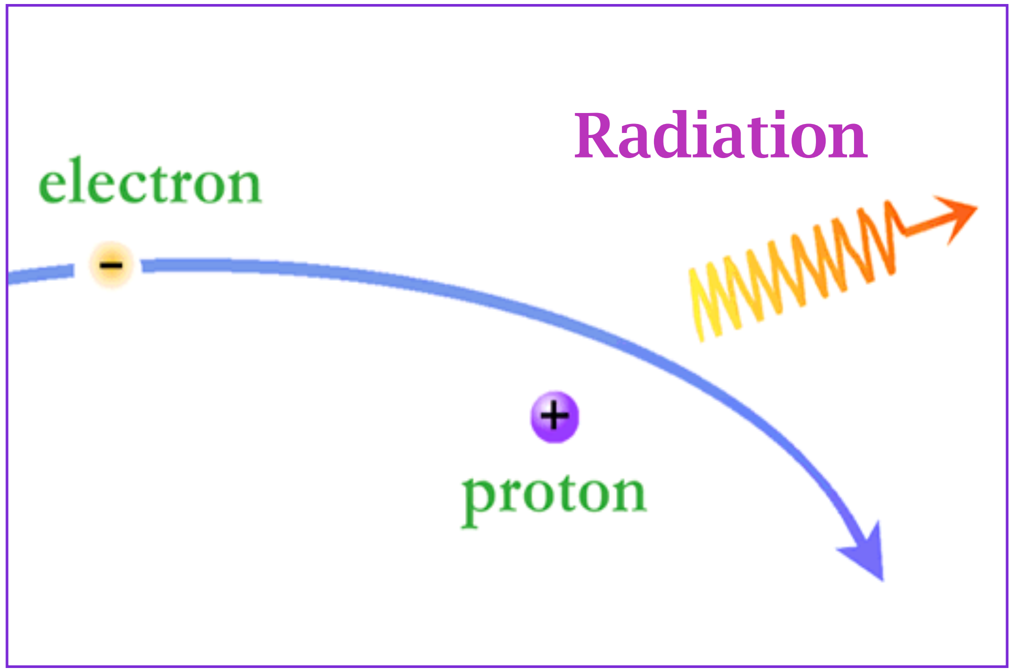

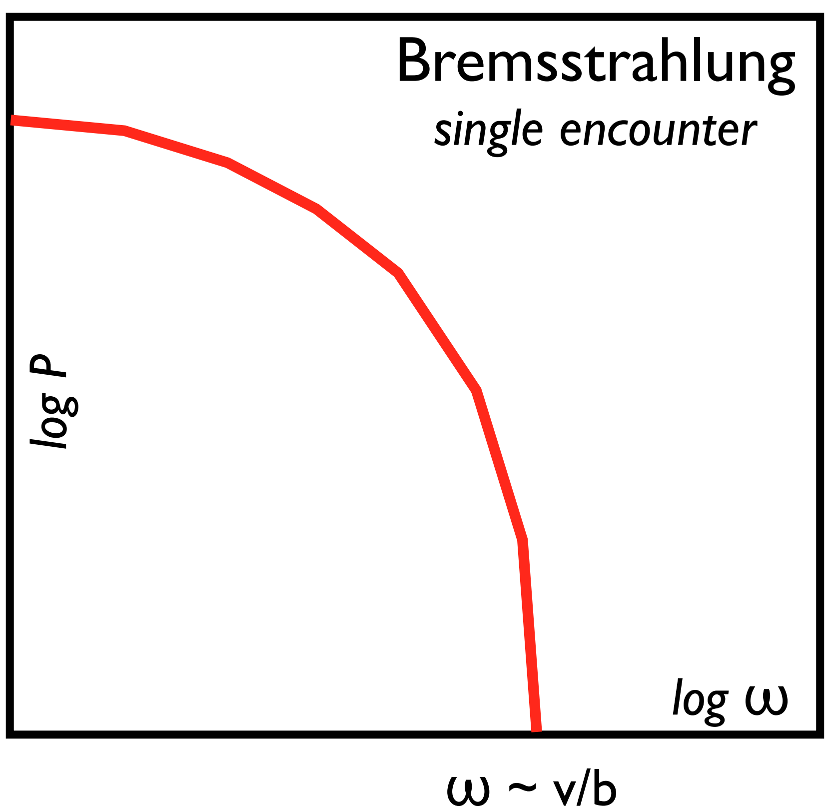

Spectrum

Electric field received by the observer is time dependent

Fourier transform of the electric field yields the spectrum

Net observed spectrum is a sum over all emitting particles

Polarization

$$\vec{E} \propto \hat{n} \times [(\hat{n} - \vec{\beta}) \times \dot{\vec{\beta}}]$$

At a single particle level, over short times, radiation is always polarized.

For slowly moving particle (or $\vec{\beta}$ nearly || to $\hat{n}$) polarization is || to the projected instantaneous acceleration.

Net observed polarization involves average over the particle's trajectory, and over the distribution of emitting particles.

Radiation Pattern

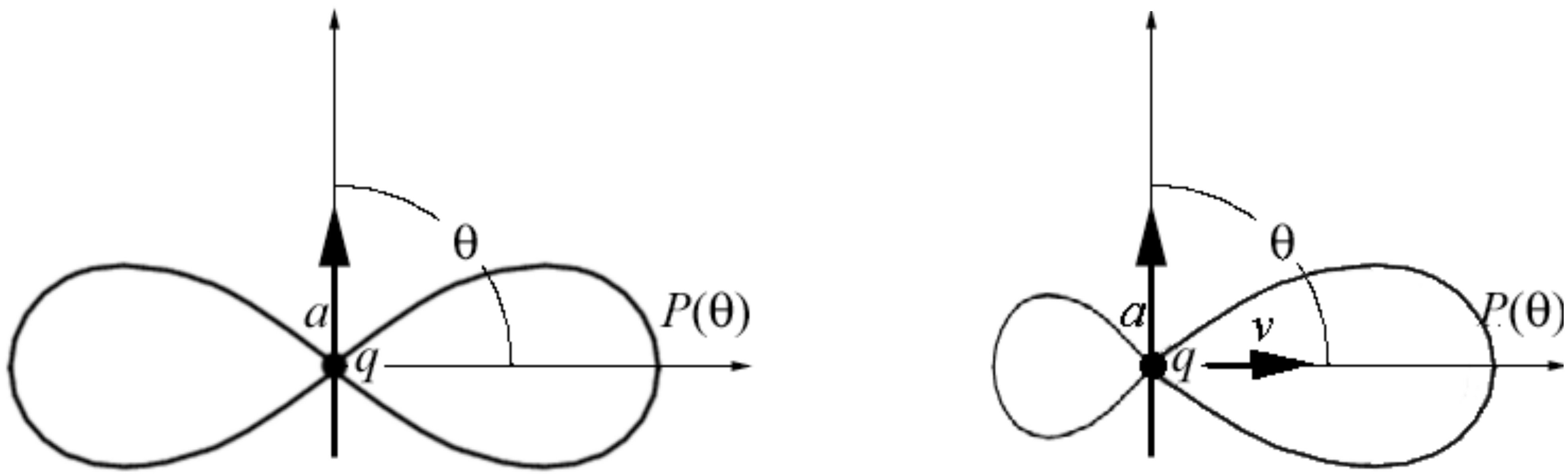

Stationary dipole

Moving dipole

Motion introduces aberration and relativistic beaming

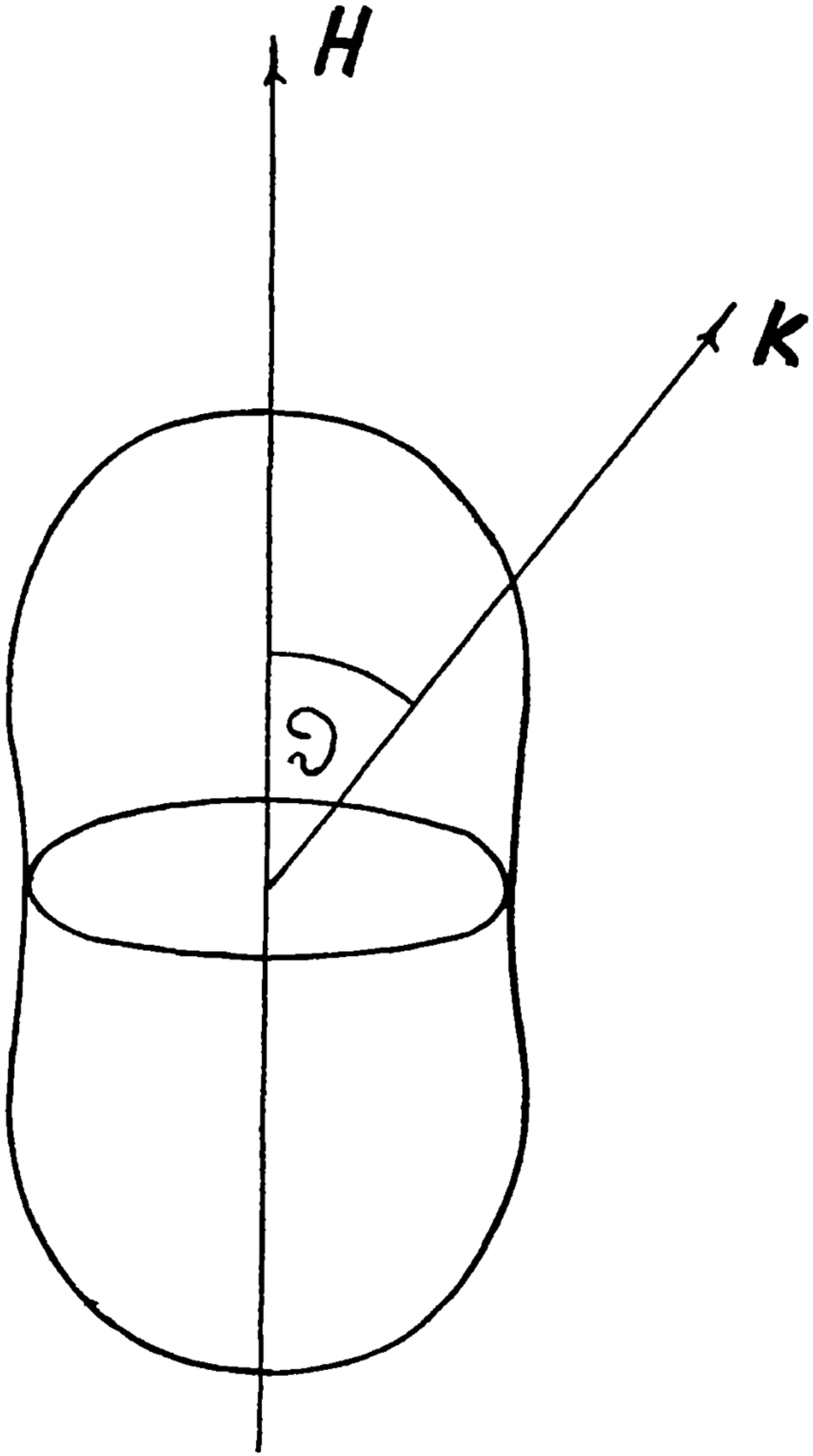

Cyclotron Radiation Pattern

circular motion

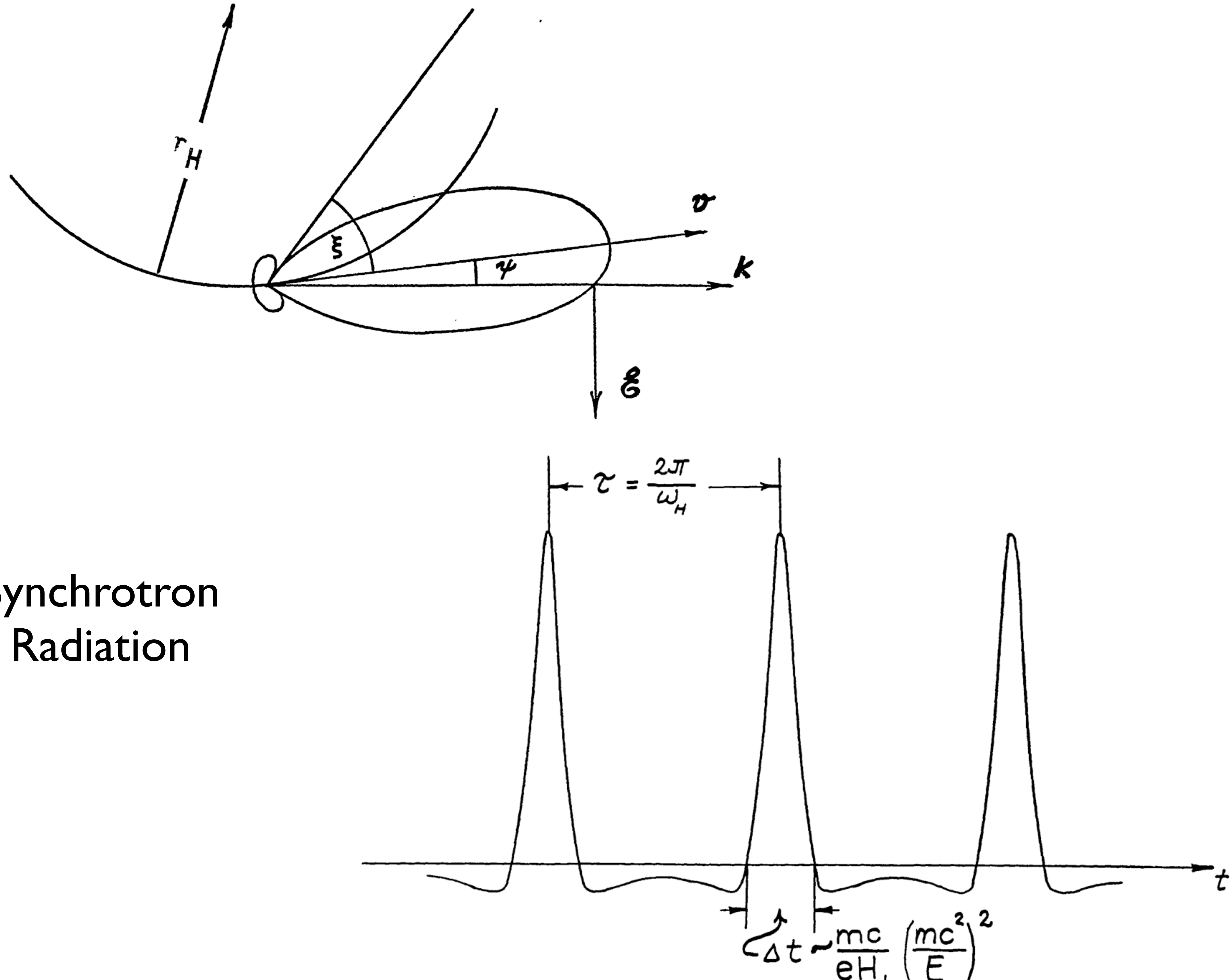

Synchrotron
Radiation

Synchrotron radiation pattern

single emitter

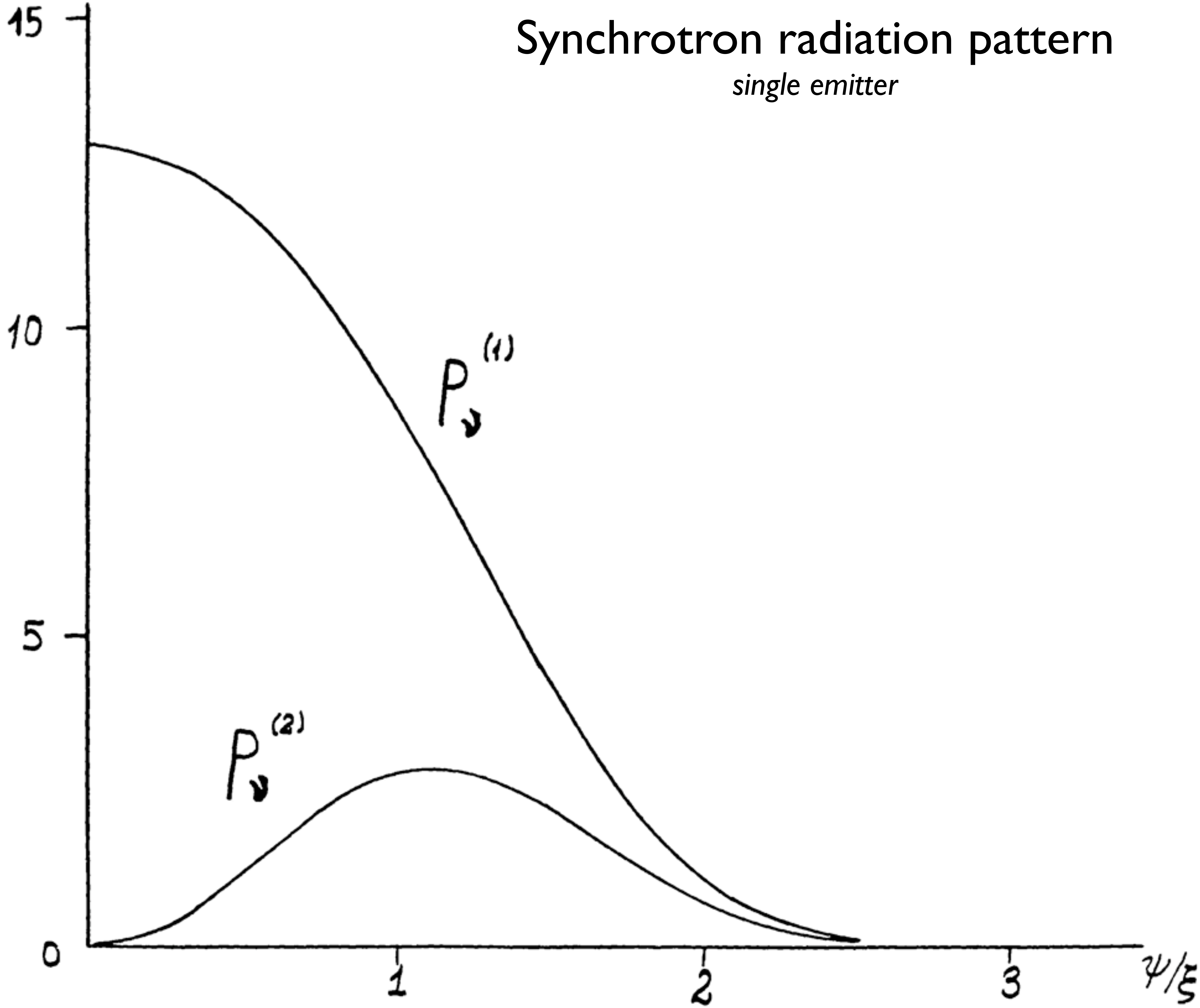

Synchrotron spectrum from single emitter

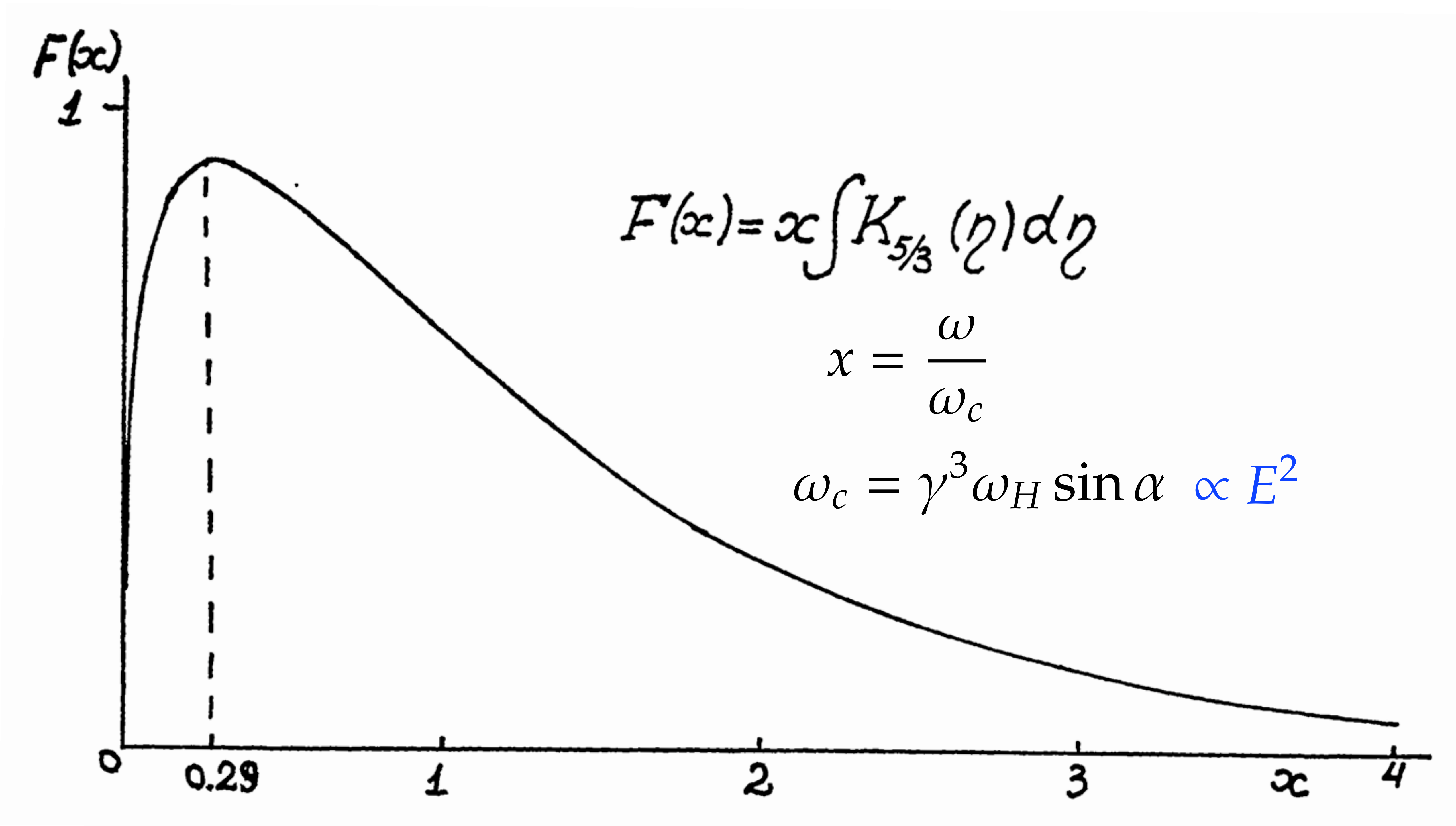

$$x = \frac{\omega}{\omega_c}$$

$$\omega_c = \gamma^3 \omega_H \sin\alpha \;\; \propto E^2$$

Radio image of the active galaxy Cygnus A
- Example of a powerful synchrotron source

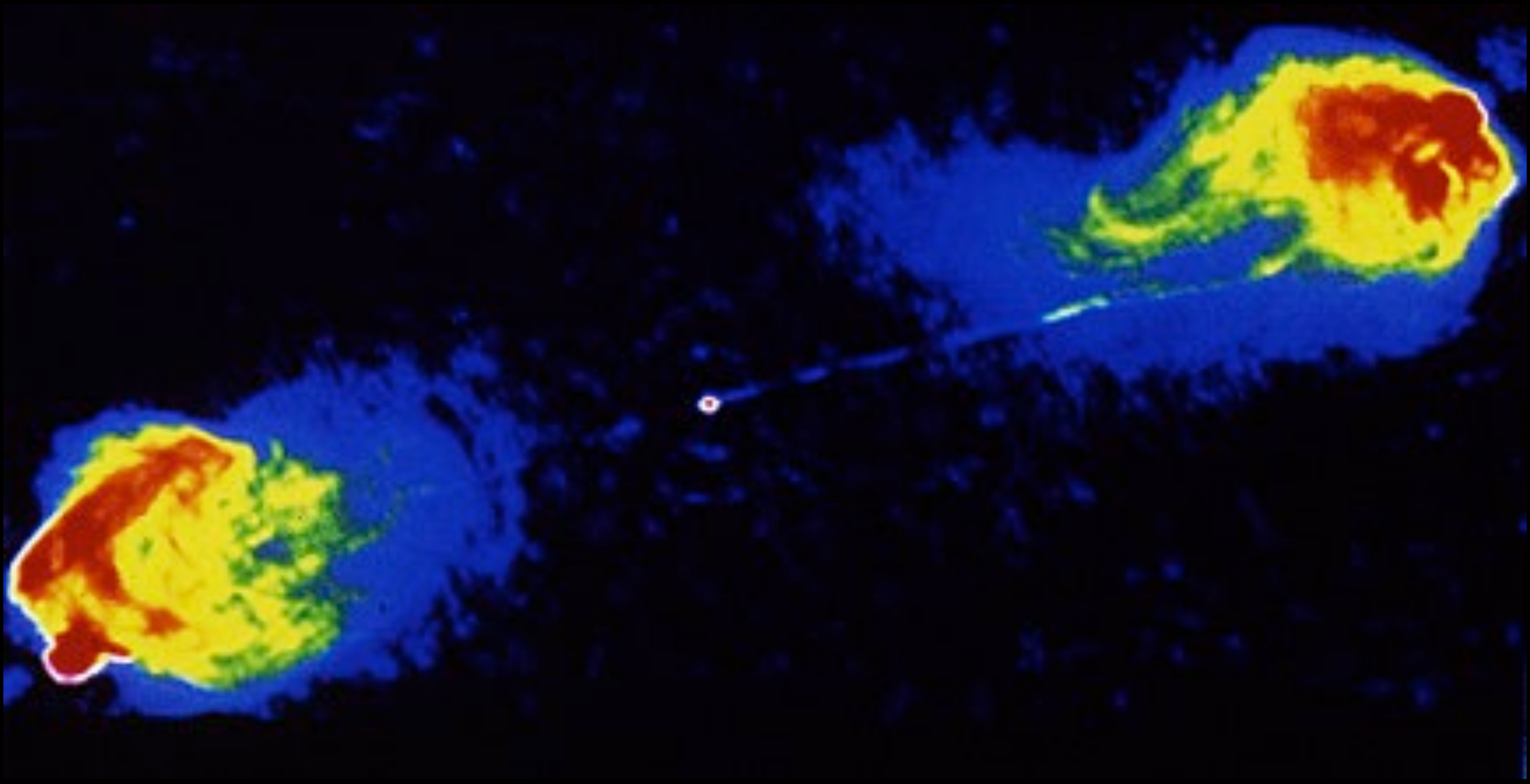

Curvature Radiation

Relativistic Charged Particles moving ***along*** *curved field lines*

- Shares most properties of Synchrotron Radiation (replace Larmor radius by the radius of curvature of field lines)

- Polarization || to the projected field lines (Synchrotron: polarization perp. to projected B)

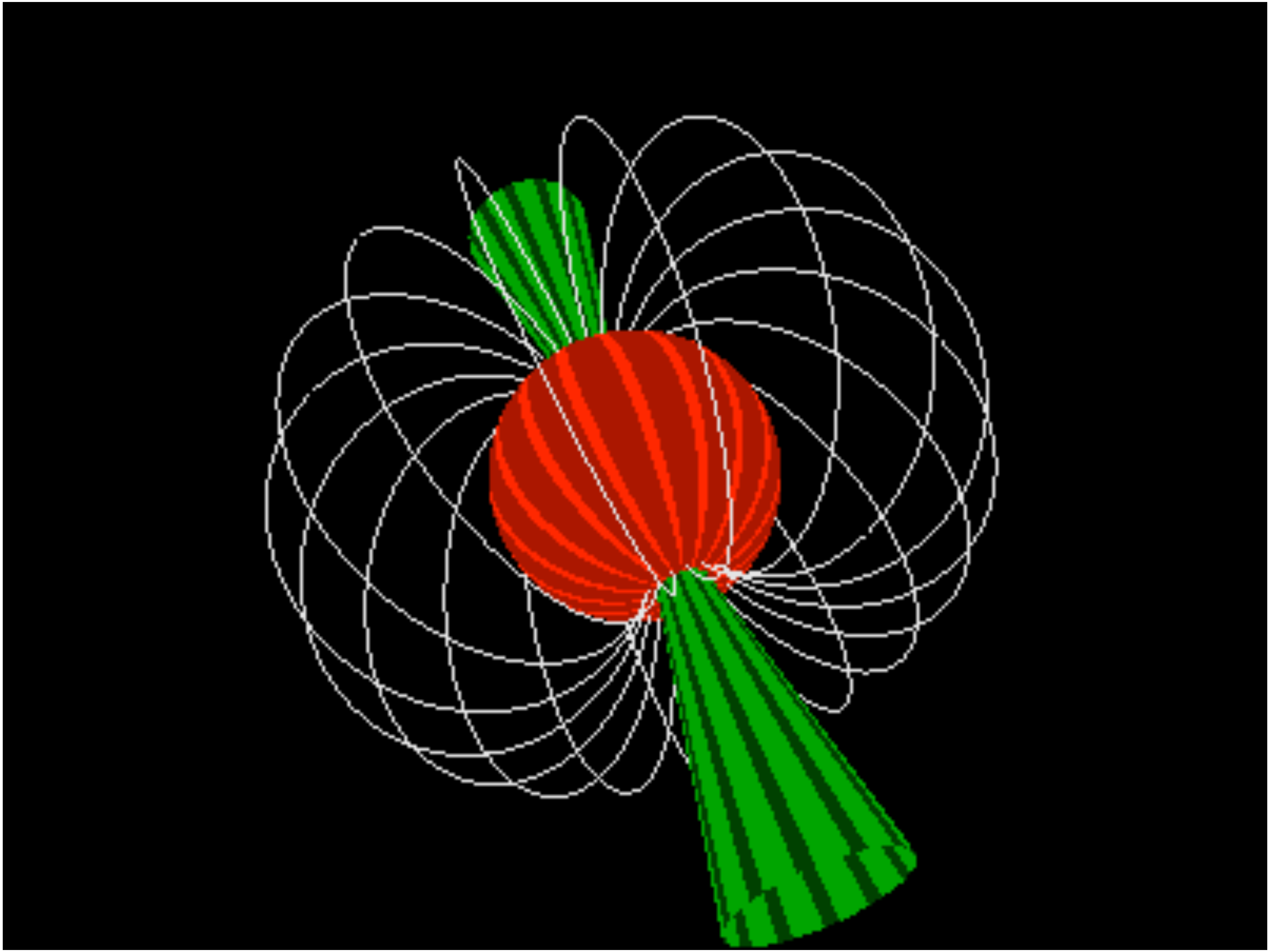

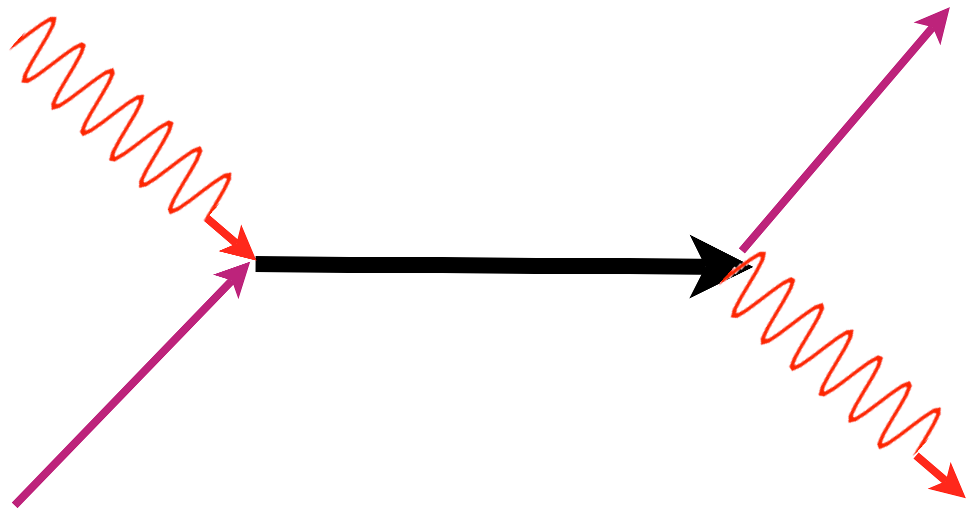

Scattering processes

Non-resonant / resonant

Inverse Compton Scattering

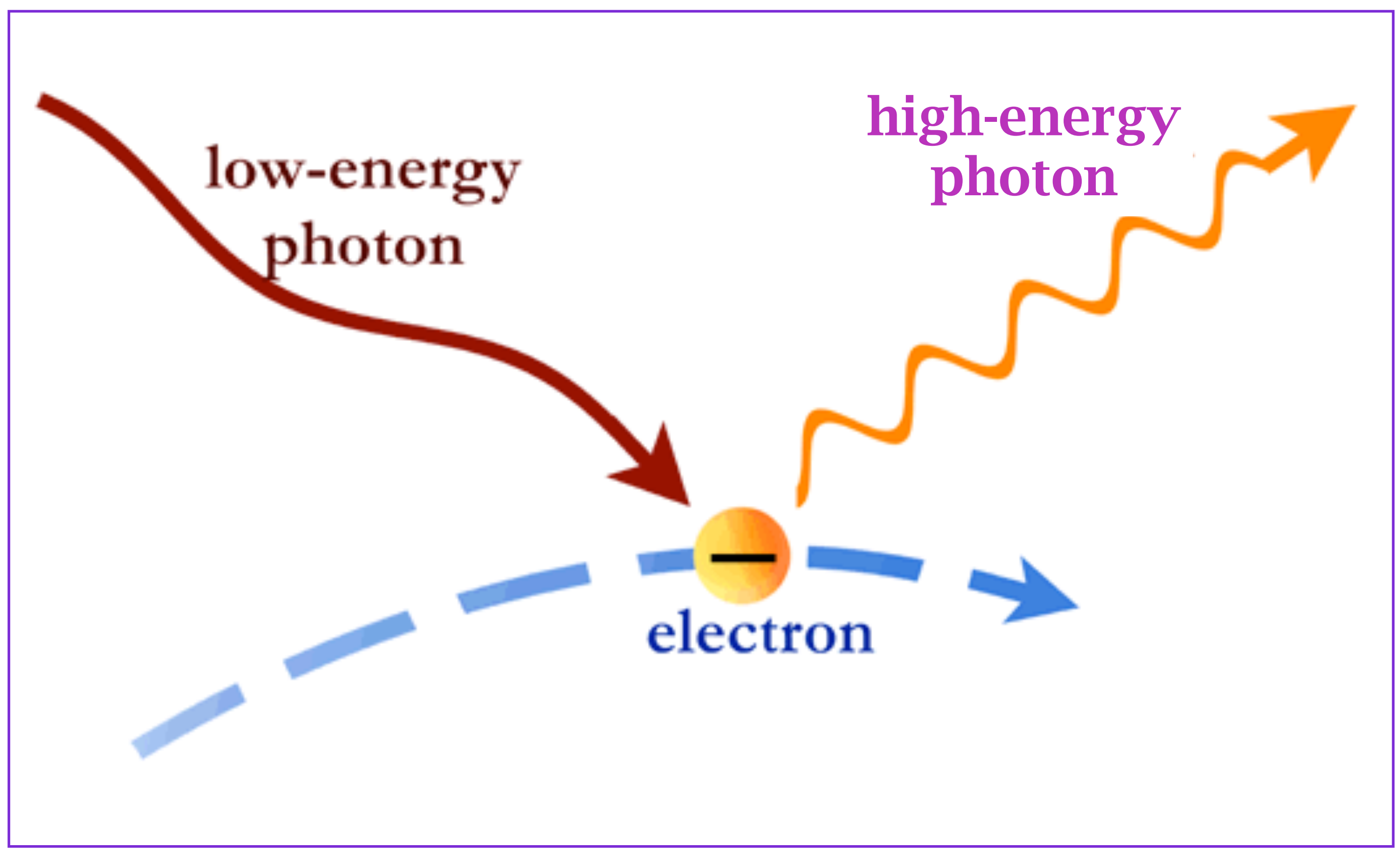

Related processes: Compton Scattering
Thomson Scattering

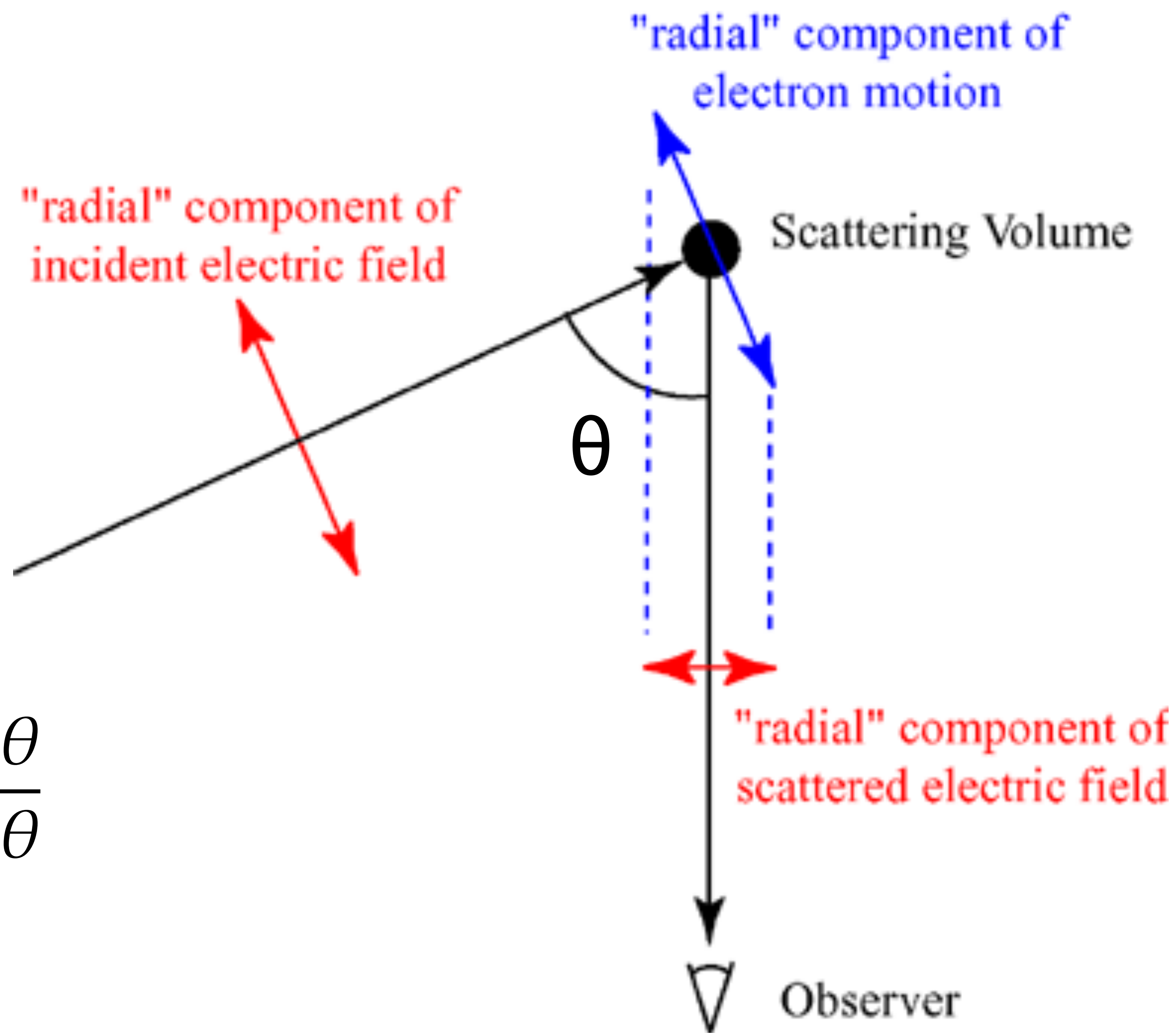

Pol. $\dfrac{1-\cos^2\theta}{1+\cos^2\theta}$

Thomson scattering geometry

Scattering cross section

Thomson $$\sigma_T = \frac{8\pi}{3} r_0^2 = \frac{8\pi}{3} \left(\frac{e^2}{mc^2} \right)^2$$

Compton $$\sigma \approx \sigma_T \left(1 - 2x + \frac{26x^2}{5} + \cdots \right), \qquad x \equiv \frac{h\nu}{mc^2} \ll 1$$

$$\sigma = \frac{3}{8} \sigma_T x^{-1} \left(\ln 2x + \frac{1}{2} \right), \qquad x \gg 1$$

Synchrotron Self Compton

Synchrotron power $$\frac{4}{3}\sigma_T c\beta^2\gamma^2 U_B$$

Compton power $$\frac{4}{3}\sigma_T c\beta^2\gamma^2 U_{\rm ph}$$

$L_{comp} \propto L_{sy}$: Compton Catastrophe : Brightness Temperature limit $\sim 10^{12}$ K

Bulk Comptonization / Compton Drag

Strong radiation beams collimated within $1/\Gamma_{\text{bulk}}$ can be produced by Inverse Compton Scattering by relativistic bulk flow of charged particles

Due to aberration effects, can generate very high polarization

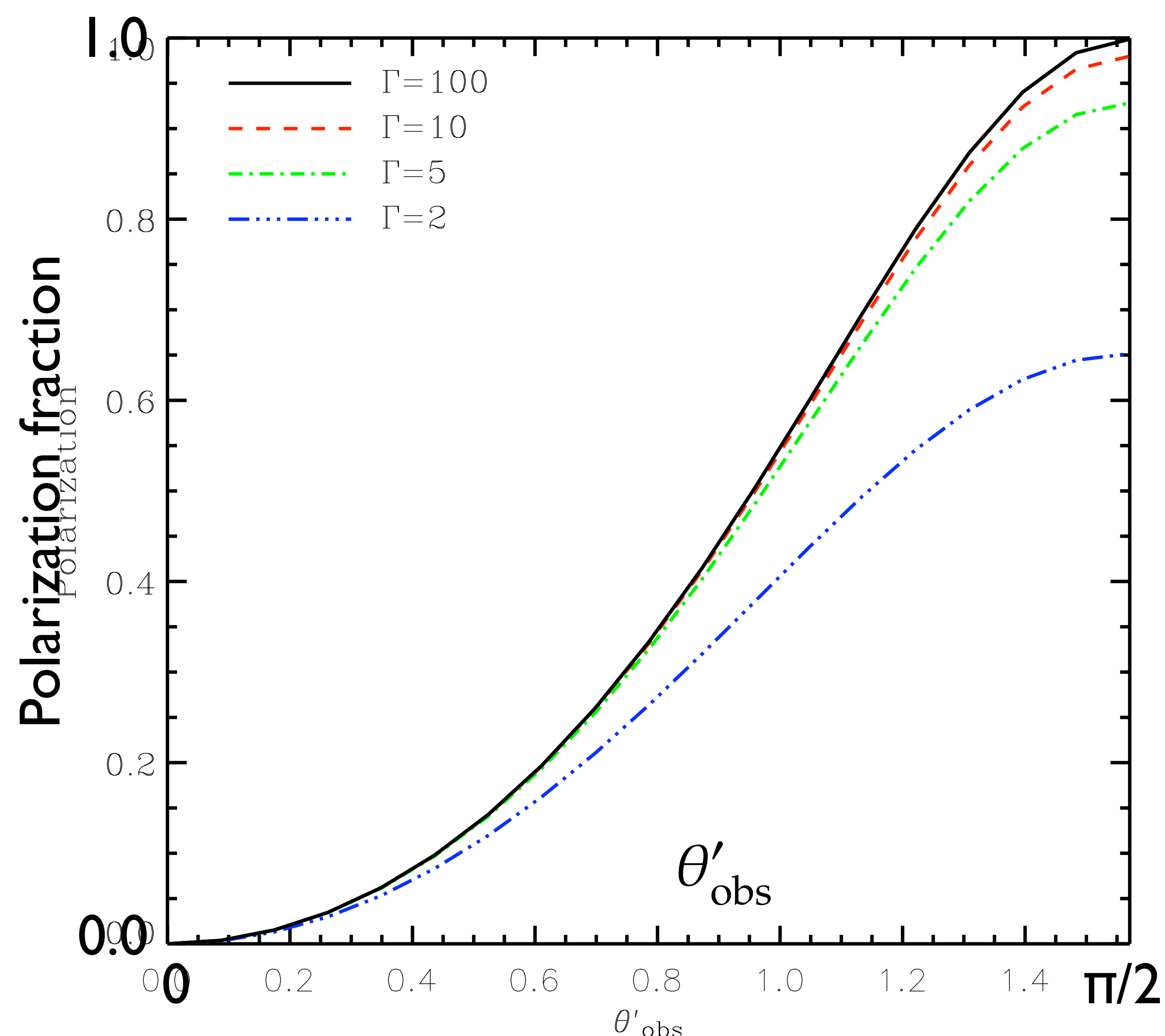

Lazzati et al 2004

Spectra

Radiation received from a source is the sum of emission from a large population of particles.

Energy distribution of the particles shape the spectra

Thermal distribution

Maxwell-Boltzmann

Non-thermal distribution

Non-Maxwellian, e.g. power-law

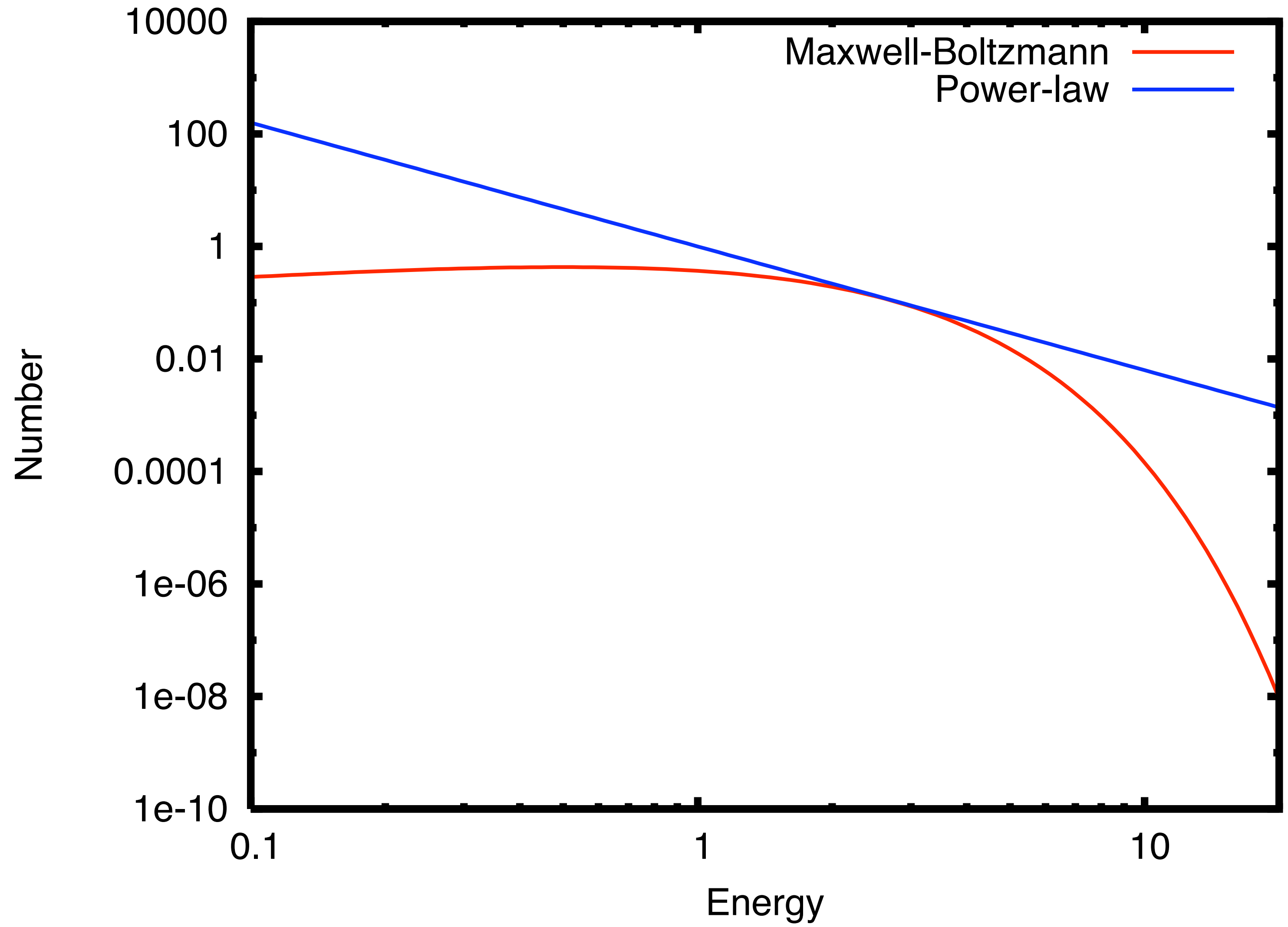

What is emitted is not what we see

Radiation is modified during propagation through matter

Radiative transfer

$$\frac{dI_\nu}{ds} = -\alpha_\nu I_\nu + j_\nu$$

$$\frac{dI_\nu}{d\tau_\nu} = -I_\nu + S_\nu$$

S_ν for a thermal source is the Planck function B_ν

$$B_\nu = \frac{2h\nu^3}{c^2}\frac{1}{\exp(h\nu/kT) - 1}$$

Blackbody function

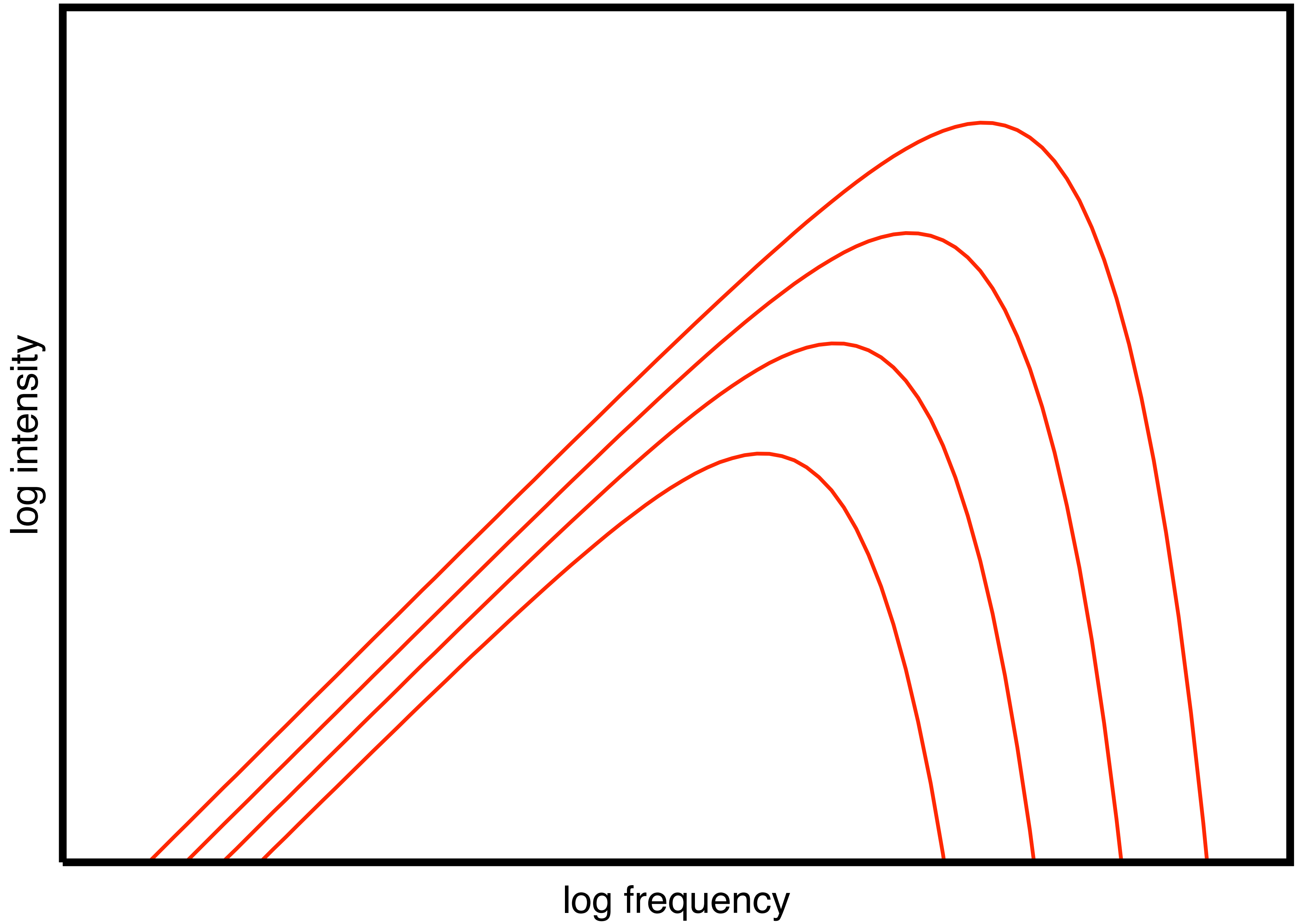

At large optical depth a thermal source will emit blackbody intensity. Emission will be received from a *photosphere*

Optical depth is frequency-dependent. A source could be optically thick at some frequencies, optically thin at others.

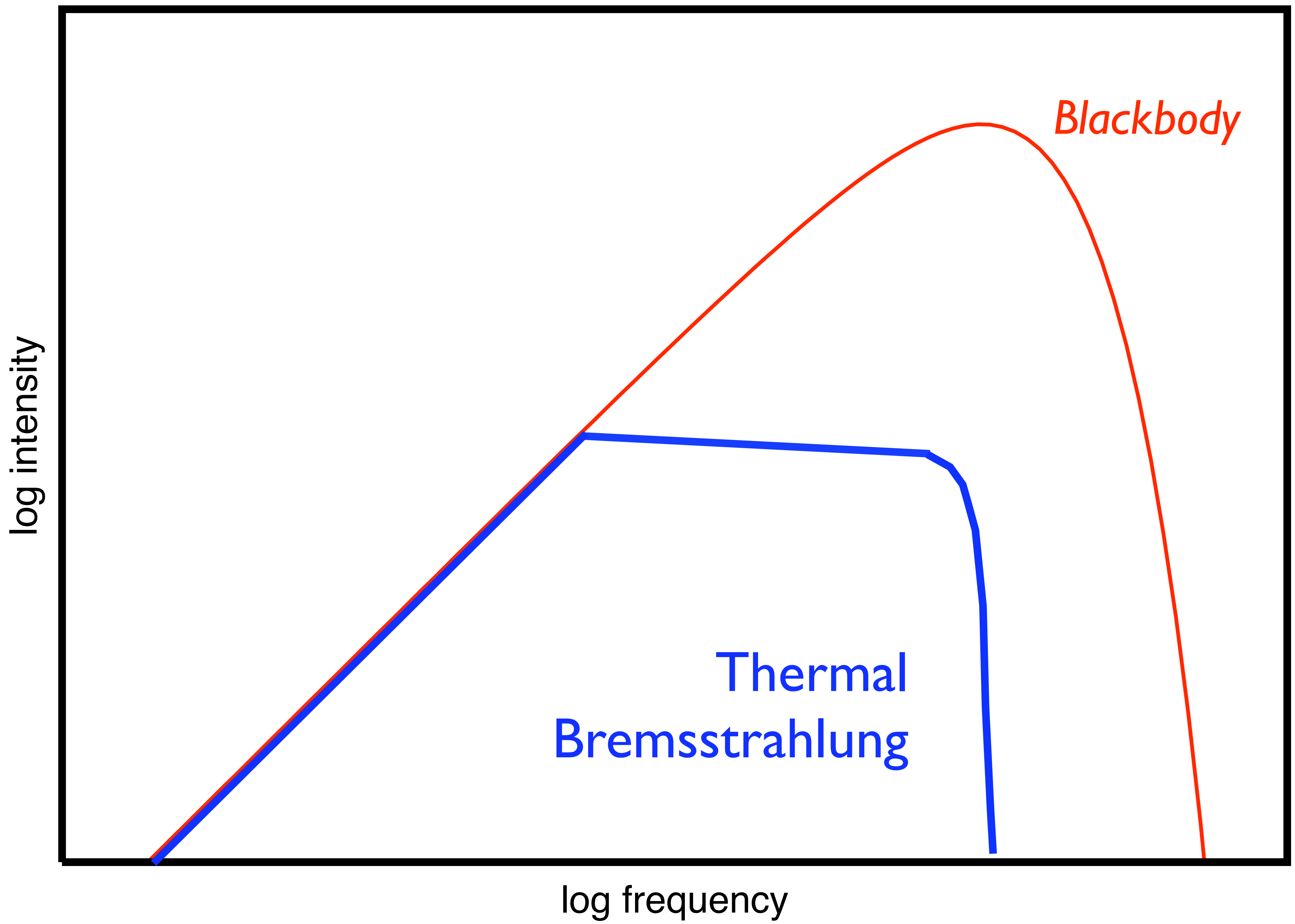
Blackbody
Thermal Bremsstrahlung
log intensity
log frequency

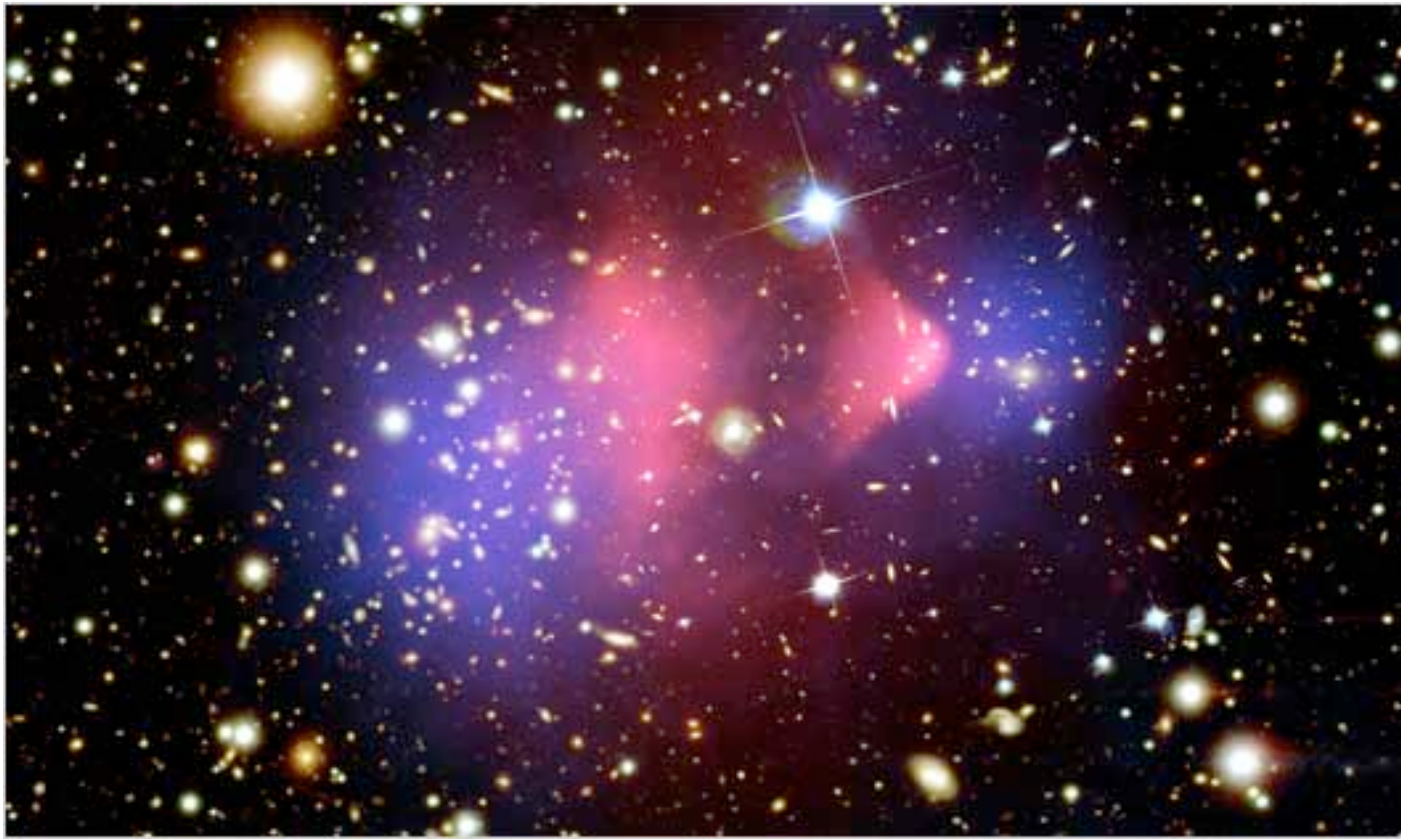

X-ray emission (pink) by hot gas in Bullet Cluster
- *Primarily Thermal Bremsstrahlung emission*

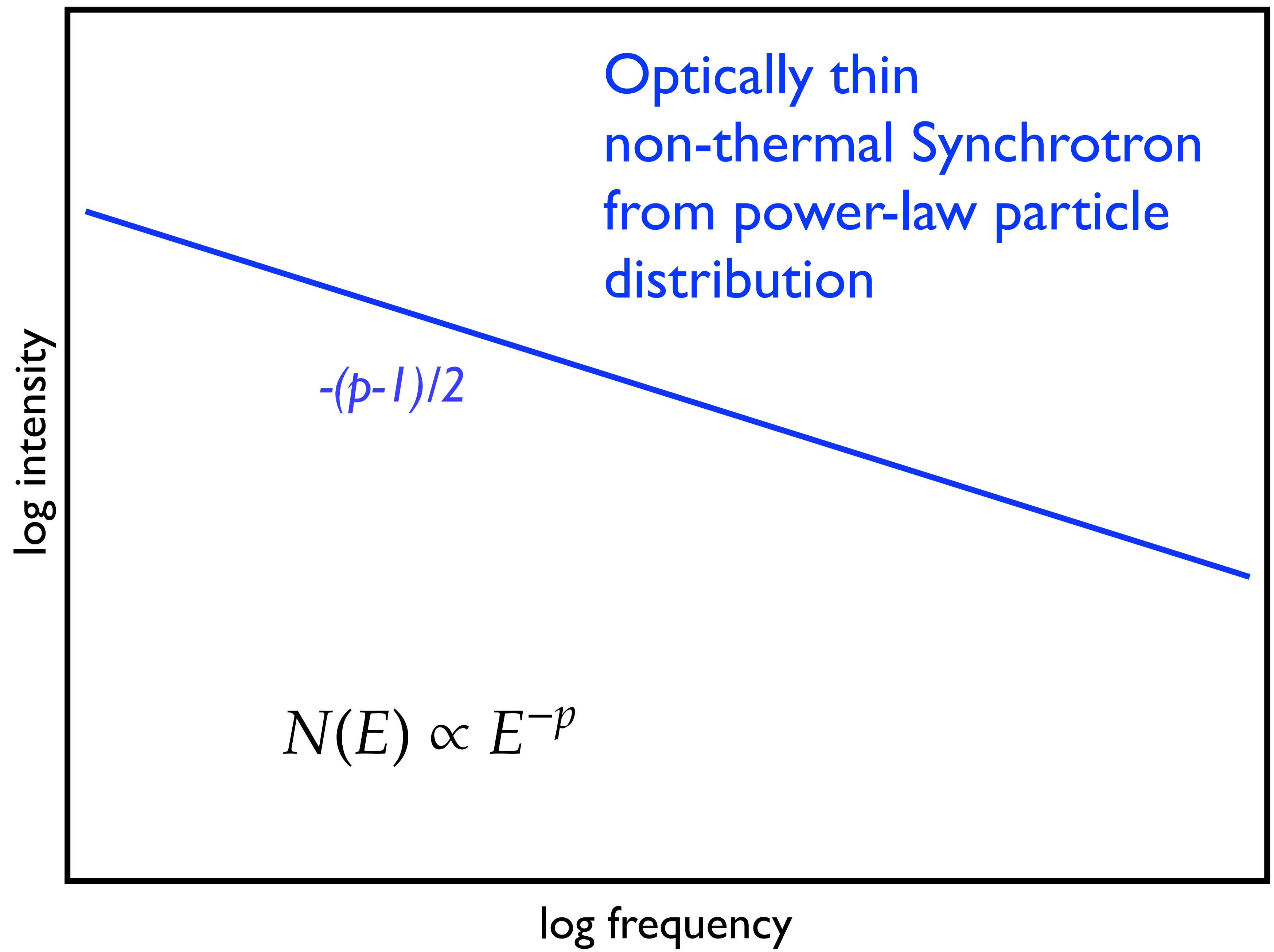

Strong polarization in ordered field: $\dfrac{p+1}{p+\frac{7}{3}}$ (up to 70%)

Spectral regimes in Synchrotron Emission

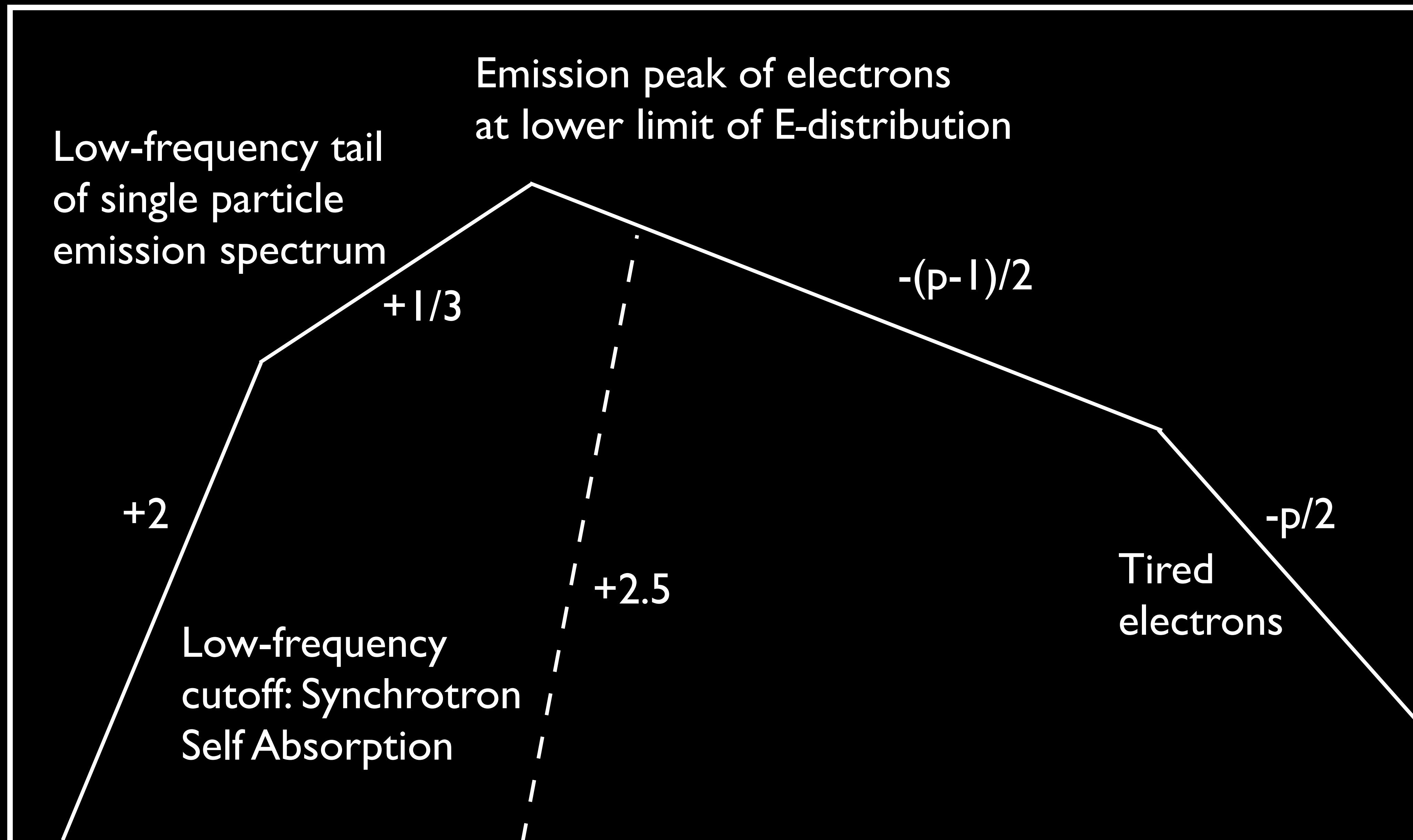

Jitter radiation can steepen the low-frequency cutoff:

- Low energy particles have longer duration of E-field pulse per orbit
- More affected by pitch angle scattering before pulse completion

(Medvedev 2000)

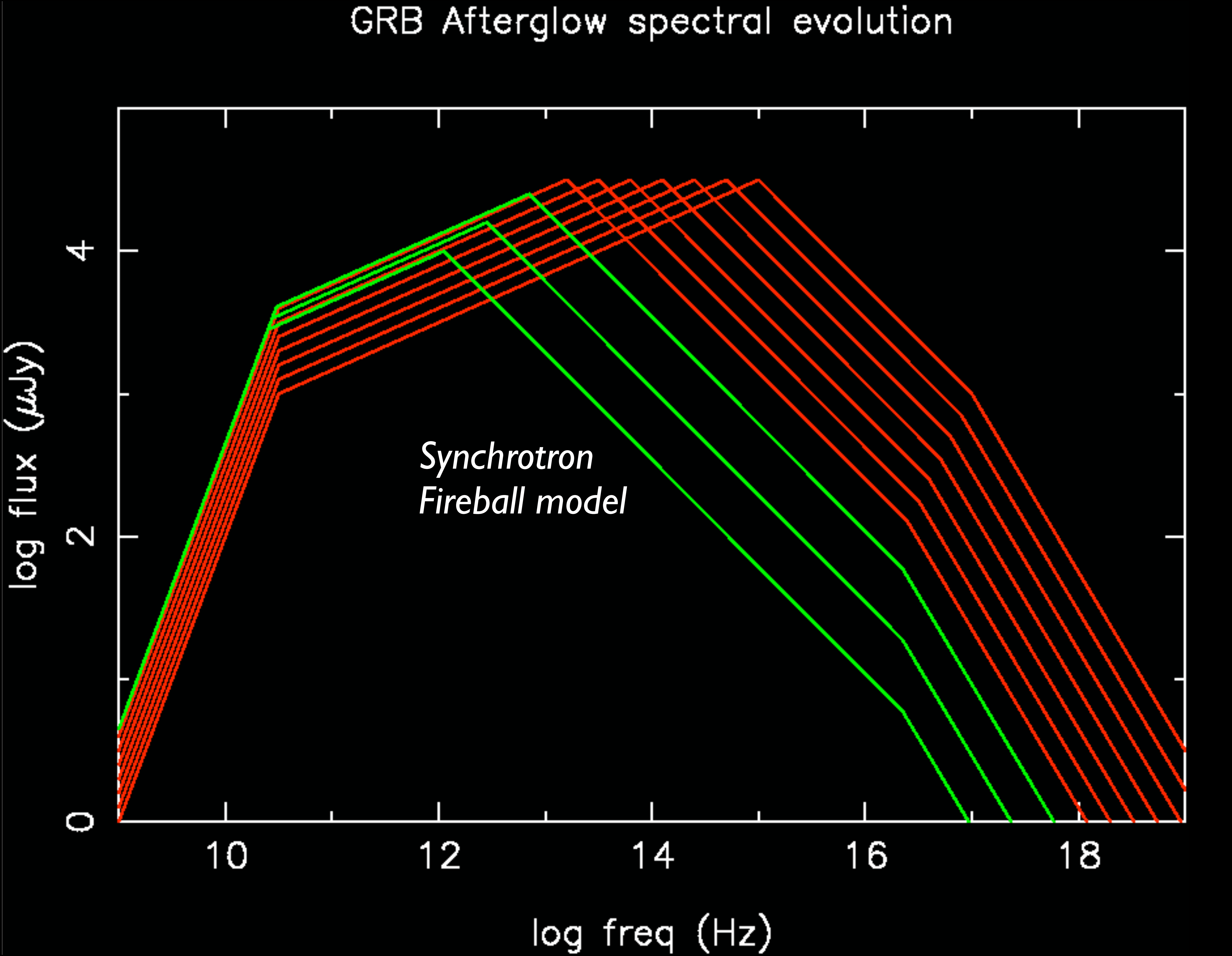
GRB Afterglow spectral evolution
log flux (μJy)
log freq (Hz)
0
2
4
10
12
14
16
18
Synchrotron
Fireball model

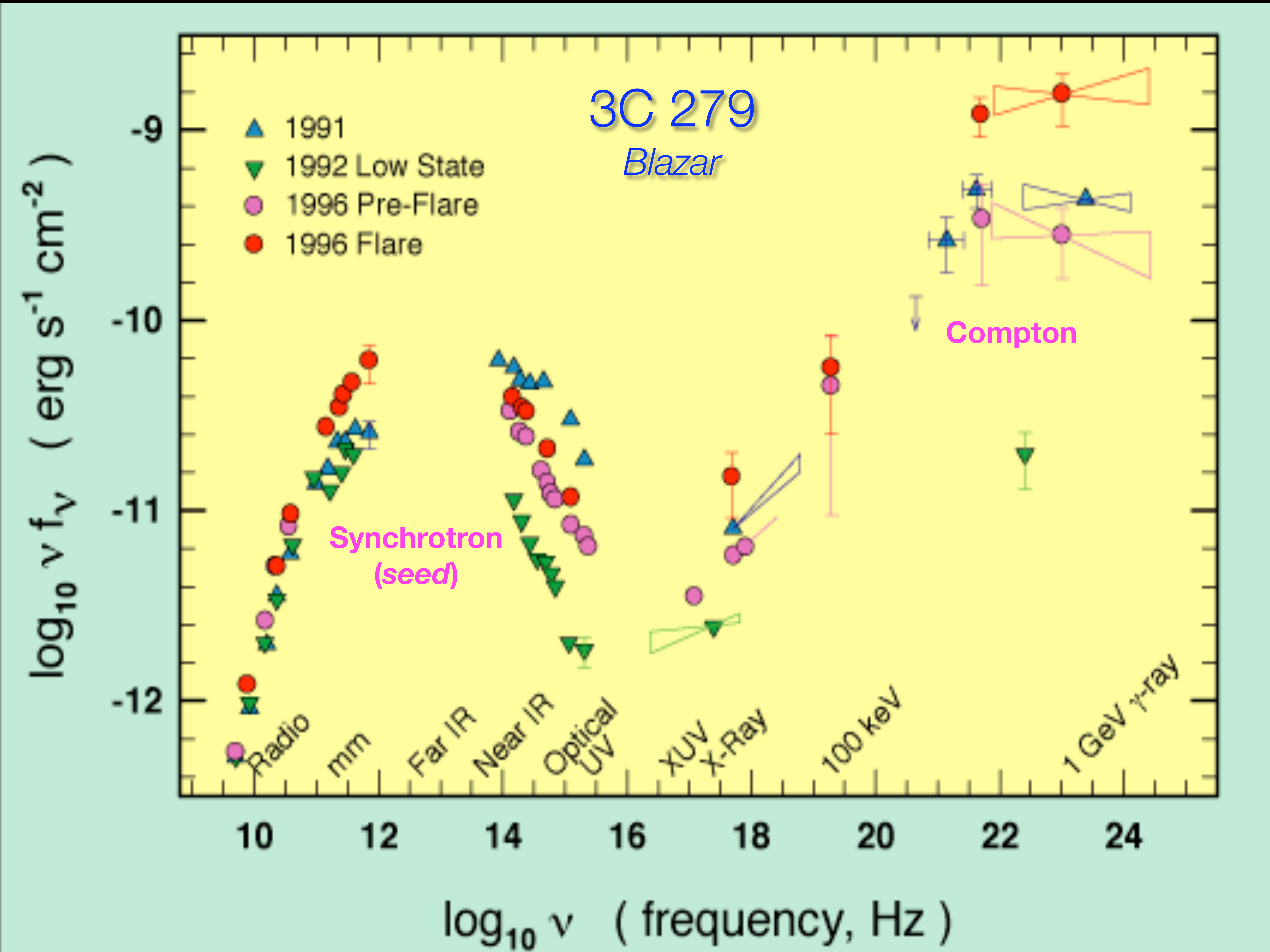

3C 279
Blazar
1991
1992 Low State
1996 Pre-Flare
1996 Flare
Synchrotron
(seed)
Compton
Radio
mm
Far IR
Near IR
Optical
UV
XUV
X-Ray
100 keV
1 GeV γ-ray
-9
-10
-11
-12
10
12
14
16
18
20
22
24
log10 ν fν (erg s-1 cm-2)
log10 ν (frequency, Hz)

What is emitted is not what we see

Radiation is modified during propagation through matter

Plasma effects

Dispersion

$$\frac{v_{\mathrm{ph}}}{c} = \left(1 - \frac{\omega_{\mathrm{p}}^2}{\omega^2}\right)^{-1/2}$$

In magnetic field,
Faraday Rotation

$$\left(\frac{v_{\mathrm{ph}}}{c}\right)_{\mathrm{R,L}} = \left(1 - \frac{\omega_{\mathrm{p}}^2}{\omega(\omega \pm \omega_B)}\right)^{-1/2}$$

Dust Extinction, Polarization

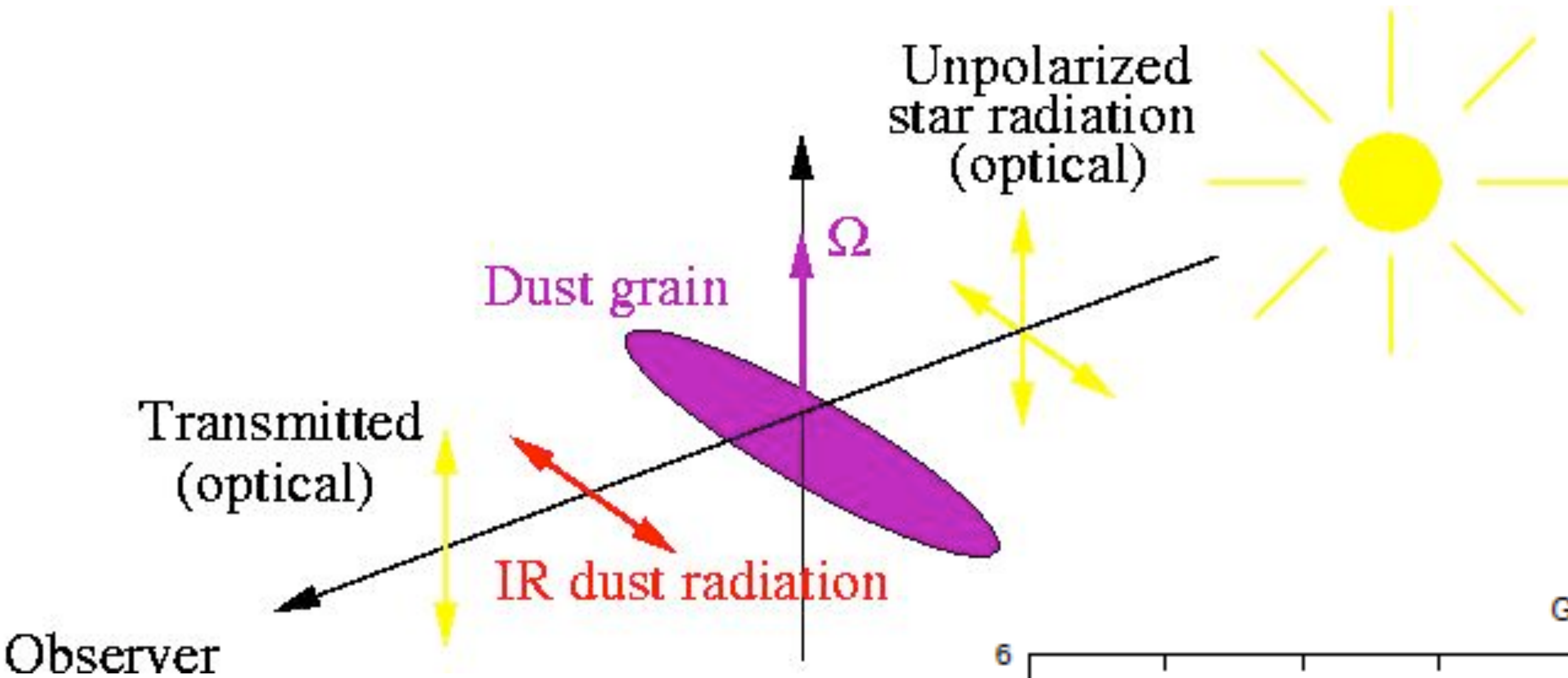

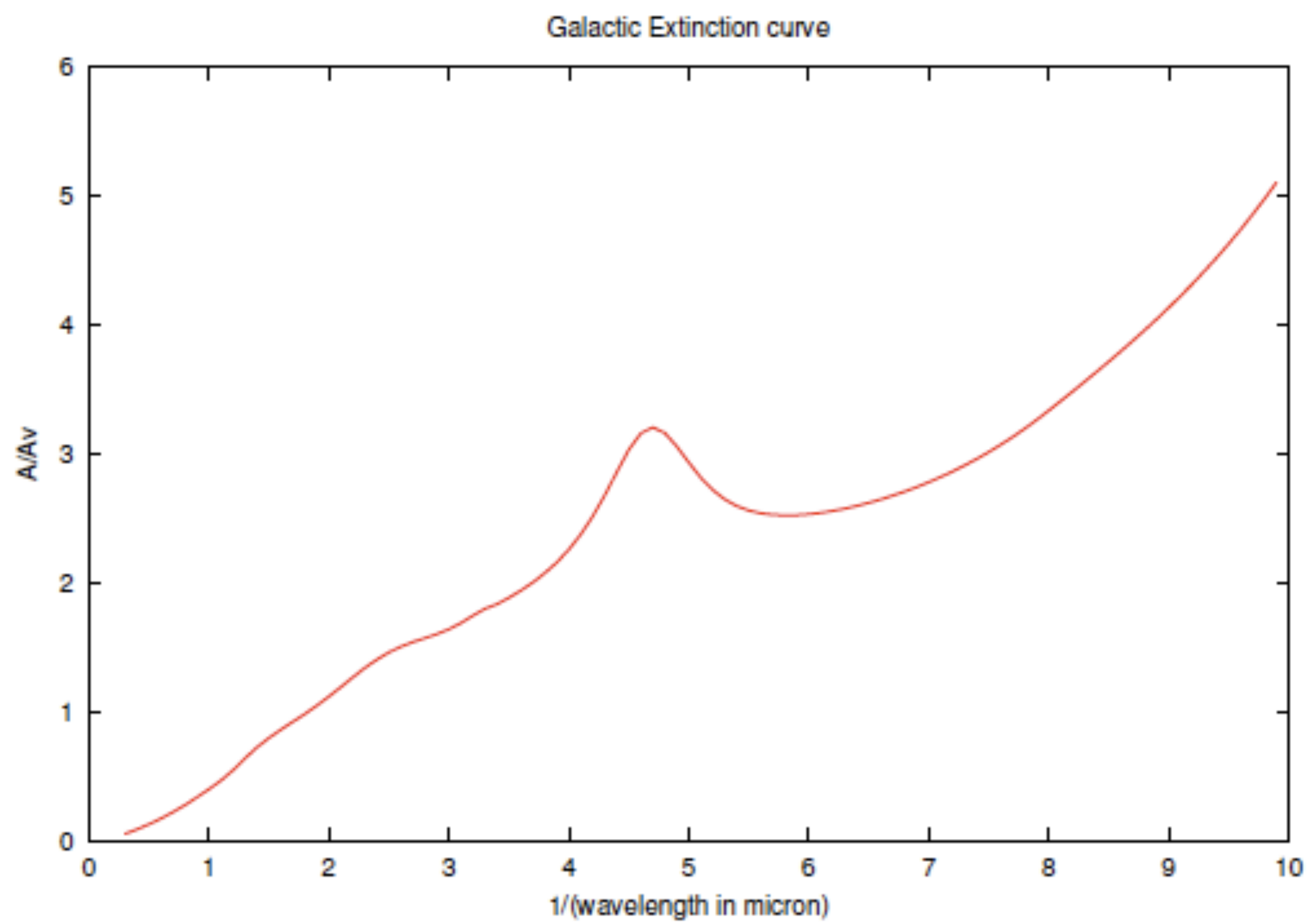

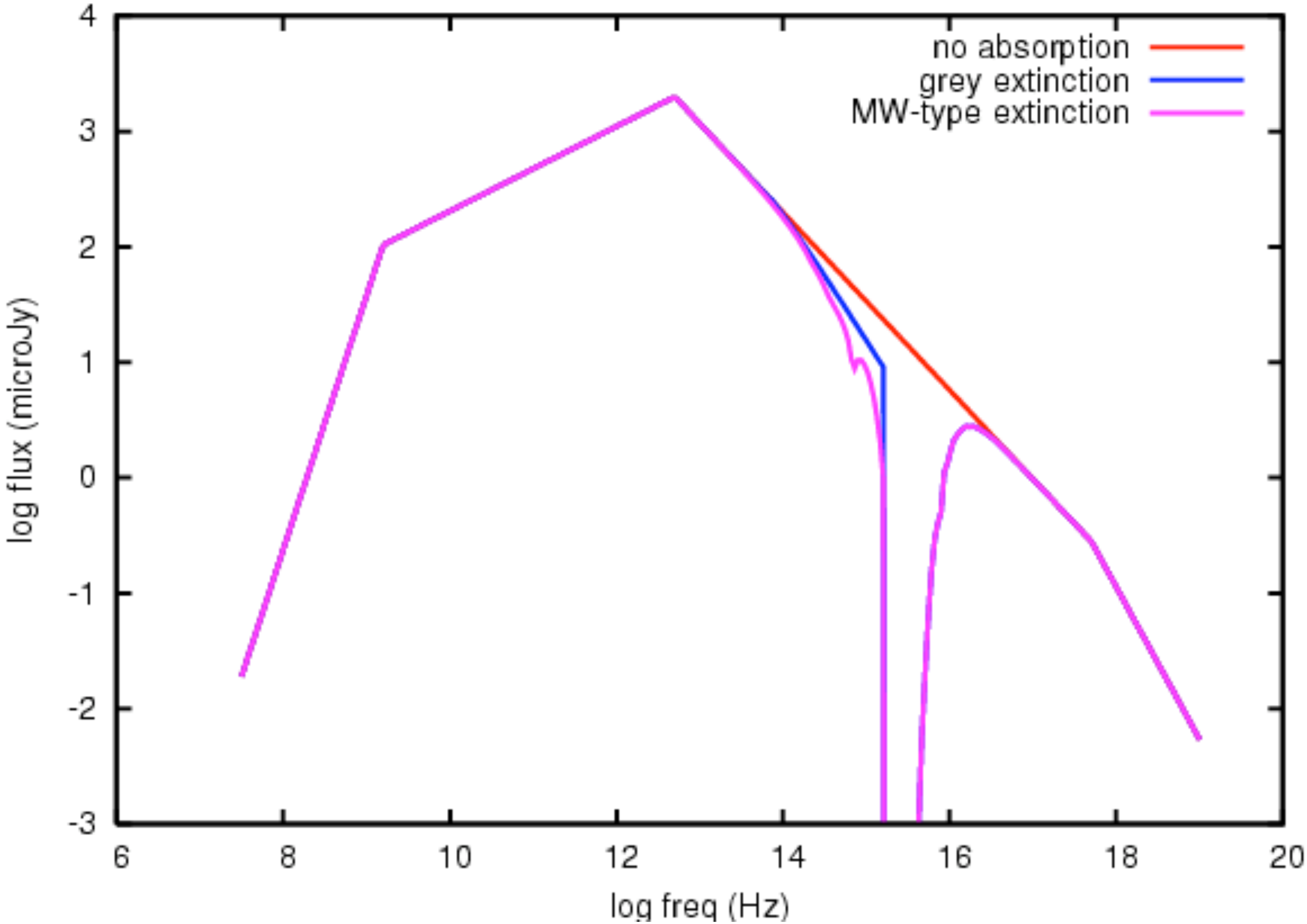

no absorption
grey extinction
MW-type extinction
log flux (microJy)
log freq (Hz)
4
3
2
1
0
-1
-2
-3
6
8
10
12
14
16
18
20

Absorption by the Earth's Atmosphere

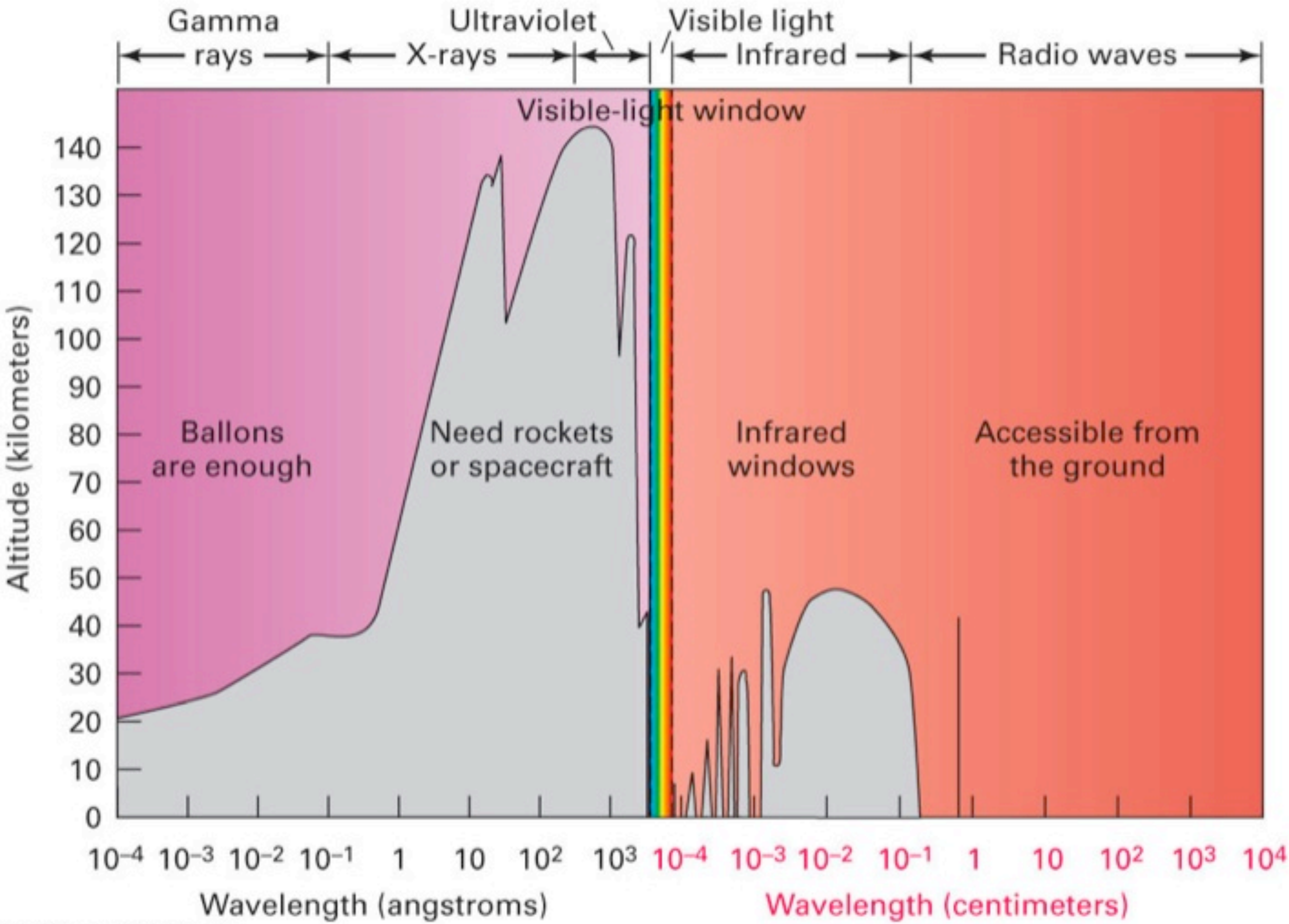

Nuclear / particle processes

Change in binding energy ➞ photon emission

- Radioactivity (e.g. Al^{26})

- Decay of heavy mesons (e.g. $\Pi^0 \rightarrow 2\gamma$)
  generated in nuclear scattering ($p + p \rightarrow \Pi^0$)

- Fusion

- Pair Annihilation

Diffuse gamma-ray emission from gal. plane

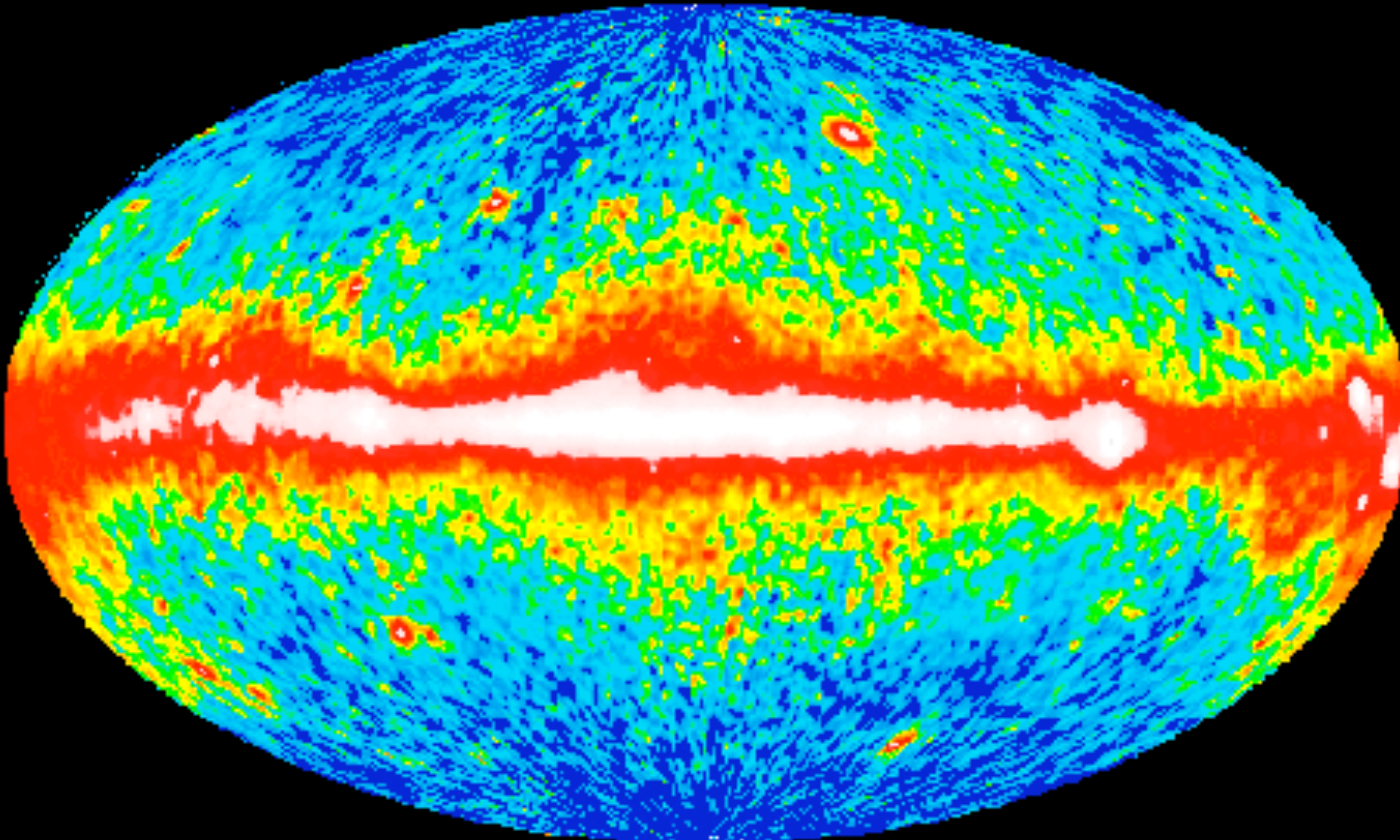

CR + gas → Π^0 → 2 γ

Pulsars

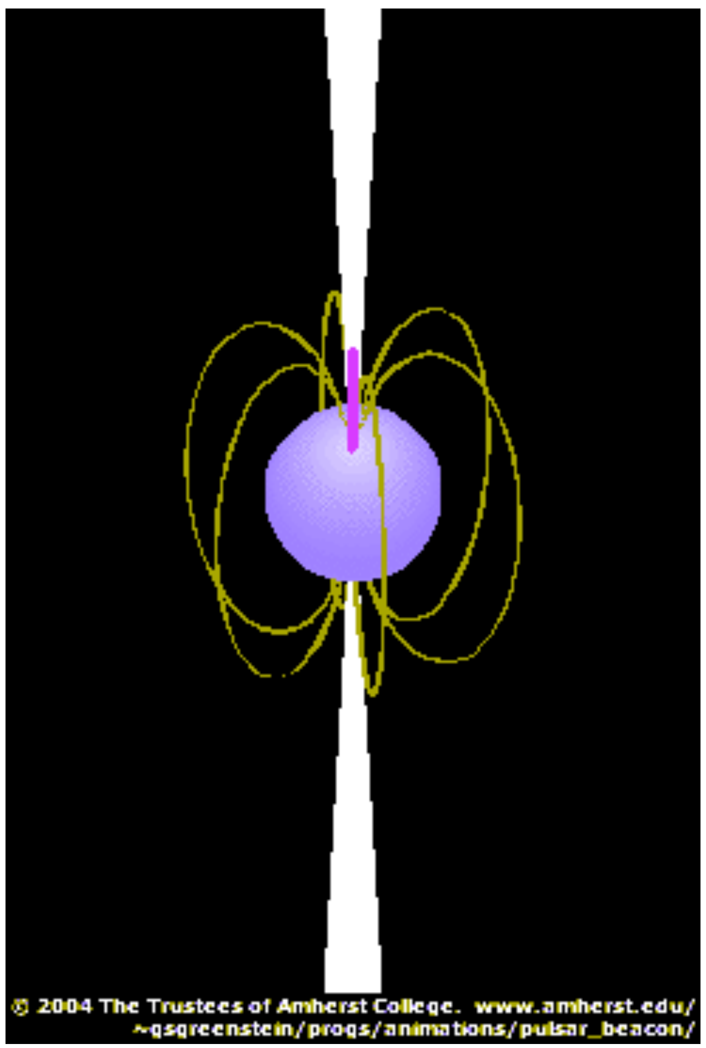
© 2004 The Trustees of Amherst College. www.amherst.edu/
~gsgreenstein/progs/animations/pulsar_beacon/

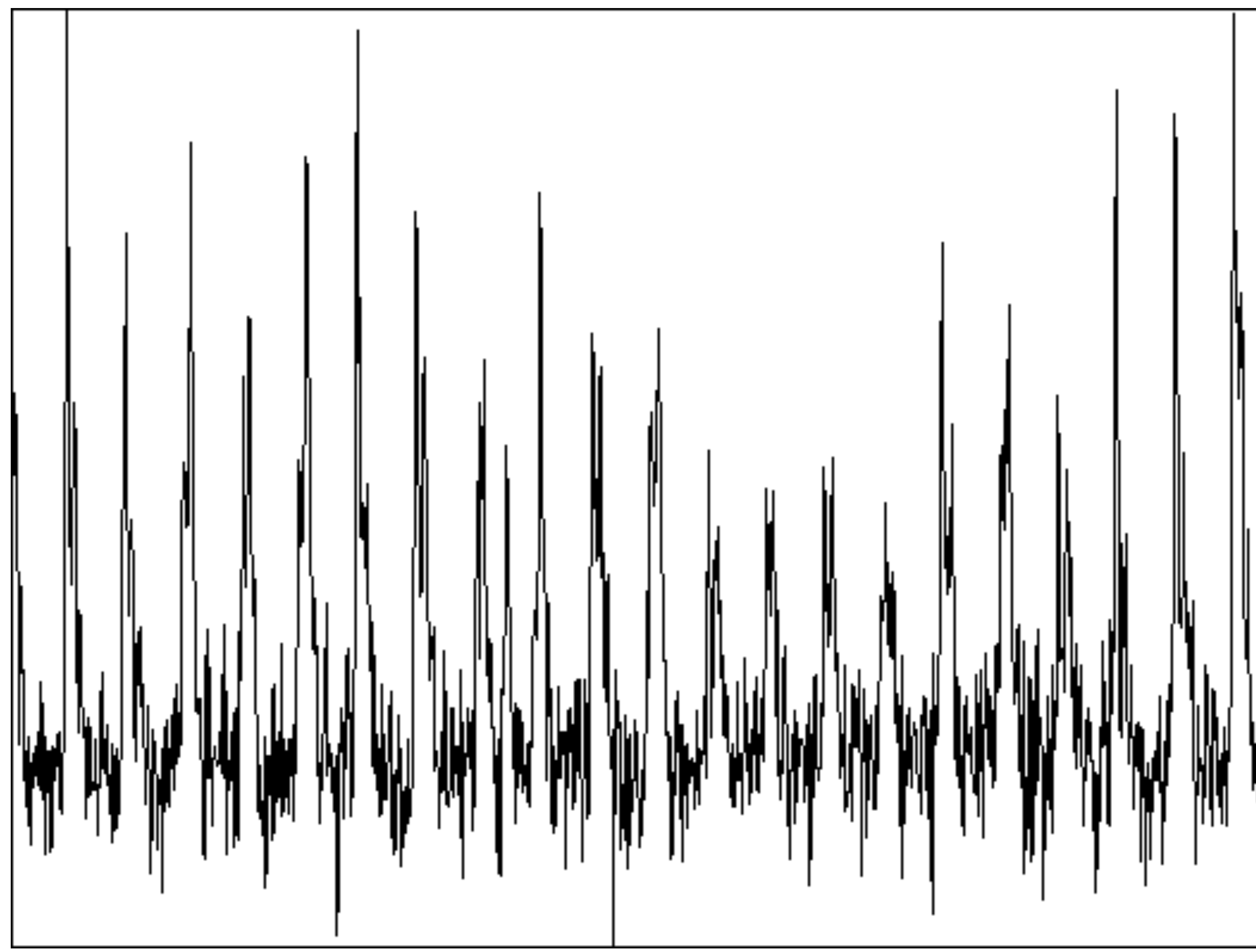

Pulsars

Non-accreting magnetized neutron stars - radiating via magnetospheric processes

Main presence at radio wavelengths (~2000)

A few dozen at higher energies.

Fermi single-handedly increased the number of gamma-ray pulsars from half a dozen to > 50. *(Abdo et al 2009)*

Surface Magnetic field ~10^8 - 10^{13} G
(Cyclotron fundamental ~ 1eV - 100 keV)

How do we know the field strength?
- Rotation-powered pulsars : spindown torque
- Accreting X-ray pulsars : cyclotron features

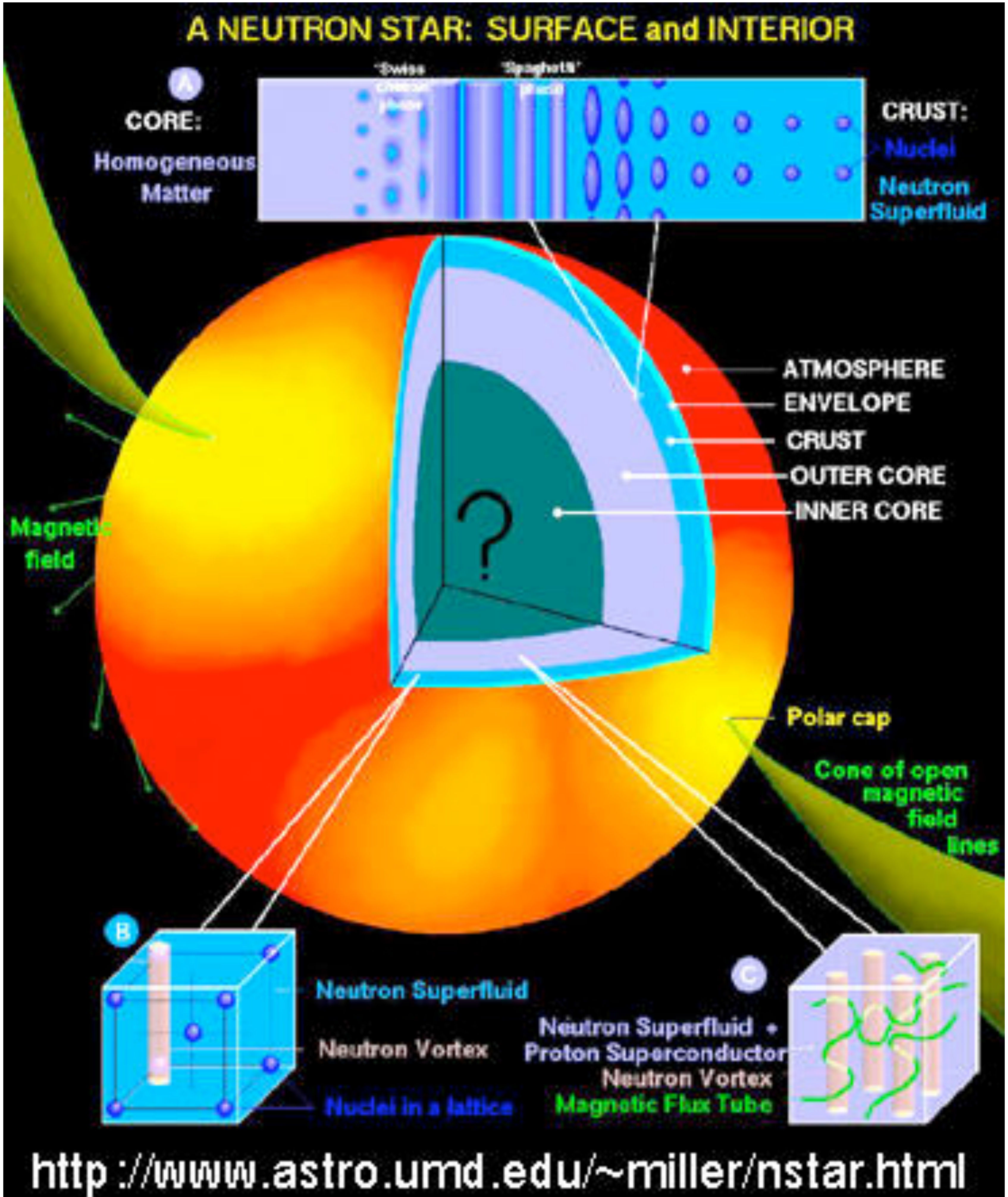

Pulsar emission is a magnetospheric phenomenon

Crab Nebula

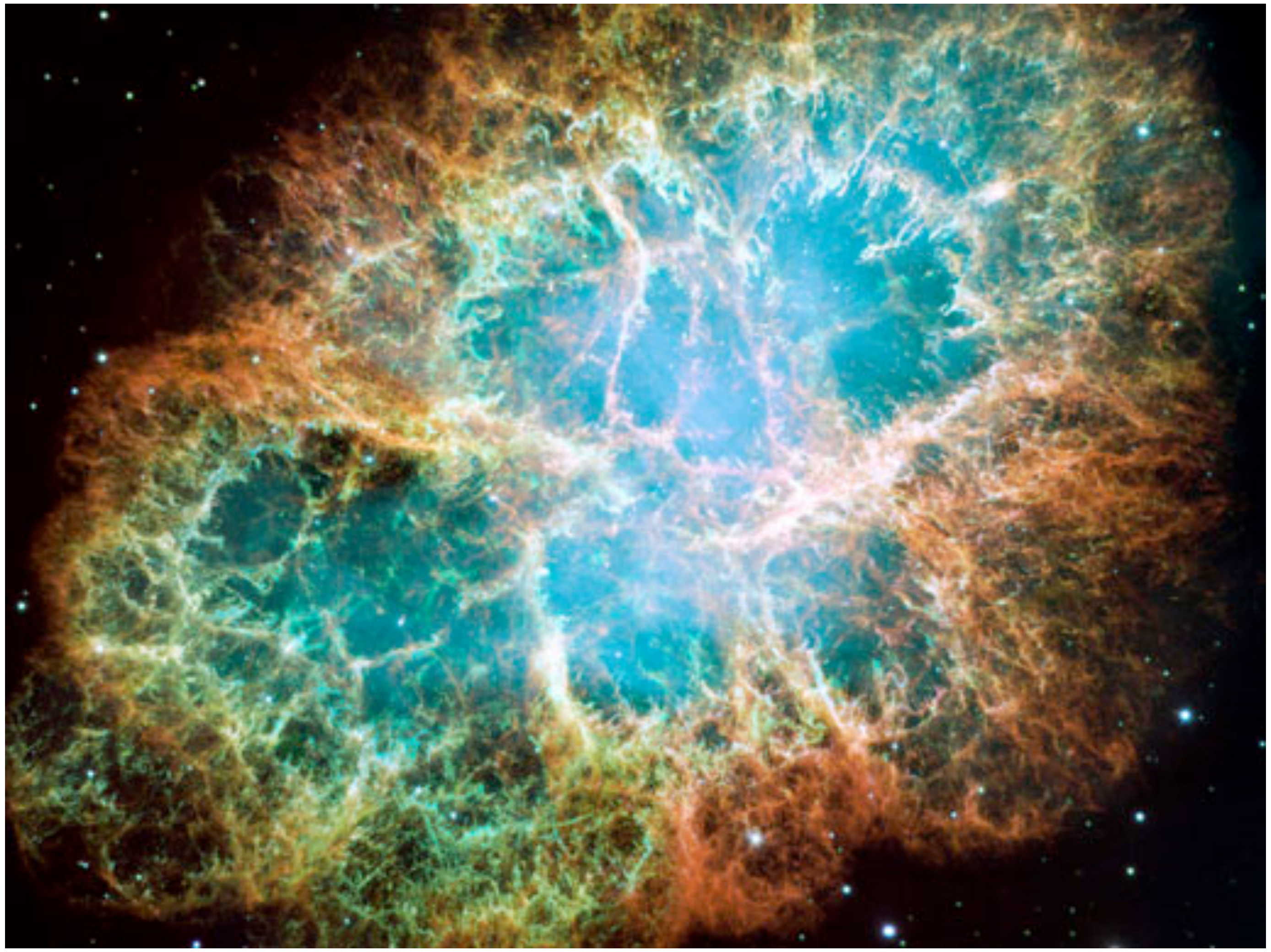

Vacuum Dipole Model

Spinning magnet generates magnetic dipole radiation

$$\textit{Radiated power} = \frac{2}{3c^3}(\ddot{m})^2 = \frac{2}{3c^3}B^2R^6\Omega^4\sin^2\alpha$$

$$= -I\Omega\dot{\Omega} \quad \textit{(Rate of loss of rotational energy)}$$

Yields $B^2 \propto P\dot{P}$

Measurement of spindown rate helps estimate *B*

$$B_{12} = \sqrt{P_{\rm s}\dot{P}_{-15}}$$

Age: ~ $P/\dot{P}$ young objects often found in SNRs

Pulsar P-Pdot diagram

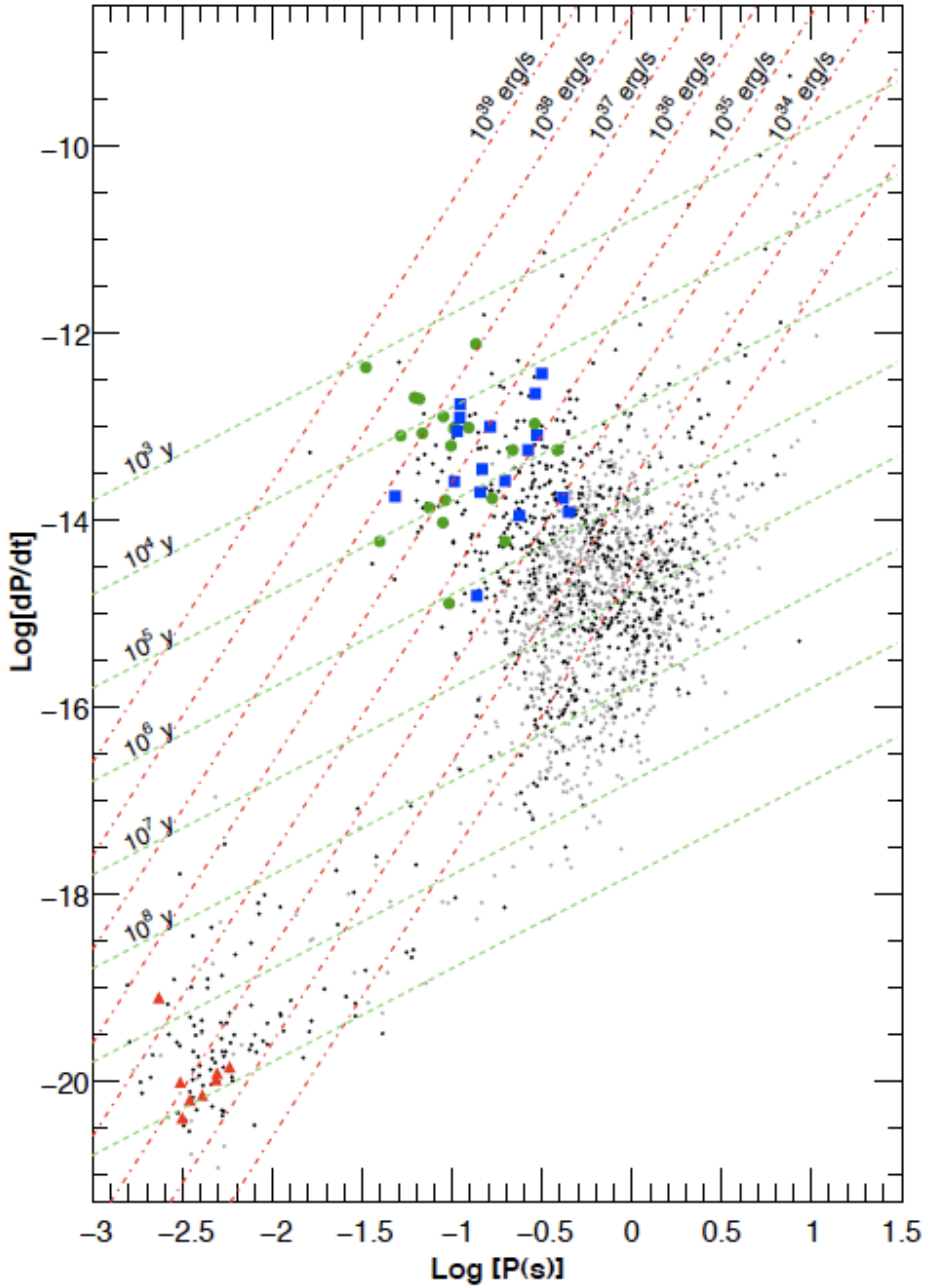

Coloured Dots are gamma-ray pulsars

(Abdo et al 2009)

Spin period-Magnetic field distribution of observed Pulsars

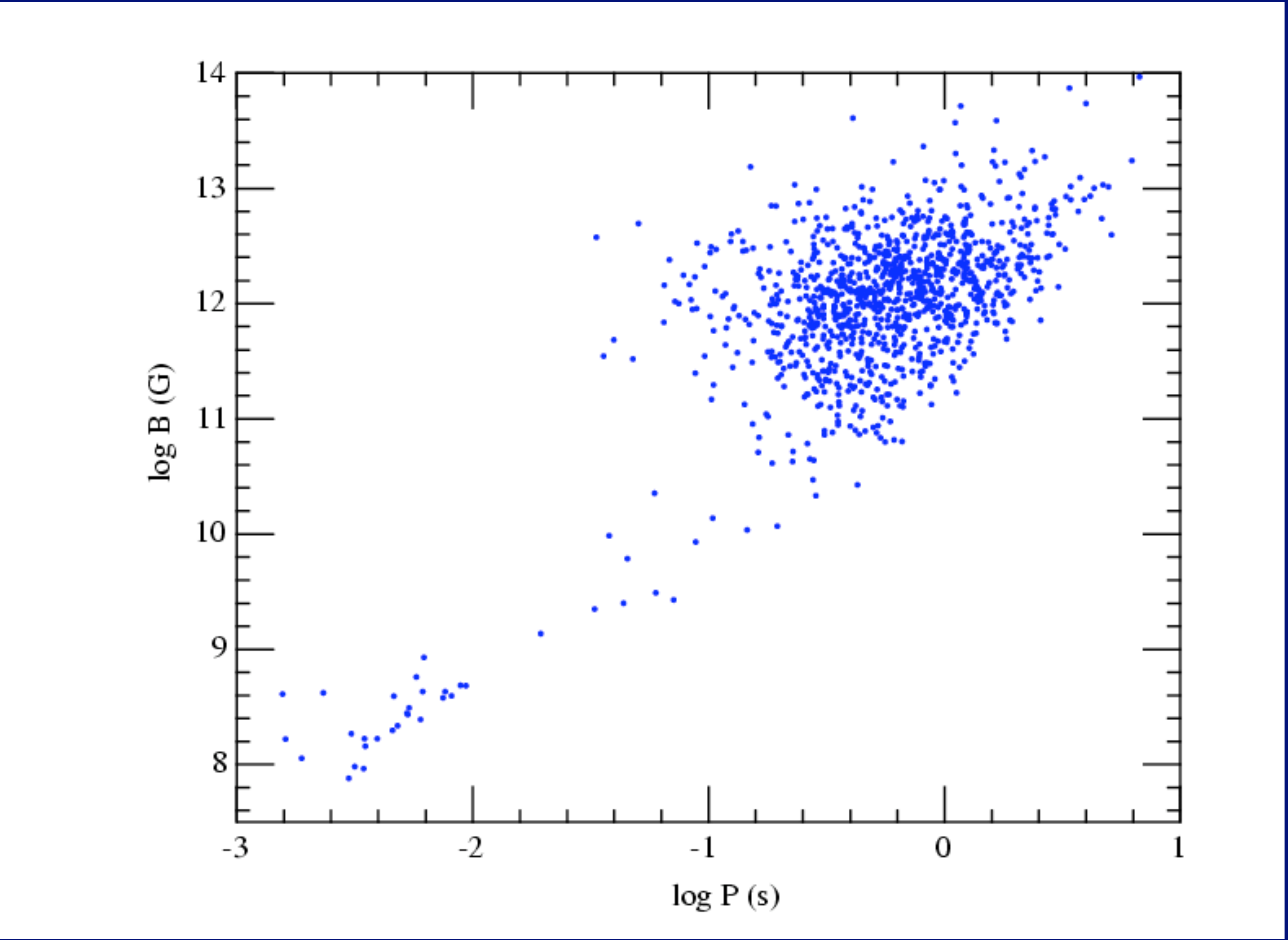

Spin period-Magnetic field distribution of observed Pulsars

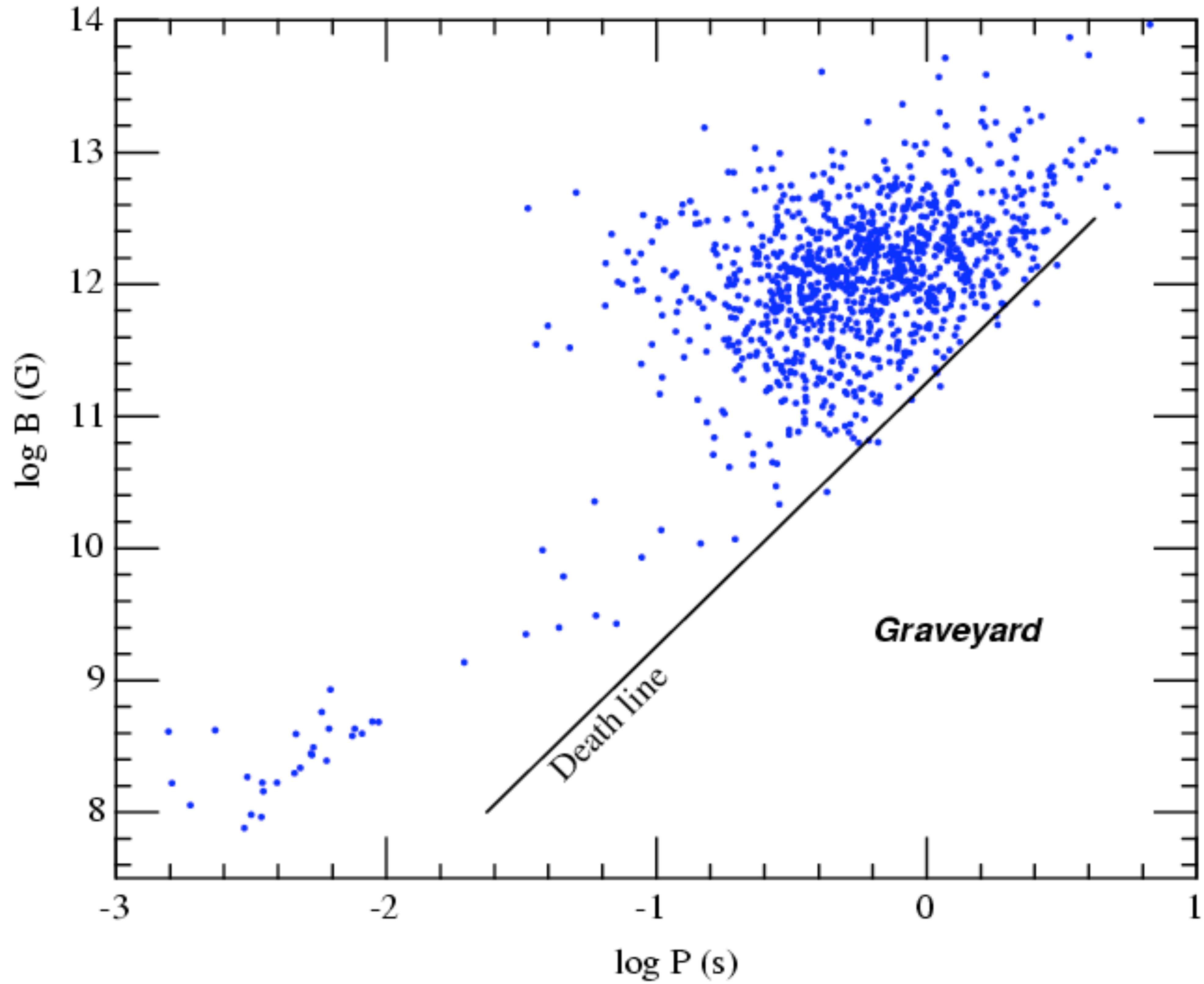

The Pulsar Magnetosphere

Basic concepts: Goldreich & Julian 1969

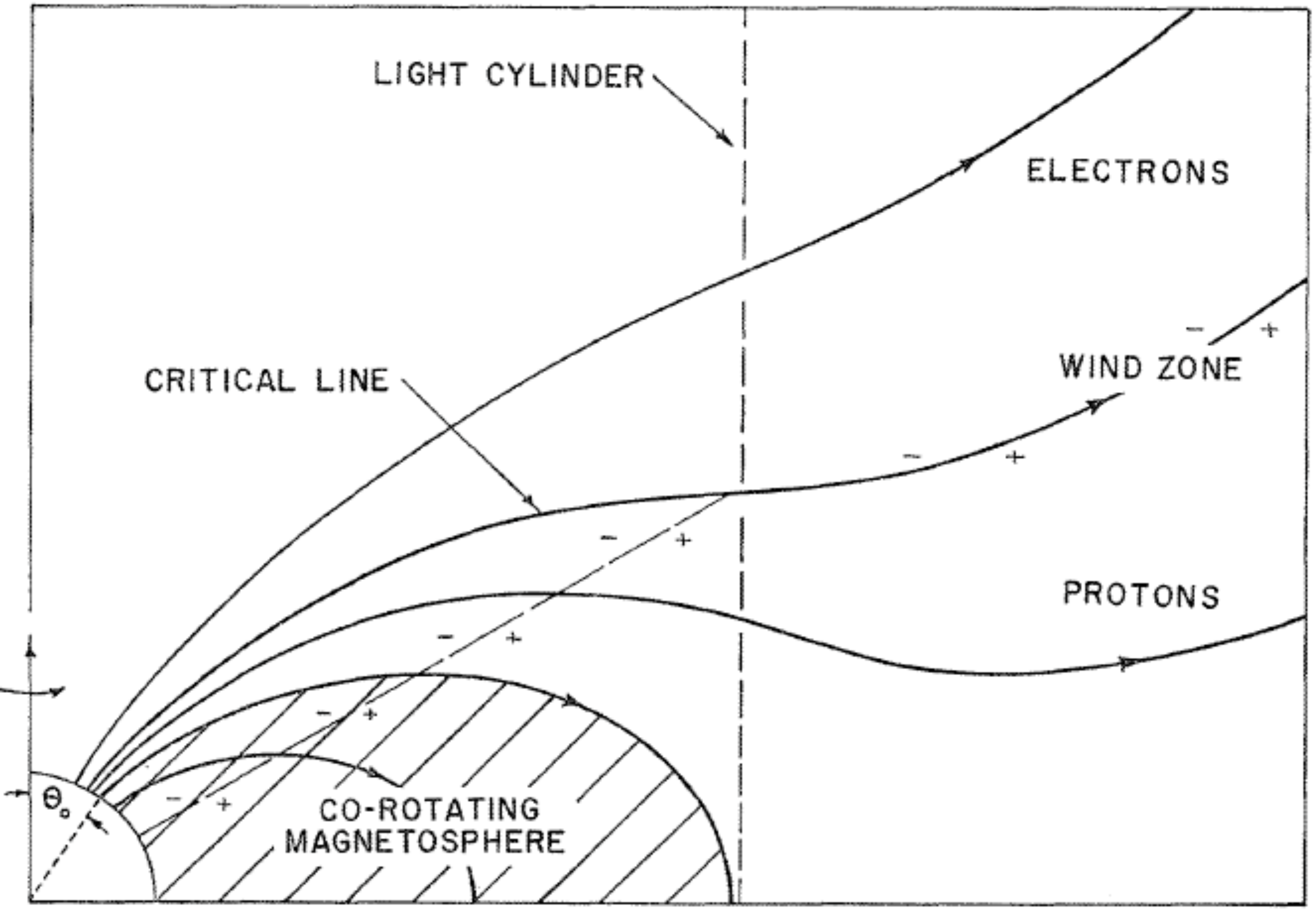

- A vacuum exterior would have potential drop exceeding 10^{15} V
- Space charge must exist, $\boldsymbol{E}\cdot\boldsymbol{B}=0$
- Co-rotating magnetosphere can be maintained up to the light cylinder, $\rho \simeq -\boldsymbol{\Omega}\cdot\boldsymbol{B}/2\pi c$
- With pair production, no. density of charged particles may far exceed ρ
- ρ passes through 0 and changes sign in the magnetosphere

Plasma on open field lines cannot co-rotate. Current flows out along these lines, creates toroidal mag. field which provides the dipole spin-down torque.

A charge-starved gap is likely on the null ρ surface at the boundary of the closed magnetosphere: The Outer Gap (Cheng et al 86, Romani 94)

Force-free magnetosphere

(Spitkovsky 2006)

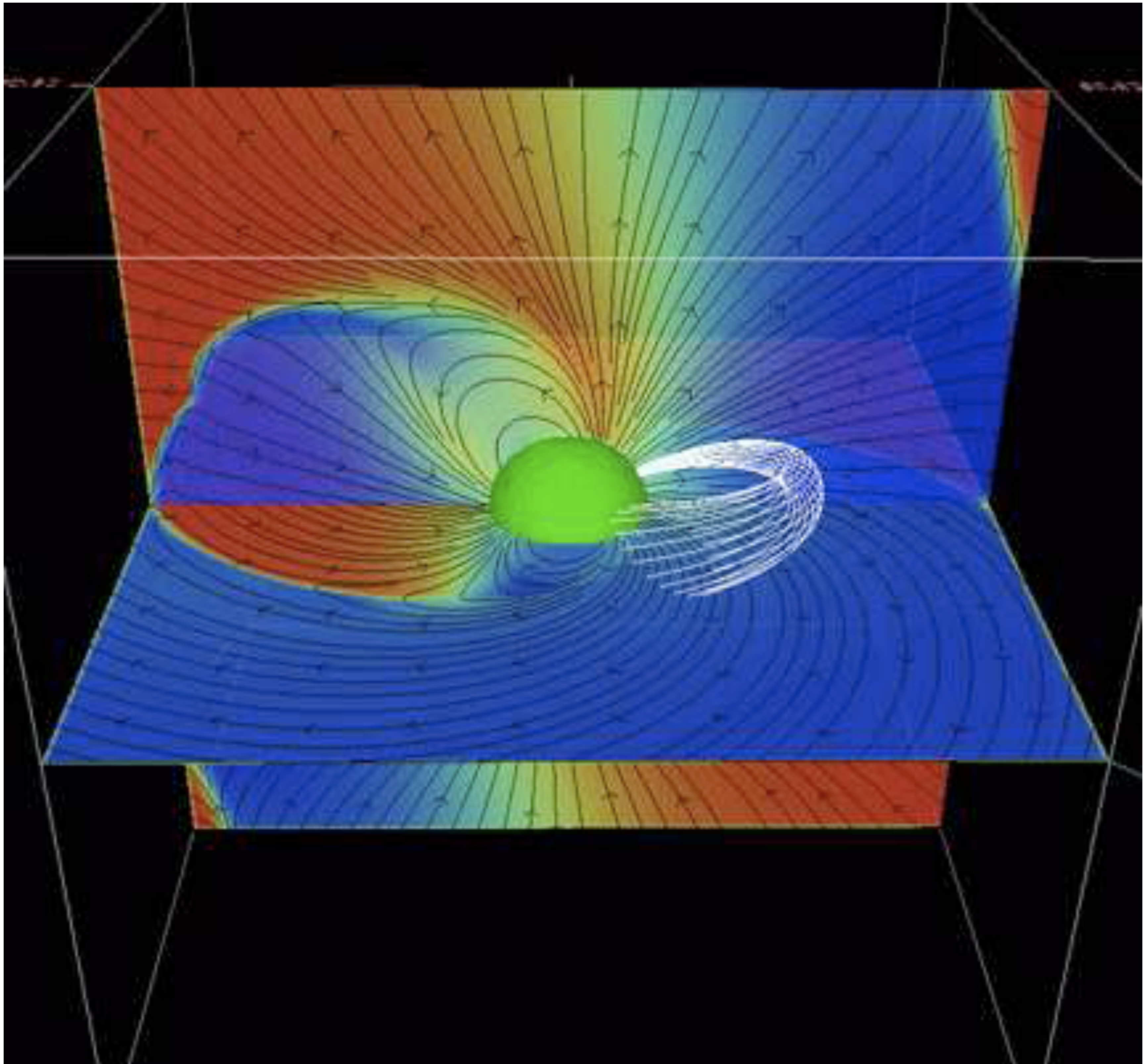

$\rho\boldsymbol{E} + (\boldsymbol{j}\times\boldsymbol{B})/c = 0$
everywhere

poor approximation near LC, current sheets

Radio Pulsar emission phenomenology

- Sharp pulses, low duty cycle : *strong beaming*
- High Brightness Temp (~10^{20} K) : *coherent emission* [Radio only]
- Frequency-dependent pulse width : *radius-to-frequency mapping*
- Strong linear polarization with S-pattern position-angle sweep : *curvature radiation, rotating vector model*
- Strong pulse-to-pulse variation but stable average profile : *stochastic phenomena within a geometric envelope*
- Drifting subpulses : *rotating carousel of sparks,* ***E****x***B** *drift*

Complications:
Cone-core dichotomy, Orthogonal polarization modes, Multiple comp., Mode changes, Nulling, non-RVM pol sweep, circular pol......

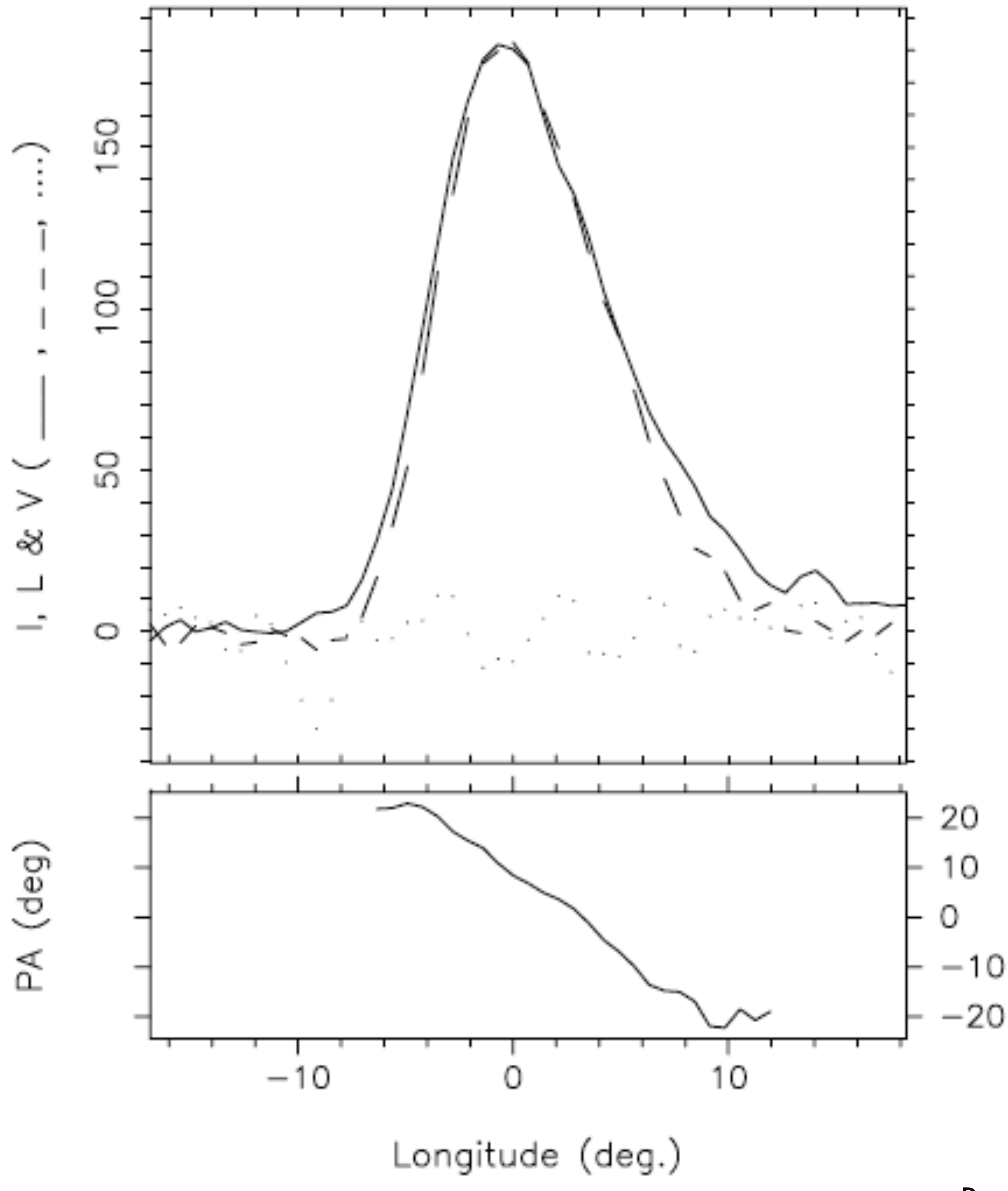

Ramkumar & Deshpande 2001

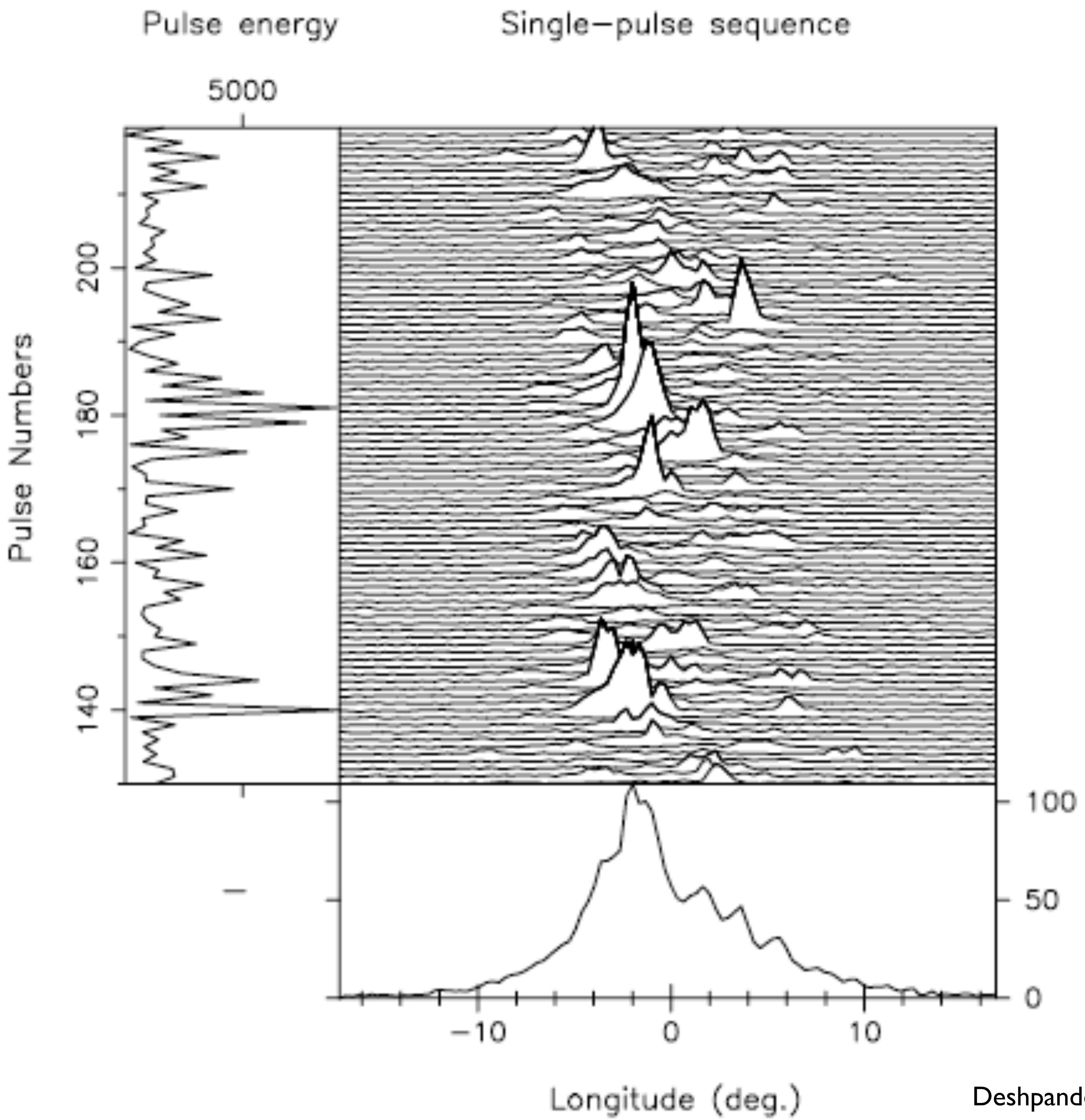

Deshpande & Rankin 99

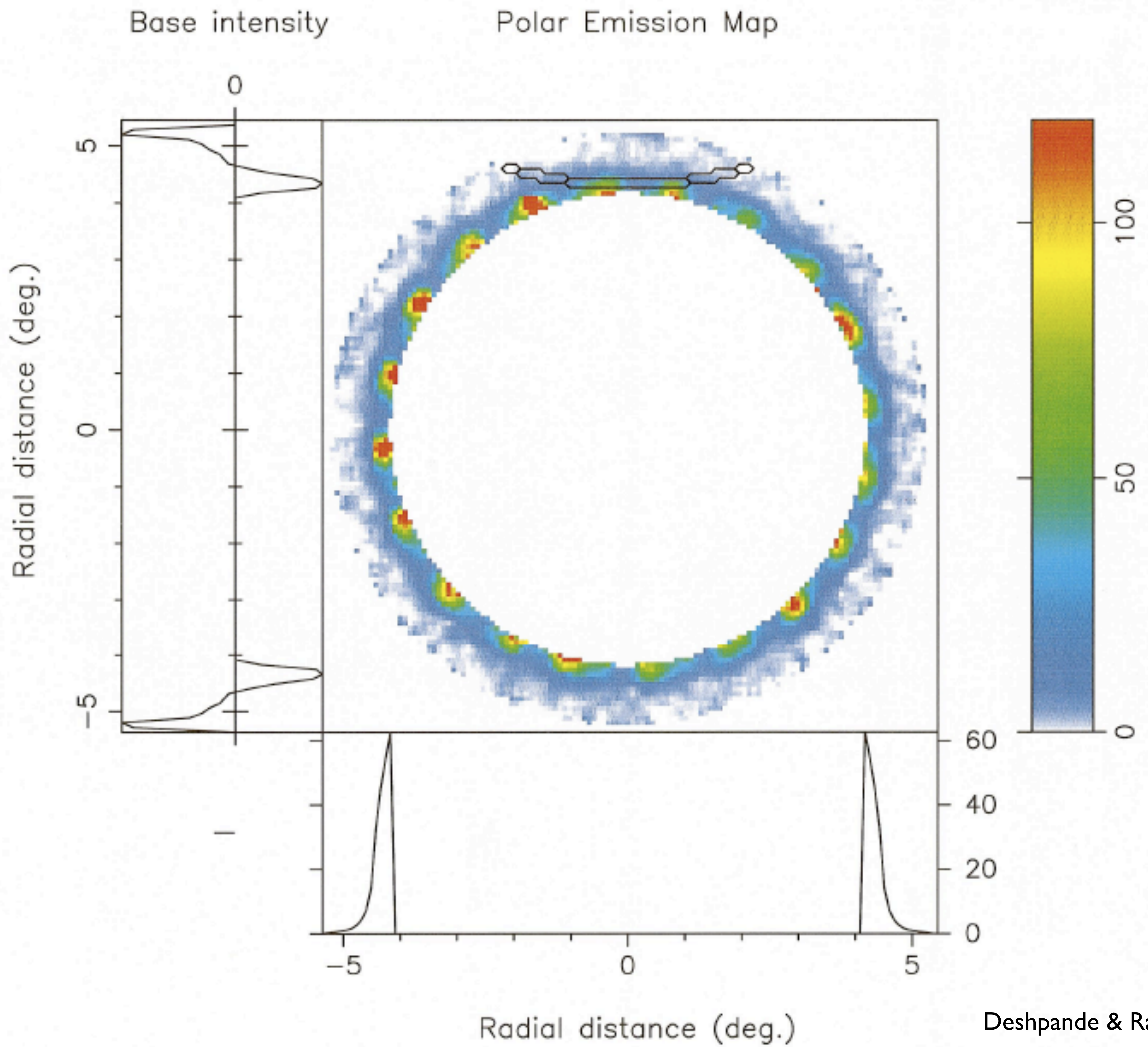

Deshpande & Rankin 99

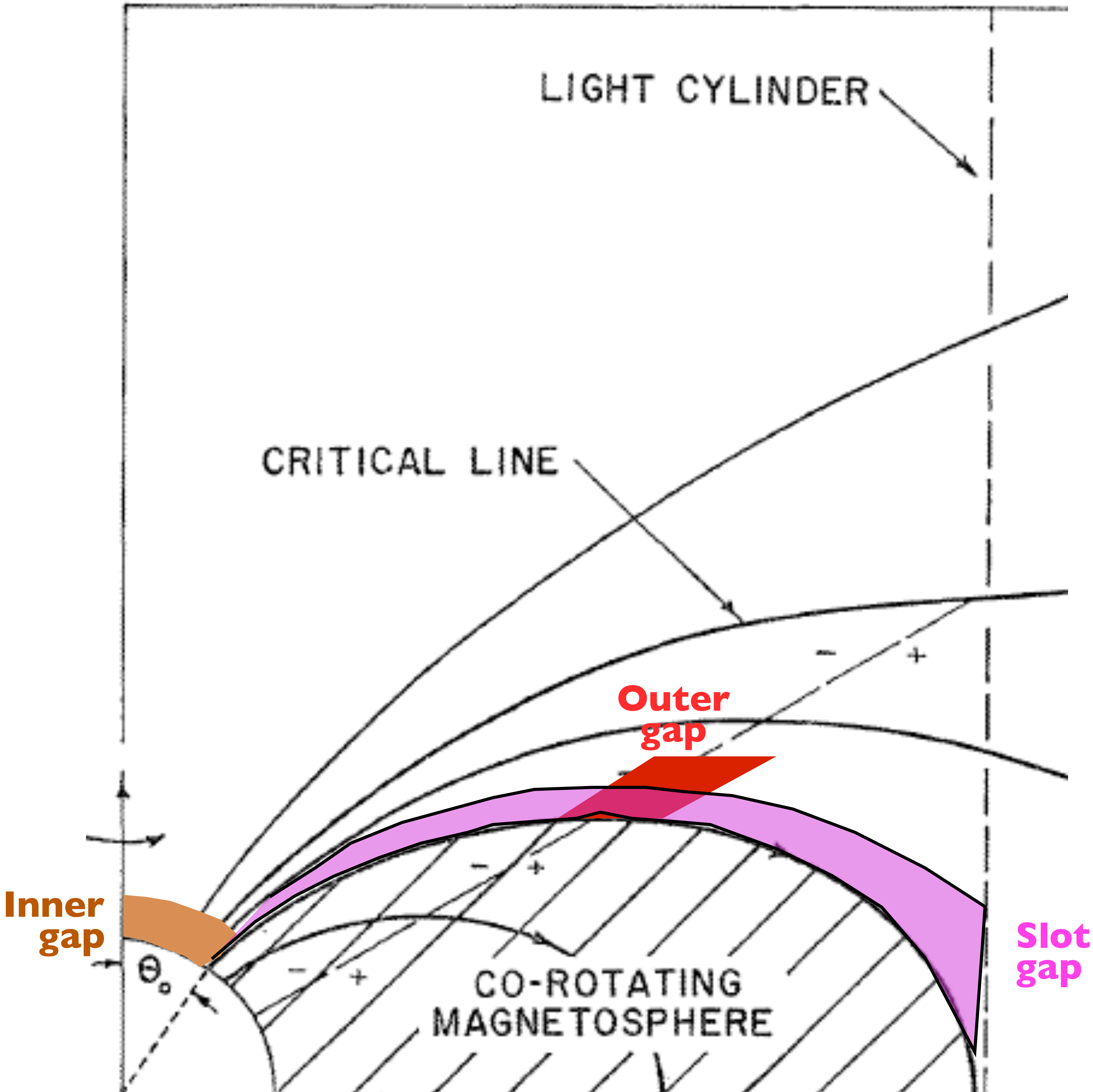

LIGHT CYLINDER
CRITICAL LINE
Outer gap
Inner gap
Slot gap
Θ_o
CO-ROTATING MAGNETOSPHERE

Outer gap modelling of gamma ray pulsation: (*Romani et al 1992.....*)

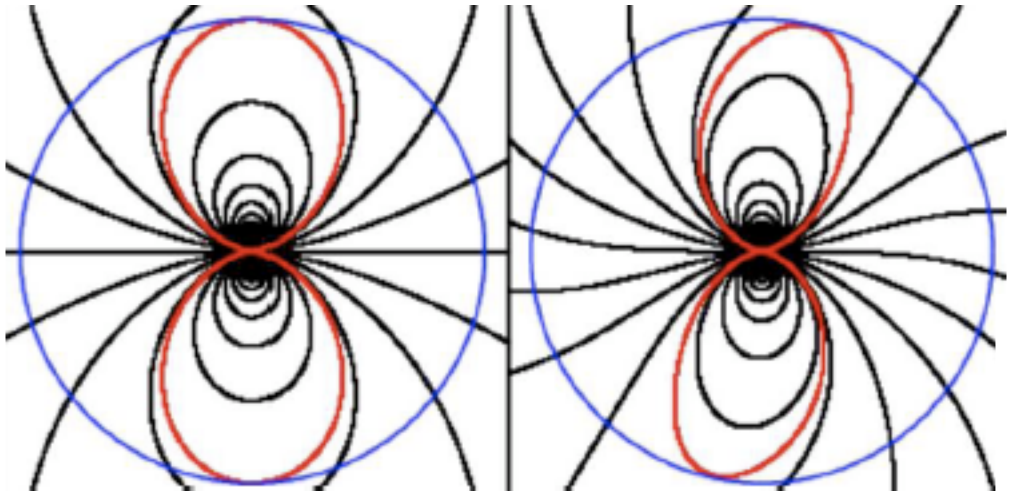

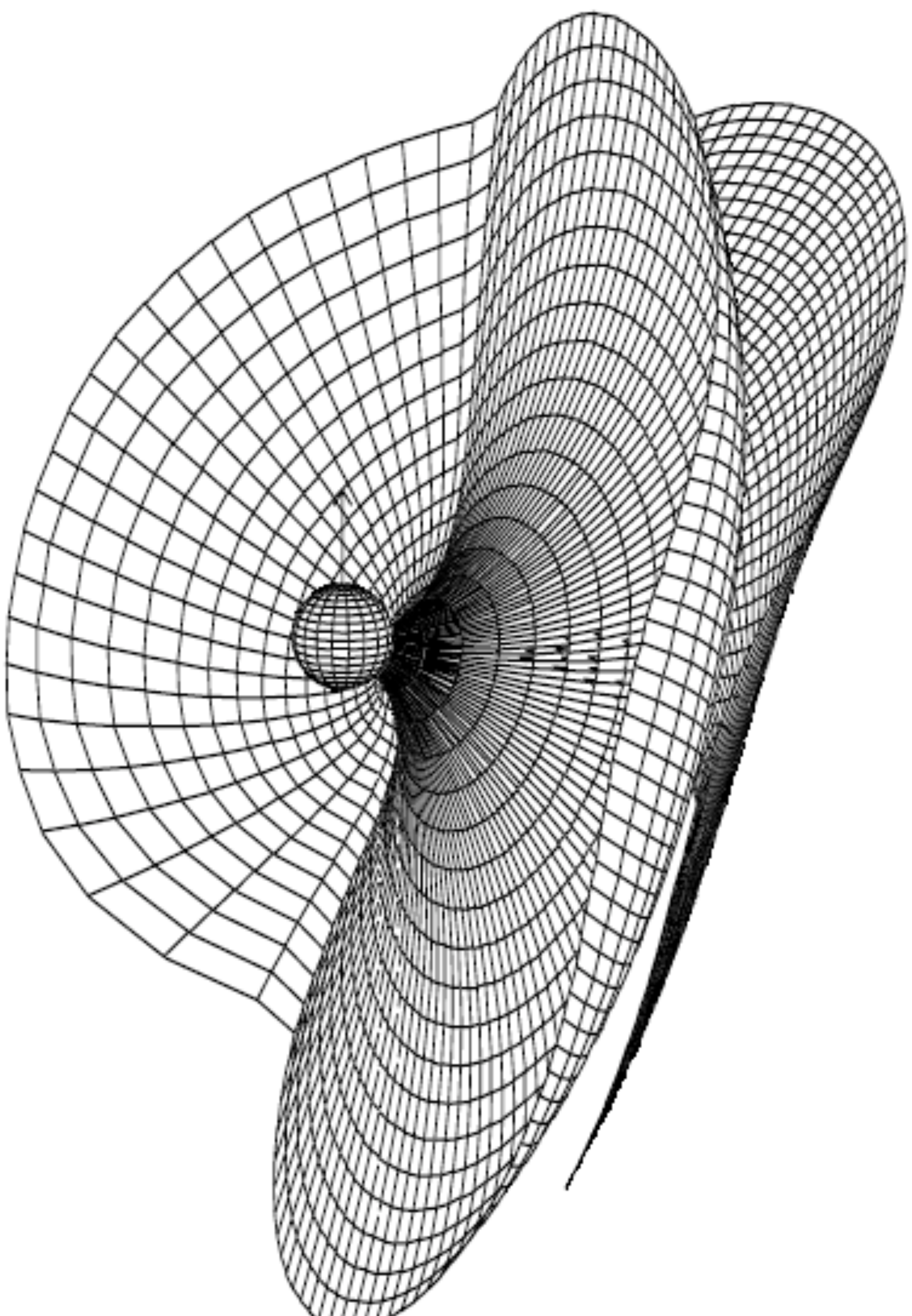

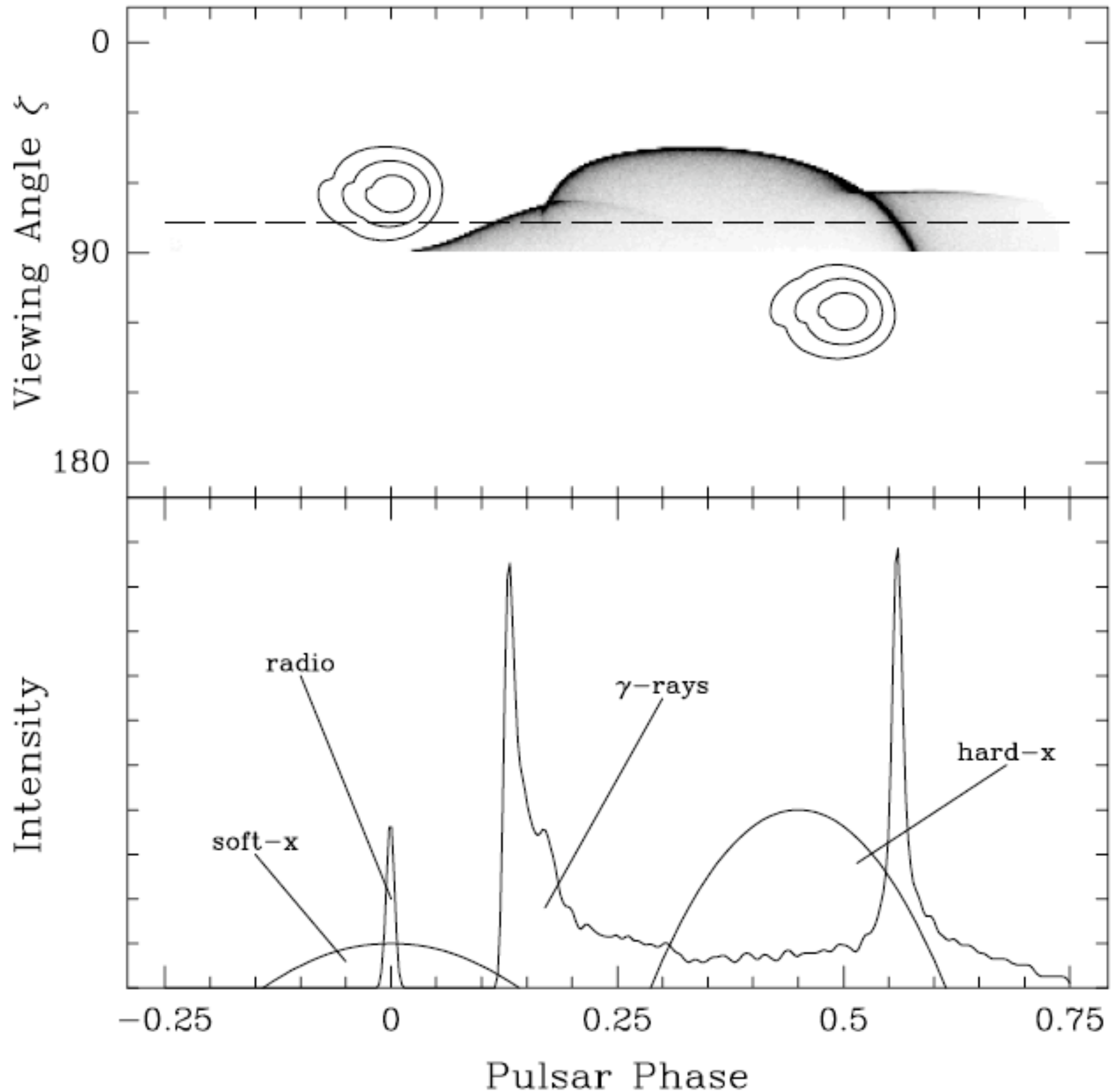

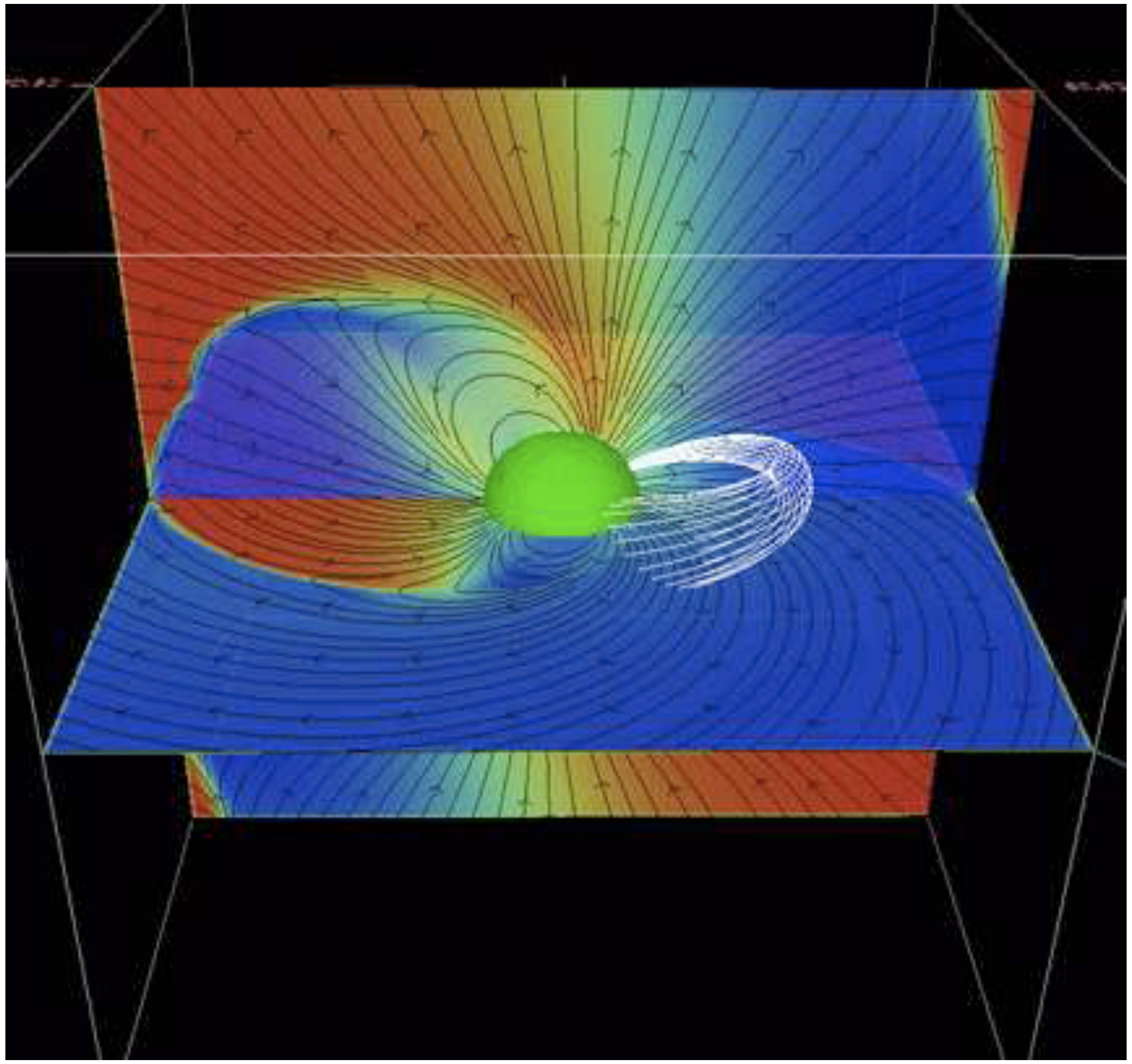

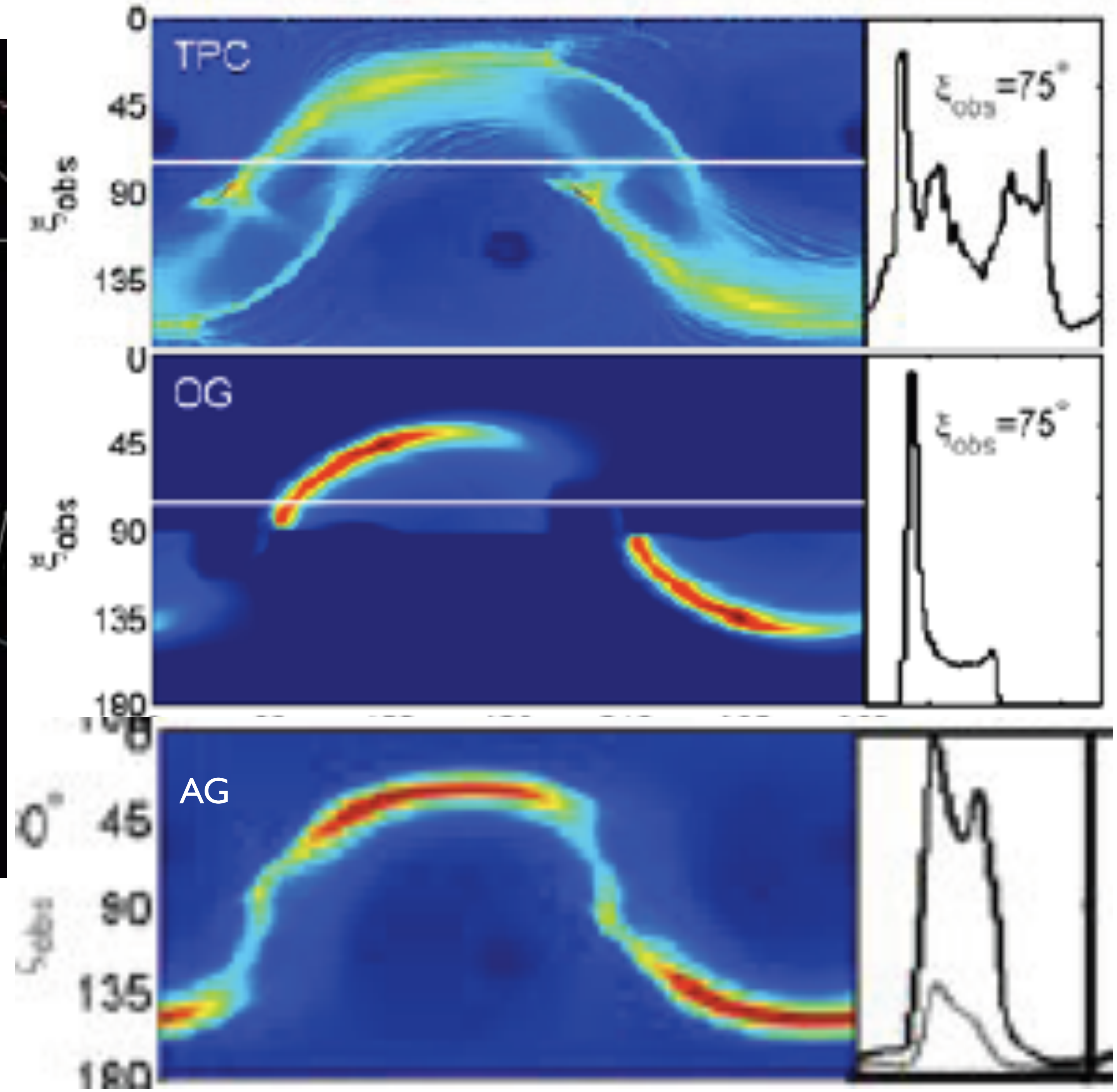

Placing an “Annular Gap” at Current Sheets in FF magnetosphere solution
(*Bai and Spitkovsky 2009*)

Pulse modelling slot-gap vs outer gap

(*Romani & Watters 2010*)

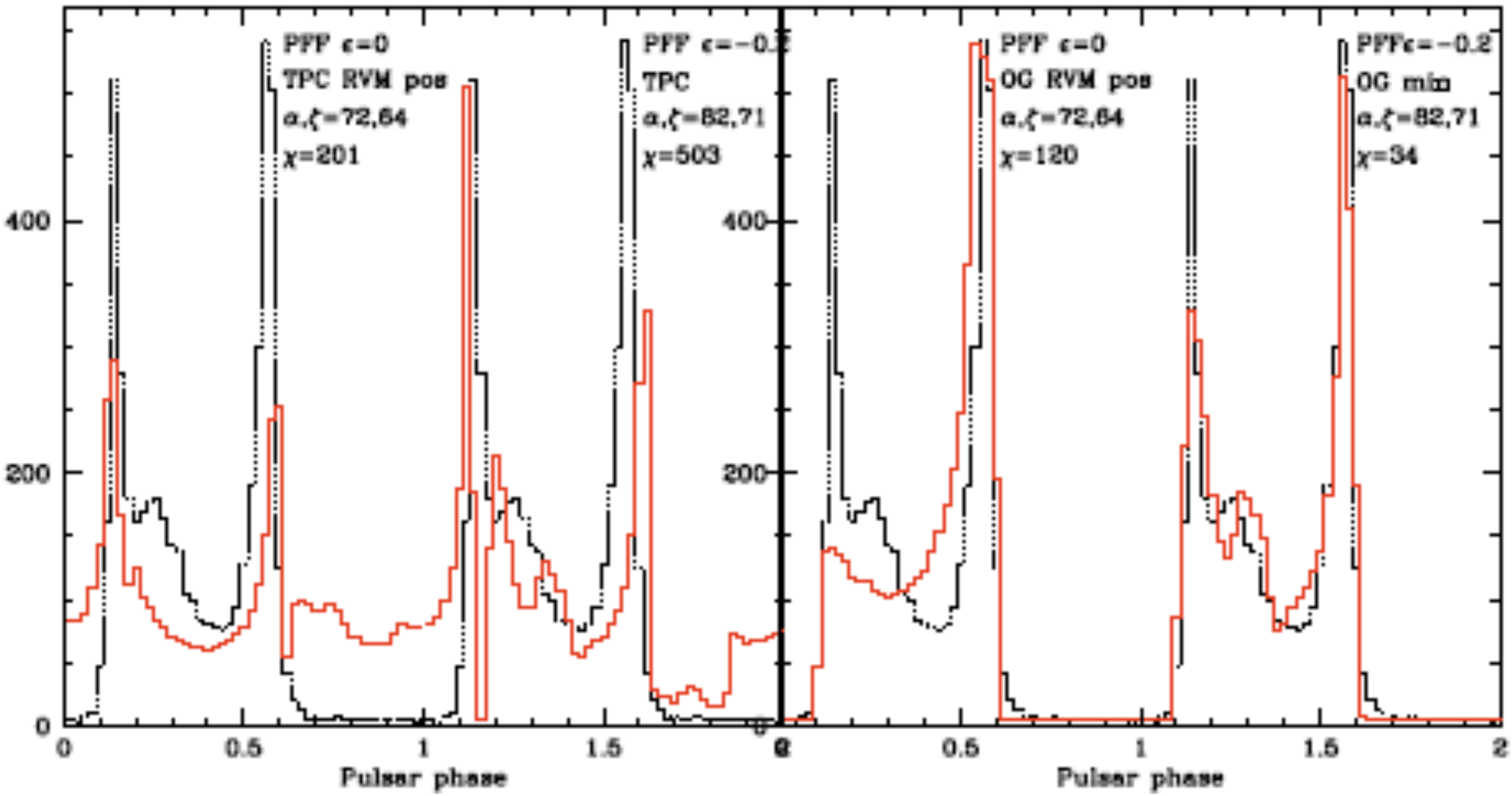

Vela Pulsar Fermi obs (black) and model (red)

Supernova Remnants

- Sites of supernova explosions
- Ejected material interacts with surrounding matter
- Shock heating of swept up gas and ejecta: X-ray emission continuum and lines characteristic of ejected species
- Shock acceleration of relativistic particles (electrons and protons)
- Synchrotron emission from electrons : *Radio - X-rays*
- Inverse Compton and Bremsstrahlung : *X* - γ
- γ-rays also produced by interactions of relativistic protons with local gas
    * secondary pairs
    * pion production and decay

Thermodynamic variables across a shock

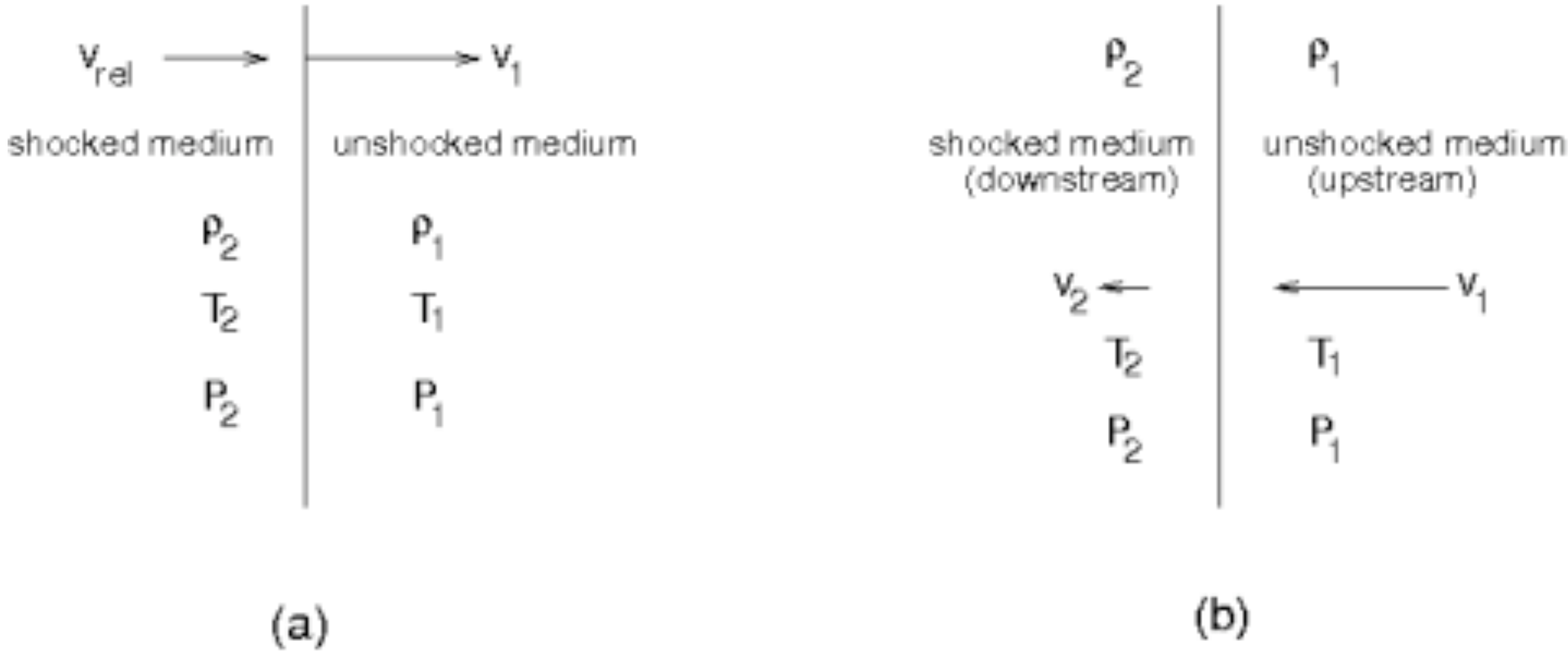

Conservation conditions:

$$
\begin{array}{lrcl}
\text{mass} & \rho_2 v_2 & = & \rho_1 v_1 \\
\text{momentum} & P_2 + \rho_2 v_2^2 & = & P_1 + \rho_1 v_1^2 \\
\text{energy} & v_2(u_2 + P_2 + \rho_2 v_2^2/2) & = & v_1(u_1 + P_1 + \rho_1 v_1^2/2)
\end{array}
$$

For a strong shock $v_2 = v_1/4$; $\rho_2 = 4\rho_1$

In a relativistic shock $n_2 = 4\Gamma_{shock}\, n_1$

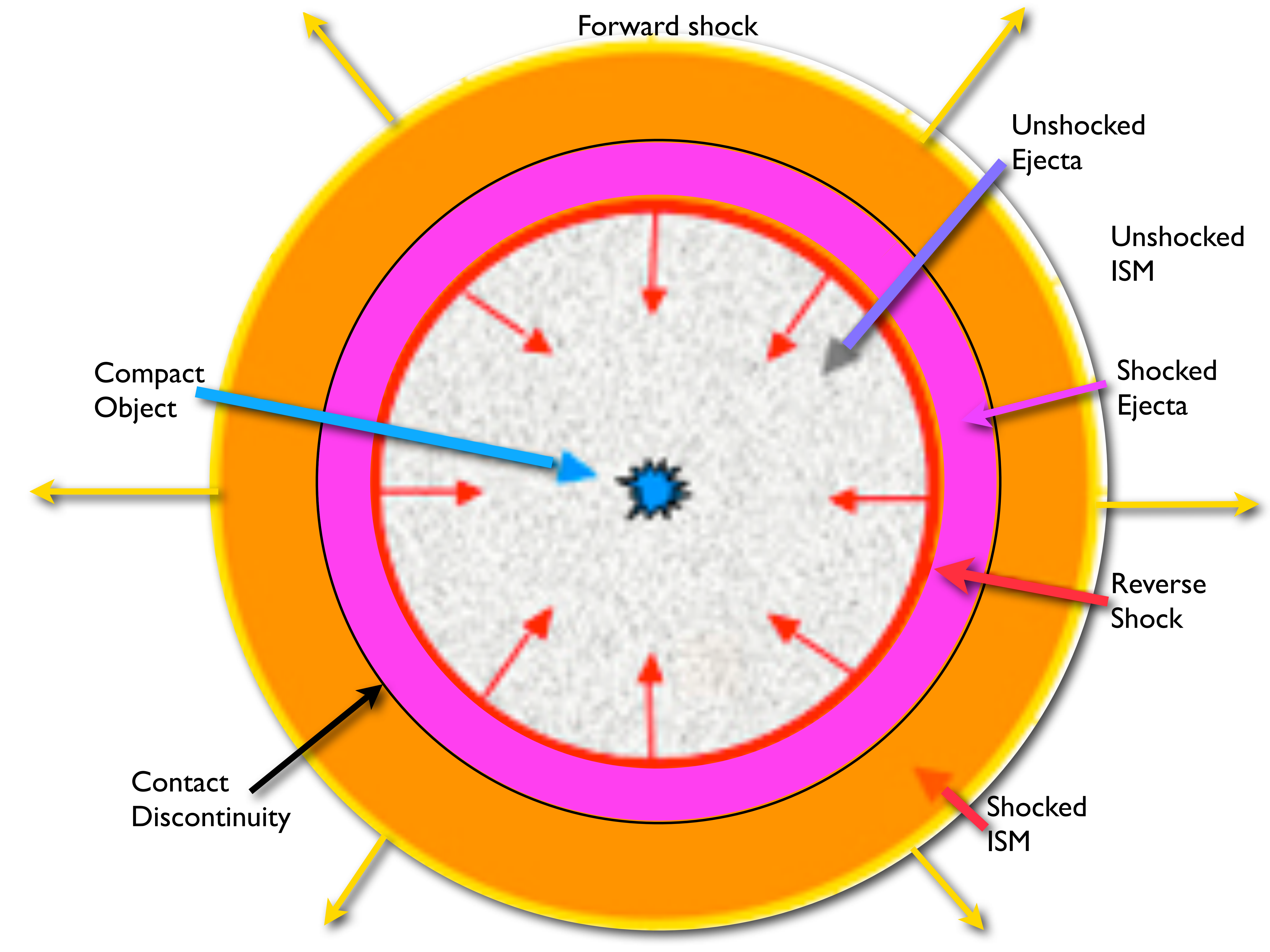
Forward shock
Unshocked Ejecta
Unshocked ISM
Compact Object
Shocked Ejecta
Reverse Shock
Contact Discontinuity
Shocked ISM

Supernova Remnants: Dynamical Phases

Early Coasting Phase (t < *a few hundred years*)

- small amount of mass sweep-up; constant expansion speed : $R \propto t$

Adiabatic Sedov Phase (*a few hundred years* < t < *several thousand years*)

- swept up mass causes deceleration; constant total energy : $R \propto t^{2/5}$

Radiative Phase (t > *a few thousand years*)

- radiative energy loss significant; expansion slows rapidly : $R \propto t^{1/4}$

Stall (t > *a few hundred thousand years*)

- expansion speed reaches interstellar sound speed; SNR dissipates

Magnetic Field is amplified behind the shock

- Swept up matter ~4 times denser; frozen-in field increases by this factor

- Contact discontinuity prone to Rayleigh-Taylor instability: drives turbulence and hence turbulent dynamo (Gull 1975)

- In very high speed (relativistic) shocks two-stream Weibel instability can efficiently generate magnetic field (Medvedev & Loeb 99)

Diffusive Shock Acceleration

Magnetic scattering of fast particles on both sides of shock
- Multiple crossings; energy gain in each cycle of crossing
- Finite escape probability in each crossing

$$\left\langle \frac{\Delta E}{E} \right\rangle_{\rm cyc} = \eta$$

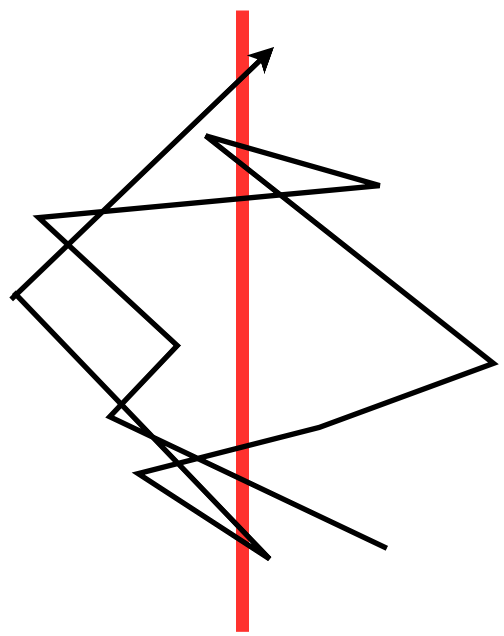

$$E_n = E_0(1+\eta)^n \;;\; N_n = N_0(1-P_{\rm esc})^n$$

$$\frac{N}{N_0}(>E) = \left(\frac{E}{E_0}\right)^{-x}, \quad x = -\frac{\ln(1-P_{\rm esc})}{\ln(1+\eta)}$$

$$N(E)dE = KE^{-p}dE, \quad p = 1 + x$$

Max. energy decided by confinement: R_L > acceleration zone escape. Radiative losses can also limit the energy acquired.

Any acceleration process in which
- **Relative energy gain ∝ time [d*E*/*E* ∝ d*t*]**
- **Escape prob. per unit time ~ constant [-d*N*/*N* ∝ d*t*]**

Will lead to a power-law energy distribution

SN shocks would accelerate all species of charged particles => **Cosmic Rays**

Veil Nebula, an old supernova remnant in Cygnus

Multiwavelength view of the remnant of Tycho Brahe's supernova

3C 10 - TYCHO'S SUPERNOVA REMNANT

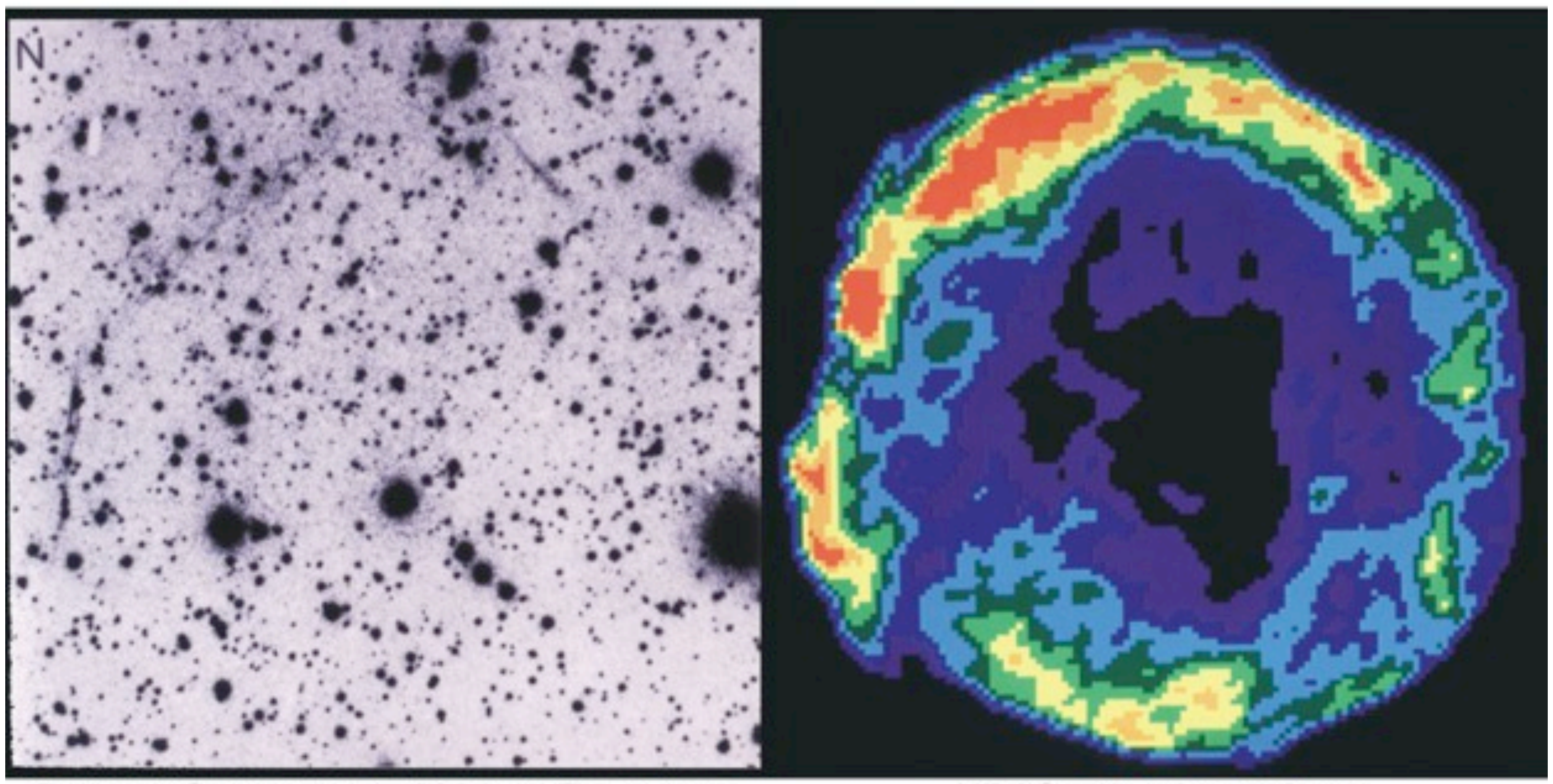

Palomar Observatory - 200 inch Telescope
Optical Image (Red Light)

NRAO - Very Large Array
Radio Image (1370 MHz)

EXPLOSION IN AD 1572

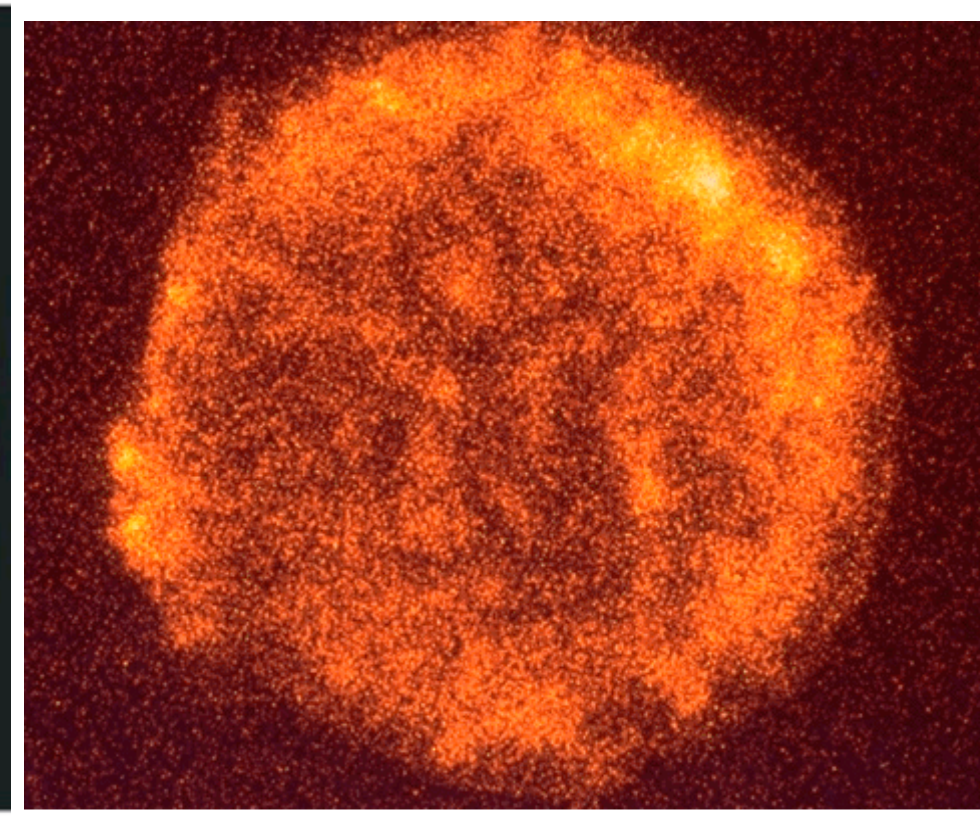

X-ray, ROSAT

Optical is faint, suffers from dust extinction

Bright radio non-thermal synchrotron emission

X-rays primarily from thermal emission by hot shocked gas

Cas A from CXO

Cas A heavy element map in reverse-shocked ejecta

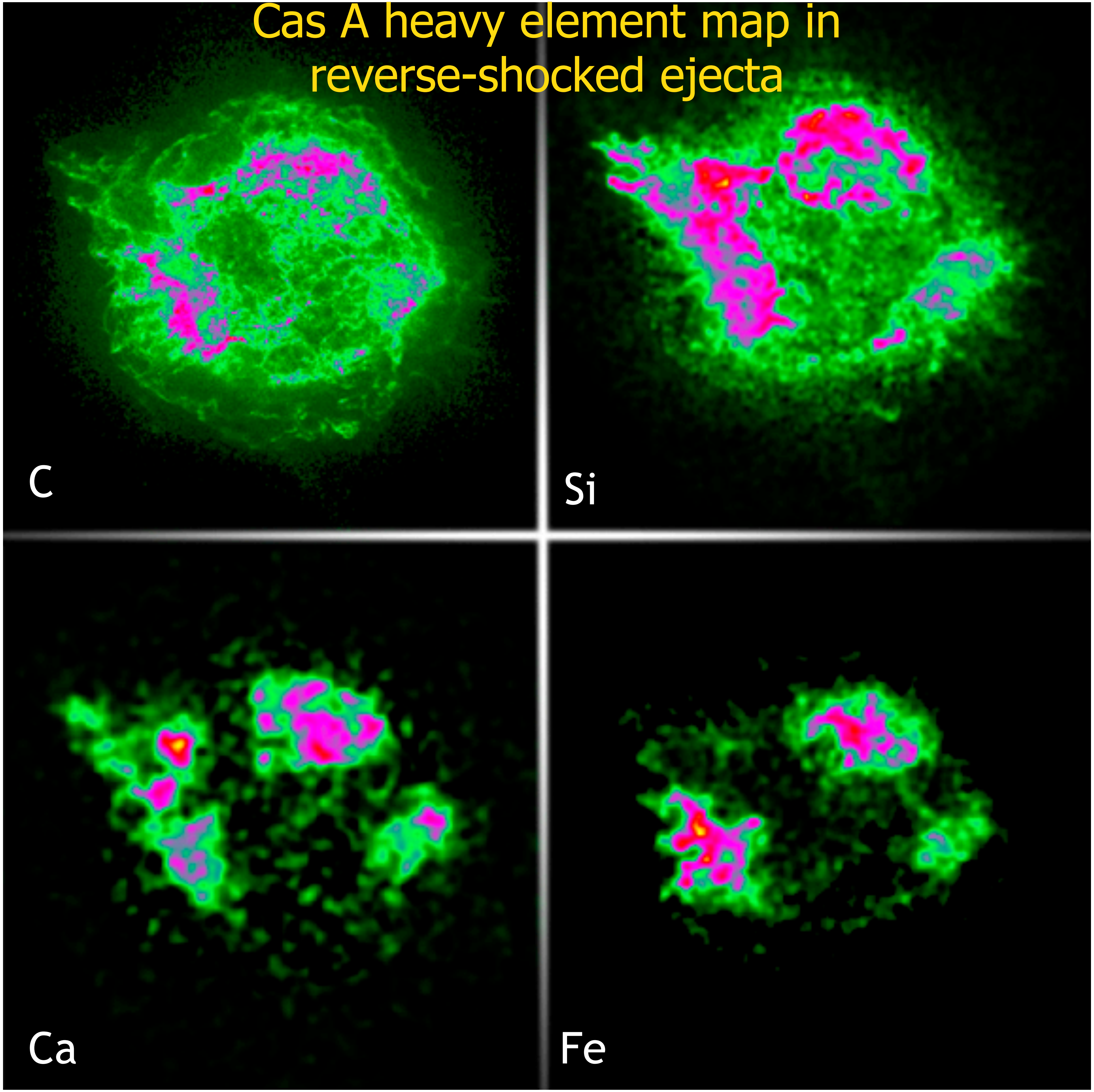

Cosmic Ray Production in Supernova Remnants

Fermi acceleration in shocks

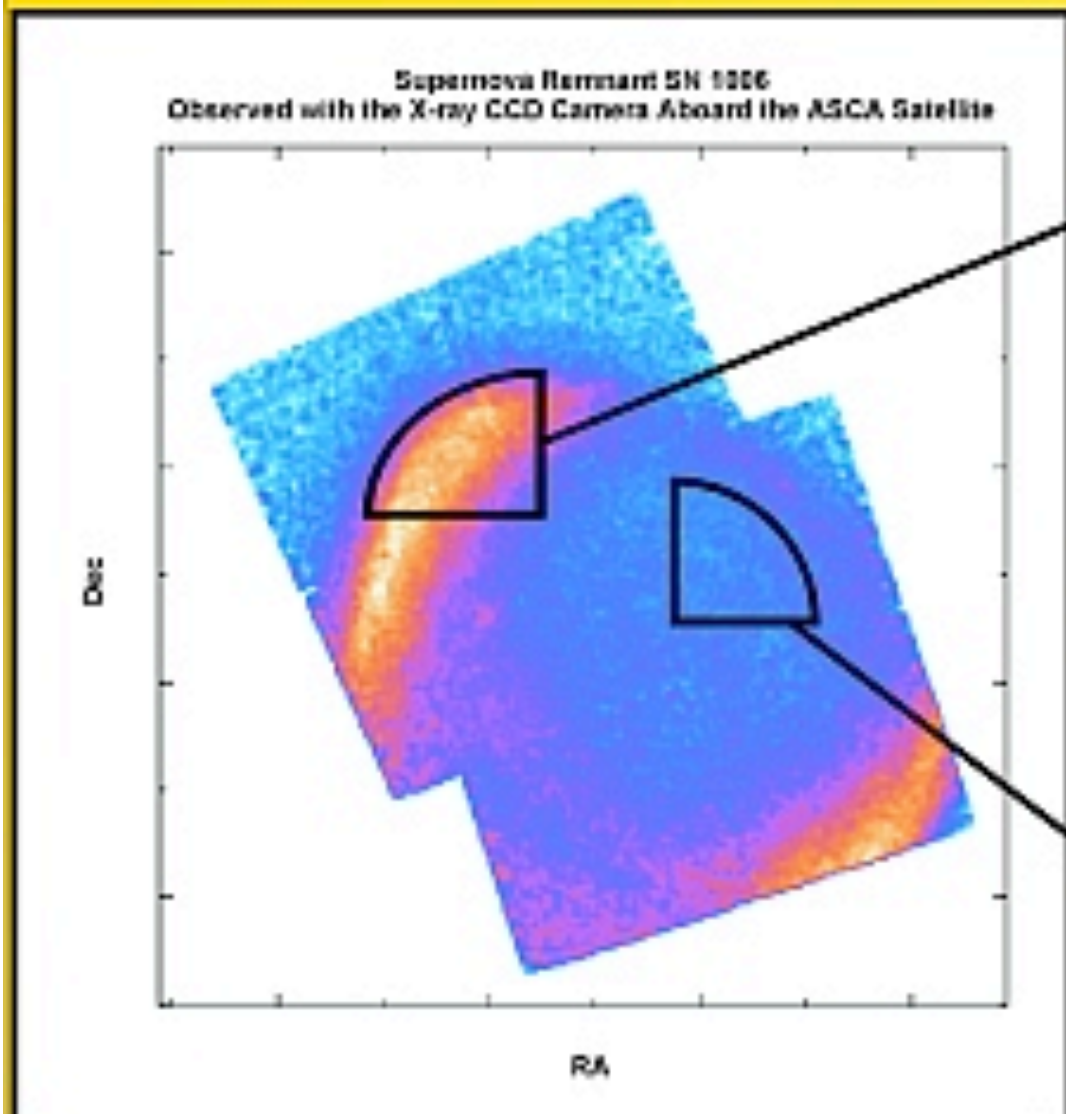

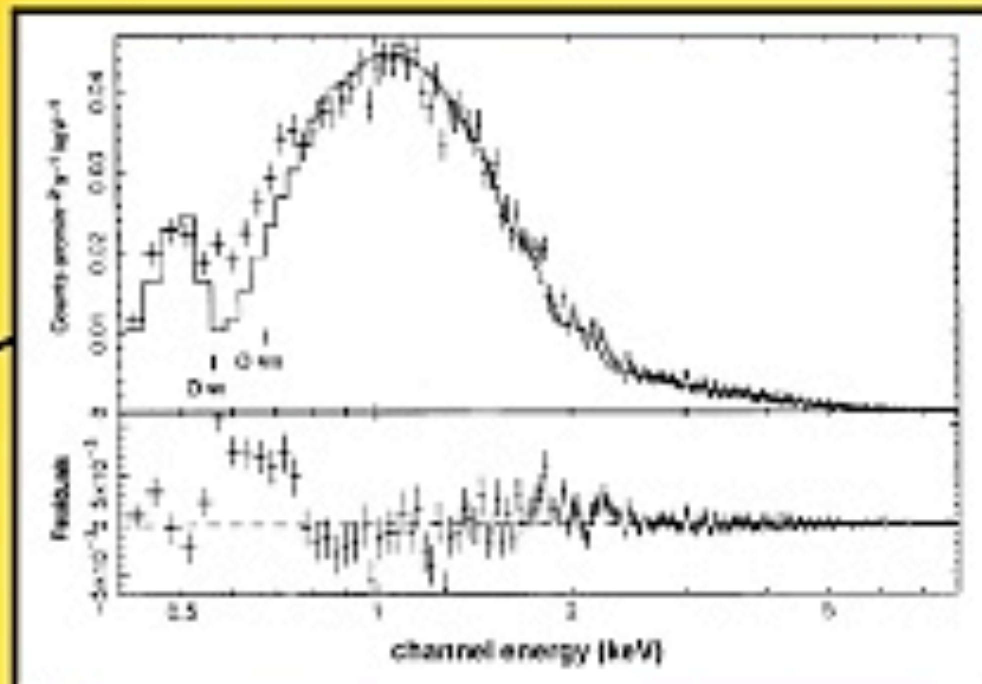

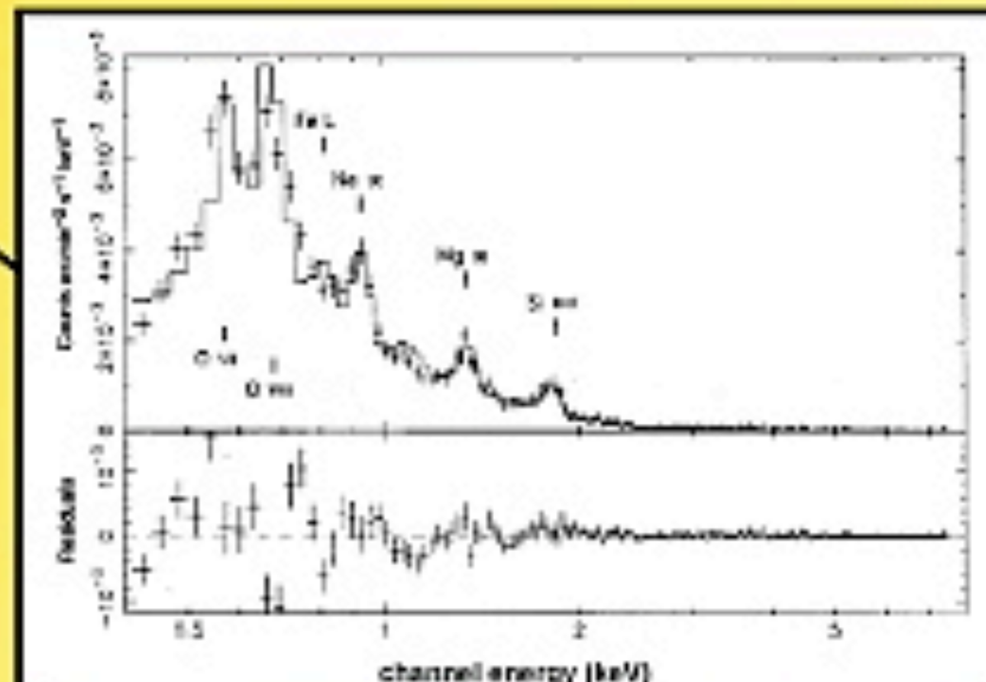

ASCA observations of the supernova remnant SN 1006 have revealed the first strong observational evidence for the production of cosmic rays in the shock wave of a supernova remnant. These results come from the detection of non-thermal synchrotron radiation from two oppositely located regions in the rapidly expanding supernova remnant. The remainder of the supernova remnant, in contrast, produces thermal X-ray emission showing Oxygen, Neon, Magnesium, Silicon, Sulfur, and Iron line emission.

(Koyama, Petre, Gotthelf, Hwang, Matsuura, Ozaki, & Holt, Nature, 378, 255, 1995)

VLA Radio image of Cas A

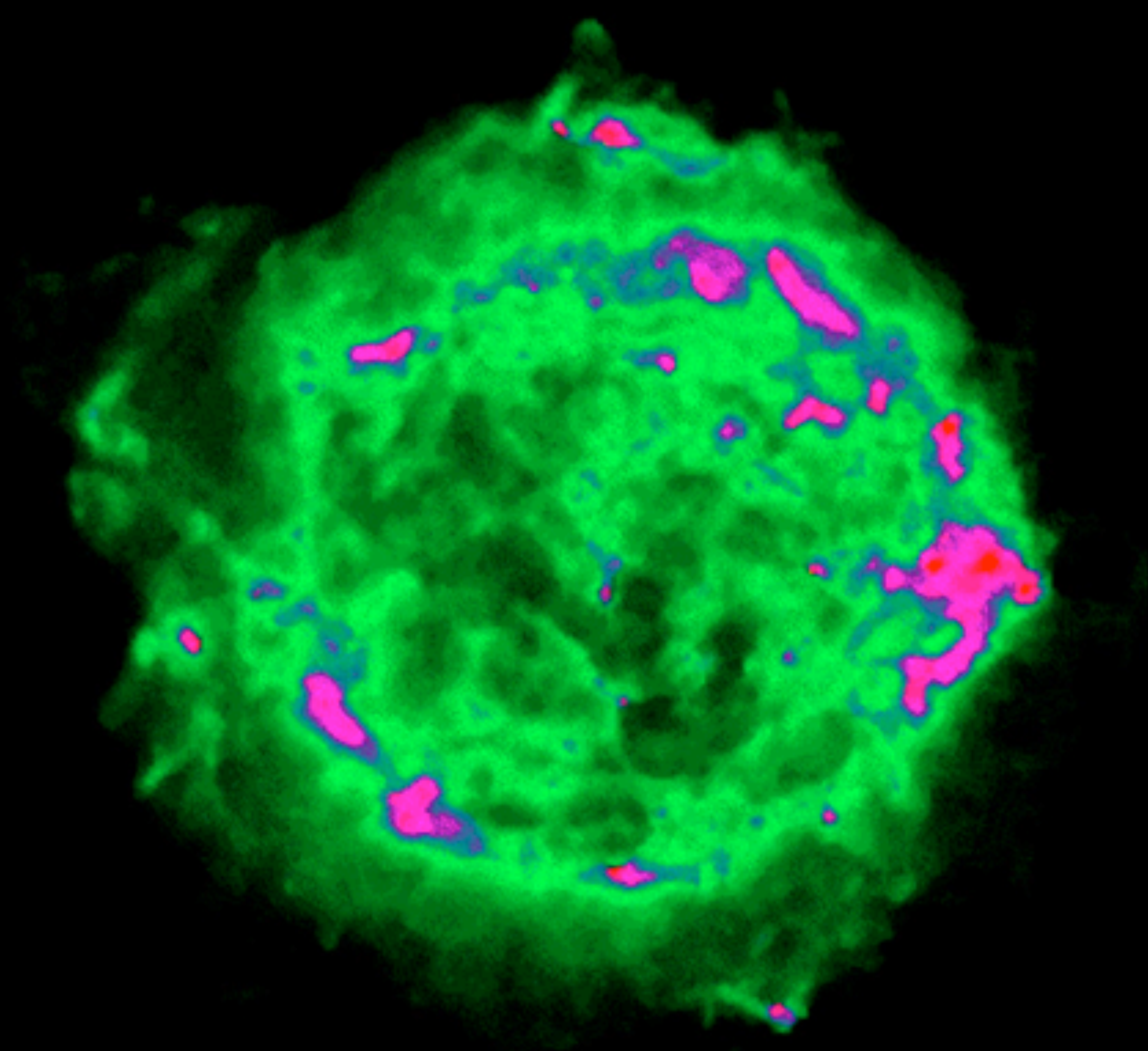

Cas A from CXO

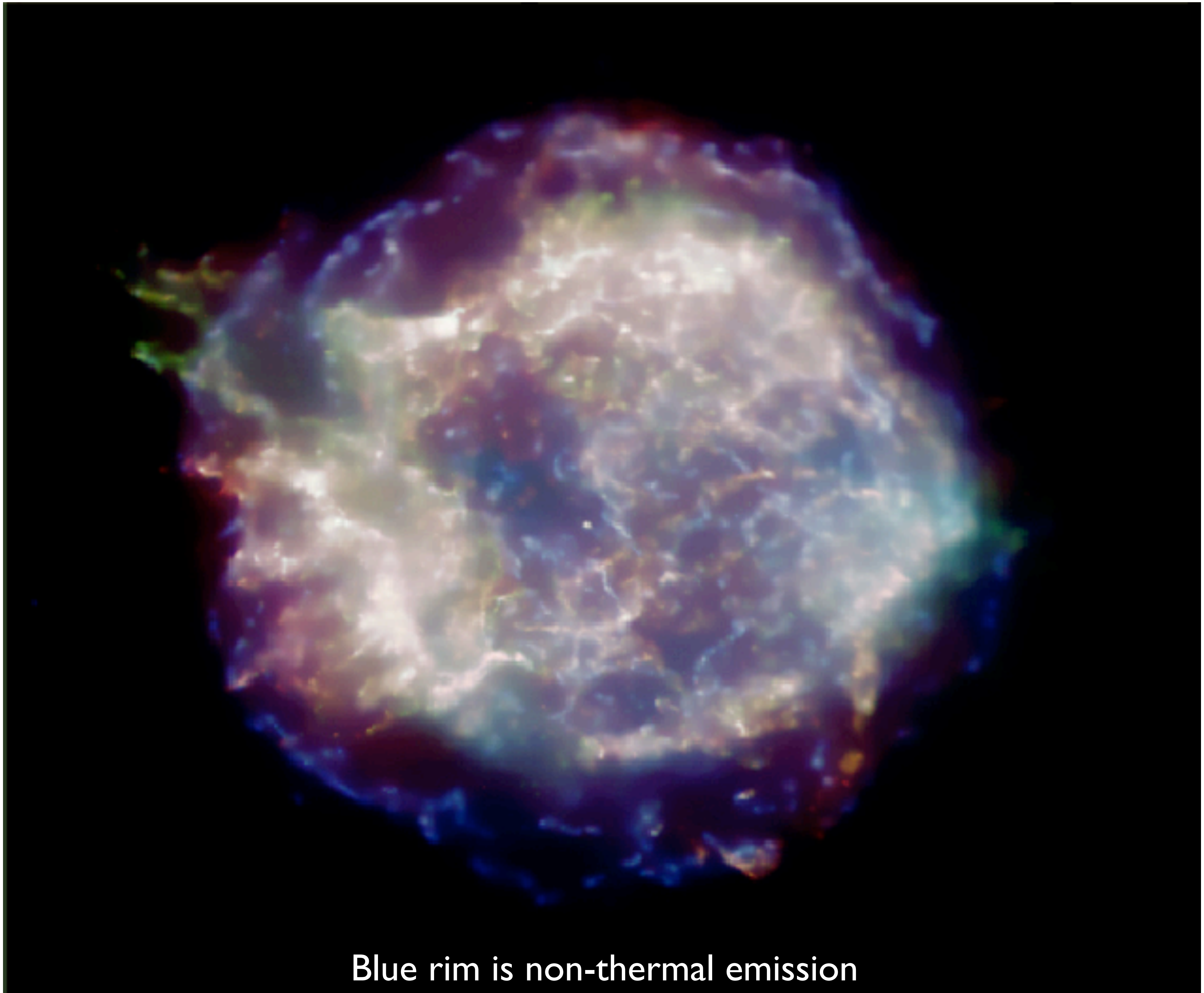

Blue rim is non-thermal emission

HESS SNR image at TeV

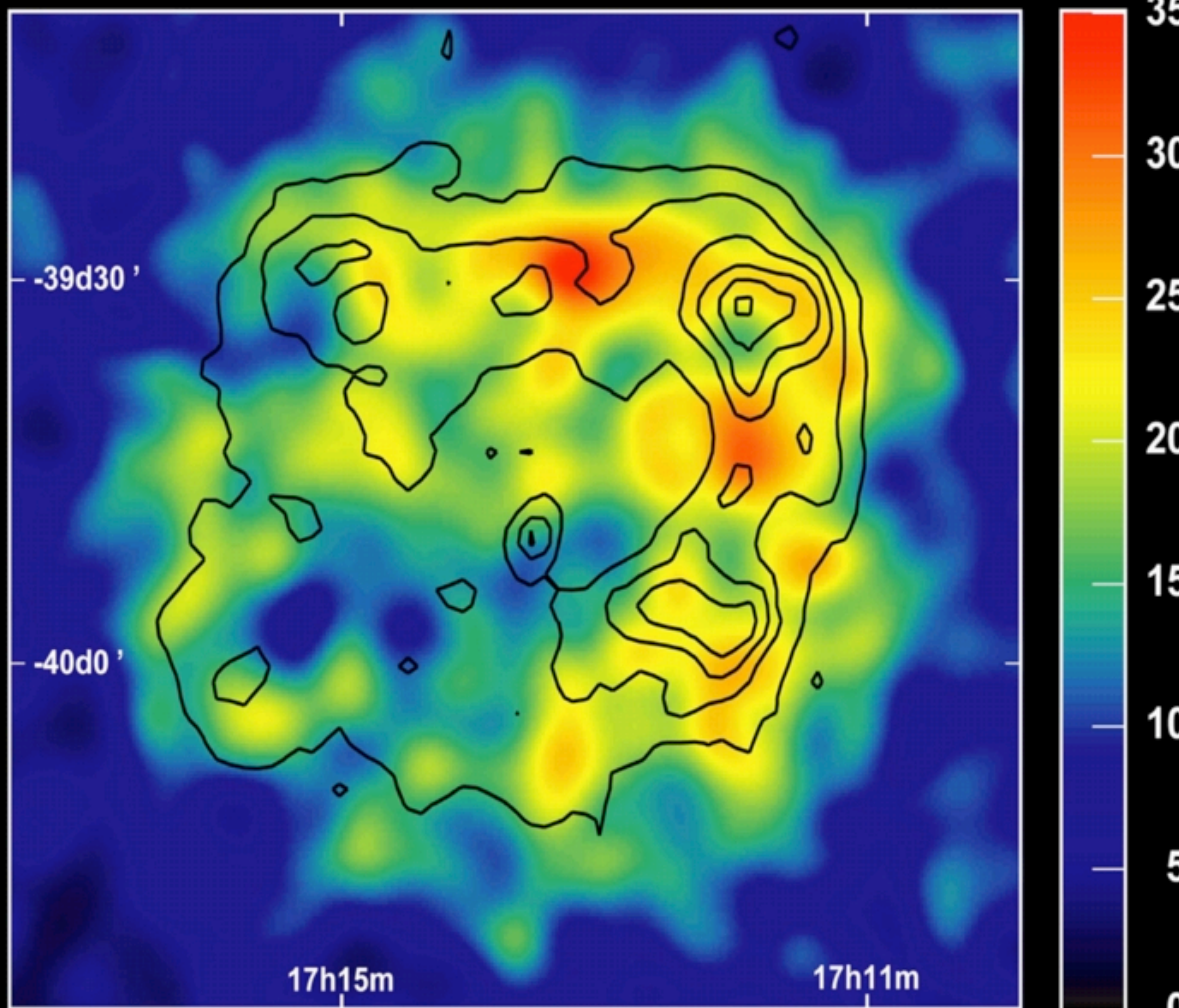

RX J1713.7-3946

Contours: X-ray

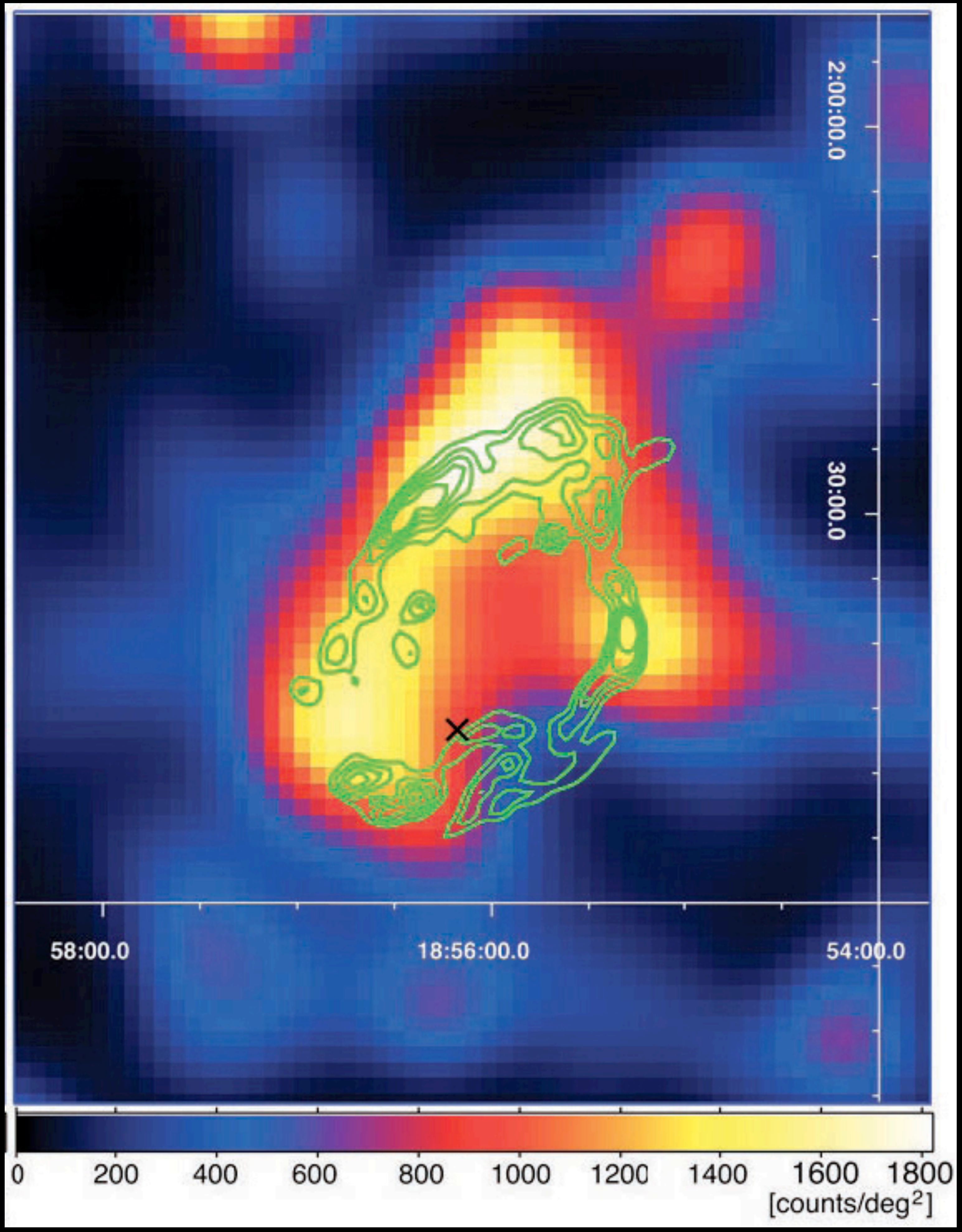

W44 imaged by Fermi LAT

Green contours: IR image

(Abdo et al 2010)

Evolution of non-thermal emission in supernova remnants

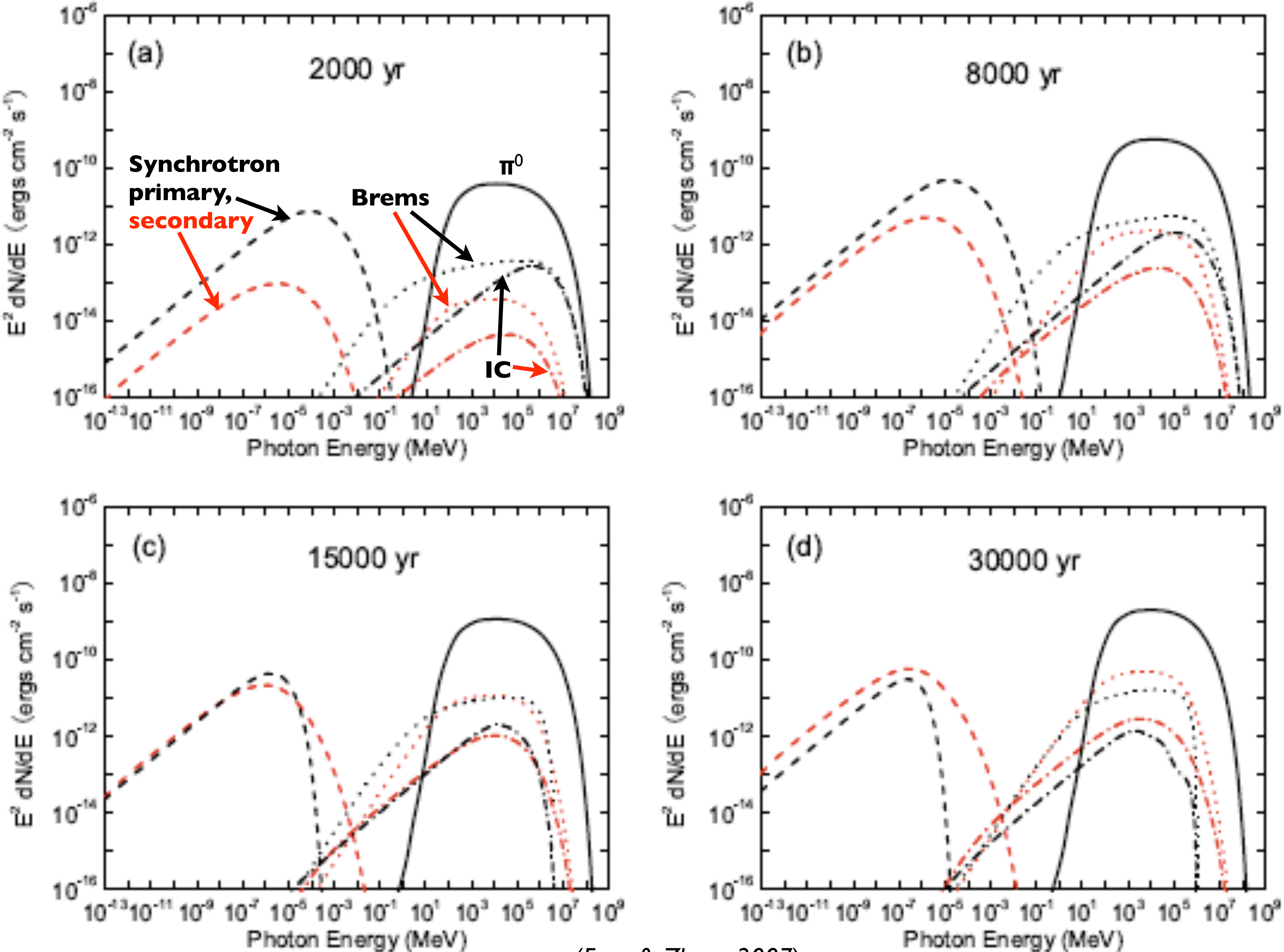

(*Fang & Zhang 2007*)